The Nucleolus as a Regulator of Chromatin Plasticity and Pluripotency

Dissertation

zur
Erlangung der naturwissenschaftlichen Doktorwürde
(Dr. sc. nat.)

vorgelegt der
Mathematisch-naturwissenschaftlichen Fakultät

der
Universität Zürich

von
Nataša Savić

aus
Serbien

Promotionskomitee

PD Dr. Raffaella Santoro (Leitung der Dissertation)
Prof. Dr. Dr. Michael O. Hottiger (Vorsitz der Dissertation)
Prof. Dr. Massimo Lopes
Dr. Paolo Cinelli
Prof. Dr. Dr. Witold Filipowicz

Zürich, 2014

“What you do makes a difference, and you have to decide

what kind of difference you want to make.”

Jane Goodall

Summary

Epigenetic mechanisms, including nuclear architecture, chromatin structure, chromatin dynamics and histone and DNA modifications, are fundamental players for correct cellular function. Chromatin organization and epigenetic signature distinguish pluripotent stem cells (ESC) from somatic cells. A less compacted chromatin structure and higher levels of histone modifications characteristic of euchromatin allow ES chromatin to assume a globally more open conformation than in differentiated cells. These chromatin properties seem to reflect a functionally important hallmark of pluripotency. How all of these changes occur during the differentiation process is yet to be elucidated.

Clustering of heterochromatin at nucleoli is a phenomena occurring in many organisms, yet its physiological relevance is poorly understood. Within the nucleolus of somatic cells, a fraction of 400 ribosomal RNA (rRNA) genes (in mouse and human cells) is transcriptionally silent, possesses epigenetic features characteristic of constitutive heterochromatin, and is stably inherited independently of cell metabolic activities. Silent rRNA genes represent a striking example of an epigenetically regulated heterochromatic domain. So far, studies concerning the regulation of epigenetic rDNA silencing investigated the mechanisms involved in the transmission of the silent heterochromatic structure of the rRNA genes through cell division (maintenance of silencing). These studies identified the nucleolar remodelling complex NoRC as the key factor that establishes and maintains silent rDNA chromatin structure during cell cycle. NoRC function requires the association of TIP5, the major subunit of NoRC, with the

non-coding RNA termed pRNA, which derives from processing of a 2kb long intergenic spacer (IGS)-rRNA transcript.

Here, we show that during ESC differentiation, rRNA genes acquire heterochromatic marks concurrently with the maturation of centric and pericentric heterochromatin. Impairment of intergenic-spacer (IGS)-rRNA processing in ESCs abrogates formation of mature pRNA and determines the lack of rDNA heterochromatin. Upon differentiation, pRNA is produced and enables the nucleolar repressor TIP5 to associate with TTF1, docking the complex to rDNA, an interaction inhibited by IGS-rRNA. Addition of pRNA to ESCs is sufficient to establish nucleolar and nuclear heterochromatin as it is found in somatic cells and impairs pluripotency, while depletion of TIP5 inhibits differentiation. The results link the epigenetic state of the nucleolus with pluripotency and commitment and unravel a further level of non-coding RNA (ncRNA) regulation through the ability of RNA processing to modulate distinct features of the same ncRNA.

Zusammenfassung

Für die Funktion einer Zelle sind epigenetische Mechanismen, sowie die nukleare Architektur, Chromatinstruktur und -dynamik, Histon- und DNA-Modifikationen grundlegende Voraussetzungen. Anhand der Chromatinorganisation und epigenetischen Signatur können pluripotente Stammzellen (ESCs) von somatischen Zellen unterschieden werden. Offene Chromatinstrukturen und die zugehörigen Histonmodifikationen sind charakteristisch für ESCs. Im Gegensatz zeichnen sich differenzierte Zellen durch ein wesentlich kompakteres Chromatin aus. Diese Chromatin-Eigenschaften stellen vermutlich ein wichtiges Kennzeichen der Pluripotenz von ESCs dar. Wann und wie diese Veränderungen während des Differenzierungsprozesses auftreten ist bislang jedoch ungeklärt.

Die Clusterbildung von Heterochromatin an den Nukleoli ist ein Phänomen, welches in vielen Organismen auftritt, und über dessen physiologische Relevanz nur wenig bekannt ist. In den Nukleoli von somatischen Zellen ist ein Anteil der ca. 400 ribosomale RNA (rRNA)-Gene (in menschlichen und murinen Zellen) transkriptionell inaktiv. Ihre epigenetische Eigenschaften sind charakteristisch für konstitutives Heterochromatin und werden stabil und unabhängig vom Zellmetabolismus weitervererbt. Diese stillgelegten rRNA-Gene sind ein Beispiel für epigenetisch regulierte heterochromatische Domänen. Bisherige Studien der epigenetischen Regulierung dieser rDNA-Domänen untersuchten den Mechanismus, der für die Vererbung von stillgelegtem Heterochromatin der rRNA-Gene während der Zellteilung verantwortlich ist (Aufrechterhaltung der transkriptionellen Inaktivierung). Diese Studien identifizierten den nucleolar remodelling complex (NoRC) als eine Schlüsselkomponente, die die

transkriptionell inaktiven rDNA-Domänen im Chromatin etabliert und über den Zellzyklus hinaus aufrecht erhält. Die Funktion des NoRC benötigt die Assoziation von TIP5 mit einer nicht-kodierenden RNA, genannt pRNA, welche als Produkt bei der Prozessierung des 2 kb langen intergenic spacer (IGS)-rRNA Transkripts entsteht.

In der vorliegen Arbeit zeigen wir, dass heterochromatische Markierungen in den rRNA-Genen während der ESC-Differenzierung gleichzeitig mit der Maturation von centromerischem und pericentromerischen Heterochromatin erworben werden. Die Beeinträchtigung der IGS-rRNA Prozessierung in ESCs verhindert die Bildung der maturen pRNA und führt zu fehlenden heterochromatischen Strukturen in den rRNA-Genen. Die Produktion der pRNA erfolgt während der Differenzierung und erlaubt die Assoziation des nukleolären Repressors TIP5 mit TTF1. Dadurch kann dieser Komplex an die rDNA binden, was zuvor durch die IGS-rRNA verhindert wurde. Alleine die Zugabe von pRNA zu ESCs ist ausreichend, um nukleoläres und nukleares Heterochromatin, ein typisches Merkmal somatischer Zellen, zu etablieren und die Pluripotenz dieser Zellen zu beeinträchtigen. Im Gegenzug wird die zelluläre Differenzierung in Abwesenheit von TIP5 inhibiert. Diese Ergebnisse weisen auf eine Verbindung des epigenetischen Status des Nukleolus mit der Pluripotenz einer Zelle und deren Bestimmung hin. Damit wird eine weitere Form der Regulation durch eine nicht-kodierende RNA (ncRNA) entschlüsselt, die der ncRNA je nach Status der RNA-Prozessierung verschiedene Eigenschaften verleiht.

Abbreviations

2i	2 inhibitors
5caC	5-carboxylcytosine
5fC	5-formilcytosine
5hmC	5-hydroxylmethycytosine
5mC	5-methylcytosine, also known as 5meC
ADP	adenosine diphosphate
ATP	adenosine triphosphate
BMP4	bone morphogenetic factor-4
bp	base pairs
CGI	CpG island
CH	CHIR99021 inhibitor
ChIP	chromatin immunoprecipitation
DNA	deoxynucleic acid
Dnmt	DNA methyltransferase
EB	embryoid body
EGC	embryonic germ cell
EpiESC	epiblast stem cell
ESC	embryonic stem cell
Fgf4	fibroblast growth factor 4
GSK3	glucogen synthase kinase-3
GST	glutathione S-transferase
His	histidine
HMG	high mobility group
HMT	histone methyltransferase
HKMT	histone lysine methyltransferase
HP1	heterochromatin protein 1
ICM	inner cell mass
IGS	intergenic spacer
IGS-rRNA	intergenic spacer rRNA
iPSC	induced pluripotent stem cell

JAK	Janus kinase
JMJD2	lysine-specific demethylase 4A
K, Lys	lysine
kb	kilobases
kDa	kilodalton
LAD	lamina associated domain
LIF	leukemia inhibitory factor
LIFR	leukemia inhibitory factor receptor
lncRNA	long non-coding RNA
LOCK	large organized chromatin domains
LSD1	lysine-specific demethylase
MAPK	mitogen activated protein kinase
MBP	methyl-CpG-binding protein
MEF	mouse embryionic fibroblast
MNase	micrococcal nuclease
mRNA	messenger ribonucleic acid
ncRNA	non-coding RNA
NOR	nucleolar organizing region
NoRC	nucleolar remodeling complex
NPC	neural progenitor cell
nt	nucleotide
NT	nuclear transplantation, also known as SCNT
PARP	poly(ADP-ribose)polymerase
PcG	polycomb group
PD	PD0325901 inhibitor
PGS	primordial germ cell
PHD	plant homeodomain
PI3K	phosphoinositide 3 kinase
Pol	RNA polymerase
pre-rRNA	precursor ribosomal RNA
pRNA	promoter RNA
PTMs	posttranslational modifications

R, Arg	arginine
rDNA	ribosomal DNA
RENT	regulator of nucleolar silencing and telophase exit
RNA	ribonucleic acid
rRNA	ribosomal RNA
qRT-PCR	quantitative real time PCR
RT-PCR	reverse transcription polymerase chain reaction
SAM	S-adenosylmethionine
SCNT	somatic cell nuclear transfer, also known as NT
SHP2	SH2 domain containing tyrosine phosphatase 2
SL1	selectivity factor 1
Snf2h	sucrose non-fermenting protein 2 homologue
Stat3	signal transducer and activator of transcription 3
TAFI	TBT-associated factor
TBT	TATA box binding protein
TDG	thymidine DNA glycosylase
TET	ten-eleven-translocation
TF	transcription factor
TGF-b	transforming growth factor beta
TIF-IA	transcription initiation factor-IA
TIF-IB	transcription initiation factor-IB
TIP5	TTF-I interacting protein 5
TrxG	trithorax
TSP, T_0, T_{1-10}	terminator elements
TSS	transcription start site
TTF-I	transcription termination factor
UBF	upstream binding factor
UCE	upstream control element
ZF	zinc finger

Table of Contents

1 Introduction

1.1 Chromatin structure

Efficient packaging of genomic DNA in eukaryotes is allowed by organization in DNA-protein complexes, termed chromatin (Lodish, 2013). The packaging of DNA into chromatin is critical both for the physical compaction of the genome into the nucleus and as a mean to regulate access to the genetic material for DNA-based transactions, such as transcription, replication, and repair. The basic unit of the chromatin is the nucleosome, which consists of 147 bp of DNA wound around the surface of an octamer of two copies each of four core histone proteins H2A, H2B, H3 and H4[2]. Adjacent nucleosomes are connected by the linker histone H1 bound to variable length of linker DNA (10-100 bp) forming a bead-on-a-string-like structure (Felsenfeld and Groudine, 2003; Wolffe, 1997). Further diversification of nucleosome core particles is obtained by varying amino acid sequence of histones, leading to a set of histone isoforms known as histone variants. In some cases, the histone variants can alter the architecture of the histone octamer, and as a consequence, of the chromatin structure (reviewed in (Sarma K, 2005)). Beyond the nucleosome, chromatin folds into successively higher-order structures that remain poorly described at a molecular level.

Several mechanisms have been described to dynamically alter the nucleosome spacing and accessibility: ATP-dependent chromatin remodelers, DNA methylation, histone modifications and incorporation of specific histone variants.

1.1.1 Histone modifications

The pioneering studies in the early 1960s have shown that histones are bearing posttranslational modifications (PTMs) (Allfrey et al., 1964). The core histone proteins are predominantly globular except for their unstructured N-terminal tails, which extend away from the globular core. Importantly, these histone tails posses a large number and different types of modified residues. These enzyme-catalyzed covalent modifications include acetylation, methylation, phosphorylation, ubiquitynation, sumoylation, ADP-ribosylation, deimination, β-N-acetylglucosamination, histone tail clipping and proline isomerization (reviewed in (Bannister and Kouzarides, 2011)). Since most of the histone modifications are reversible, this marking system represents a fundamental regulatory mechanism for chromatin function (Jenuwein and Allis, 2001). Modifications not only regulate higher-order chromatin structure by affecting inter-nucleosomal interactions, but they recruit effector proteins and complexes with specific enzymatic activities such as remodeling enzymes that utilize the energy derived from the hydrolysis of ATP to reposition nucleosomes (Strahl and Allis, 2000).

Each histone tail within the nucleosome is characterized by multiple posttranslational modifications, which is creating a distinct chromatin signature. Histone modifications are occurring in a variety of different combinations, of which each affects gene transcription and chromatin structure. This combinatory occurrence of histone modification led to the concept of the histone code (Jenuwein and Allis, 2001; Strahl and Allis, 2000). The histone code extends the information given by genetic code and together with DNA methylation and

nucleosome remodeling processes and their cognate regulatory proteins is classified under the general term “epigenetic mechanisms”.

1.1.1.1 Histone Methylation

Methylation of histone residues can mediate both active and repressive signals, which regulate gene transcription through recruitment of specific downstream effector proteins.

Histone methylation mainly occurs on the side chains of lysines (Lys, K) and arginines (Arg, R), in the N-terminal tails of histone H3 and H4 as well as in the glogular domain of histones. Histone methylation is performed by histone methyltransferases (HMTs) which catalyze the transfer of a methyl group from S-adenosylmethionine (Tsai et al.) to a lysine or arginine residue. All known histone methyltransferases contain a conserved methyltransferase domain termed SET (Su(var)3-9, Enhancer-of-zeste, Tritorax) (Lachner and Jenuwein, 2002).

Histone lysine methyltransferase (HKMT) possess a high level of substrate specificity with respect to their target lysine and also modify the appropriate lysine to a specific degree (i.e., mono-, di- and/or tri-methyl state). For example, the methylation pattern of histone 3 lysine 9 (H3K9) is established by different HMTs; G9a and GLP, which exist predominantly as a G9a-GLP heteromeric complex, are the primary mono- and di-methylases (H3K9me1 and H3K9me2), whereas SUV39H2 di- and tri-methylates a mono-methylated substrate. Tri-methylation of lysine 9 of histone 3 (H3K9me3) represents a specific mark for epigenetic transcriptional repression that is specifically recognized by heterochromatin protein 1 (HP1) and is linked to heterochromatin condensation and gene silencing

(Bannister et al., 2001; Lachner et al., 2001). Another important example of specific histone lysine methyltransferase activity are the trithorax (TrxG) and Polycomb (PcG) multiprotein complexes which contain histone methyltransferases. TrxG and PcG have reciprocal functions: TrxG proteins work together to activate transcription while PcG proteins repress transcription (reviewed in (Muller and Verrijzer, 2009)). TrxG histone modifiers, TRX and ASH1 methylate histone H3 lysine 4 (H3K4) active mark (Strahl and Allis, 2000). PcG complexes are made up of polycomb repressive complex 2 (PRC2) and polycomb repressive complex 1 (PRC1). PRC2 (EHZ2) complex deposits the H3K27me3 inactive chromatin mark while PRC1 interprets this code(Levine et al., 2004). The regulatory effects of PcG and TrxG are broad and are mediated through various histone modifications and nucleosome remodelling. Some of the specific examples in embryonic stem cells are discussed in Chapter **1.2.3**.

Recently, the search for enzymes for reversal reaction to lysine methylation identified lysine-specific demethylase 1 (LSD1) compatible with mono- and dimethylated lysine substrates which is in different complexes able to demethylate H3K4me1/2 and H3K9me2 (Shi et al., 2004). The first enzyme identified as a tri-methyl lysine demethylase was JMJD2 (lysine-specific demethylase 4, also known as KDM4) that demethylates H3K9me3 and H3K36me3 (Whetstine et al., 2006).

1.1.2 DNA methylation

Like histone methylation, DNA methylation also plays a role in regulating gene expression of cells. DNA methylation is highly conserved epigenetic modification

of DNA, which occurs on the cytosine base of the DNA within CpG dinucleotides in prokyriotes as well as in eukaryotes. The most of vertebrate genome contains few CpG dinucleotides and they tend to be converted to 5-methylcytosines (5mC). Unmethylated CpGs are very offten found locally very dense, organized in clusters called CpG islands (CGIs). DNA methylation is generally considered as a mark of silent, inactive chromatin and is inversely correlated with gene activity, although this association is dependent on CpG density. CpG-rich promoters are associated with ubiquitously expresses “housekeeping” genes and with regulatory genes expressed during development. In contrast, CpG-poor promoters are generally associated with tissue-specific genes.

DNA methylation is carried out by DNA methyltransferases (DNMTs) catalyzing the transfer of methyl group from S-adenosyl-methionine (Tsai et al.) to CpG dinucleotides of genomic DNA (Jeltsch, 2006).

Methylation patterns are established *de novo* during embryonic development and stably inherited upon cell divisions. The maintenance of DNA methylation during replication depends on DNMT1, which attaches a methyl group to hemimetylated DNA. The de novo establishment of DNA methylation is performed by DNMT3A and DNMT3B, which are able to act on hemimethylated and unmethylated CpG-dinucleotides. The role of DNMTs in embryonic stem (ES) cells has been analyzed using homozygous mutants. Inactivation of genes encoding DNMT3A and DNMT3B blocks *de novo* methylation in ES cells and mouse embryos. These methyltransferases are required for normal mammalian development but have no influence on the maintenance of imprinted methylation patterns (Okano et al., 1999). In mouse development, mutation of Dnmt1 gene results in embryonic

lethality (Li et al., 1992). Moreover, DNMT1-/- ES cells divide and maintain pluripotency in culture, but show elevated mutation rates and fail to survive after being induced to differentiate (Chen et al., 1998; Jackson et al., 2004). These and other studies have shown the importance of DNA methylation for maintaining genome stability, the establishment and the maintenance of stable cellular identities, transposable element silencing, genomic imprinting and X chromosome inactivation (reviewed in (Wu and Zhang, 2010b)).

The effect of DNA methylation on gene expression may be direct or indirect. Some DNA binding proteins (e.g. transcription factors) are only able to interact with their target sequence if unmethylated (Clark et al., 1997), whereas CpG methylation directly abolishes their interaction with DNA and leads to lower transcription level. On the other hand, methylated DNA can be specifically recognized by a set of proteins called methyl-CpG-binding proteins (MBPs), which belong to three different structural families in mammals: the MBD family, the Kaiso and Kaiso-like proteins and the SRA domain proteins. These proteins were shown to associate and recruit chromatin repressor factors such as histone deacetylases, thus establishing silent chromatin at methylated CpG sequences (Defossez and Stancheva, 2011).

Compared with other epigenetic modifications, DNA methylation is thought to be relatively stable (Wu and Zhang, 2010a). However, studies in the past decade have revealed that this modification is not as static as once thought. Loss of DNA methylation can occur through a passive or an active process. Active DNA demethylation is the enzymatic process that results in the removal of the methyl group from 5-methylcytosine (5meC) by breaking a carbon-carbon bond. By

contrast, passive DNA demethylation refers to the loss of the methyl group from 5meC when DNMT1 is inhibited or absent during successive rounds of DNA replication. Examples of both processes can be found at early development where, after fertilization, the paternal genome rapidly undergoes genome-wide active demethylation and remains as such in the consecutive rounds of cells divisions. In contrast, the maternal genome experiences gradual, passive demethylation. The three mammalian TET (ten-eleven-translocation) family proteins, namely TET1, TET2 and TET3, are dioxygenaze that successively oxidize DNA 5-methylcytosine to 5-hydroxymethylcytosine (5hmC), 5-formilcytosine (5fC) and 5-carboxylcytosine (5caC). All three forms of oxidized methylcytosine are known to be present in numerous mammalian tissues. 5hmC has been found present as 5-10% of 5mC level in embryonic stem cells and even higher in neurons. 5fC and 5caC are present at much lower levels than 5hmC, 0.03% and 0.01%, respectively, of the level of 5mC in ESCs. These low levels can at least partially be explained by their enzymatic removal by thymidine DNA glycosylase (TDG) base excision repair and possibly decarboxylation by yet unknown enzymes (reviewed in (Pastor et al., 2013)).

1.1.3 Euchromatin and heterochromatin

More than a century ago, distinct chromatin regions were observed within the genome by staining with basic dyes. The barely visible regions, termed euchromatin decondense during interphase whereas the strongly stained heterochromatin remains constantly stained throughout the cell cycle (reviewed in (Fransz et al., 2003)). Euchromatin and heterochromatin represent not only

structural types, but also main functional states of chromatin. Euchromatin is gene rich, contains irregular nucleosomal array and it is easily accessible by transcription factors. On the contrary, heterochromatic genome regions are gene poor, late-replicating and highly condensed which tends to be refractory for transcription. The heterochromatin is further subdivided in two types, facultative and constitutive (reviewed in (Dillon and Festenstein, 2002)). Facultative heterochromatin is characterized mainly by high levels of H3K27me3 (Cao et al., 2002), and the related PRC1-catalysed ubiquitination of H2AK119 (Grewal and Elgin, 2007). Constitutive heterochromatin is strongly enriched in H3K9me3, H4K20me3 and H3K64me3, as well as in DNA methylation (Daujat et al., 2009; Peters et al., 2001; Schotta et al., 2004), but deprived of histone acetylation and is mainly found at centromeric, pericentromeric, and telomeric regions.

Heterochromatic regions often clusters together, whereas the more open euchromatic regions are dispersed in the nucleoplasm or underlie nuclear pores (Meister and Taddei, 2013). Remarkably, heterochromatic clusters are not randomly distributed within the nucleus, but are enriched at the nuclear periphery and around the nucleolus (Gonzalez-Sandoval et al., 2013). This suggests that the spatial distribution of heterochromatin may be regulated, and could, in turn, influence chromatin-based functions. In support of this, nuclei of different tissues have distinct and recognizable distributions of euchromatin and heterochromatin (Solovei et al., 2013). Generally, inactive genes are sequestered in a tissue-specific manner at the nuclear periphery of differentiated cells, whereas activated, developmentally controlled promoters are sequestered in the nuclear center. This has recently been documented for genes of three distinct tissue types in *Caenorhabditis elegans*, and has been shown for a number of loci during

mammalian hematopoietic differentiation (Hubner et al., 2013; Meister et al., 2010). These observations, together with the fact that changes in heterochromatin organization are widely used as clinical markers of neoplastic transformation (Zink et al., 2004), argue that chromatin within the nucleus has an intrinsic and potentially useful order (Gonzalez-Sandoval et al., 2013).

1.2 Embryonic stem cells

Embryonic stem cells (ESCs) derive from the inner cell mass (ICM) of a blastocyst, an early-stage preimplantation embryo (in mouse, E3.5). They are characterized by their potential to self-renew indefinitely and to differentiate into any of the three germ layers: endoderm, mesoderm and ectoderm. These attributes that define the pluripotency state render ESC particularly attractive as models to study early developmental decision-making (commitment) as well as its execution (differentiation). Only cells in the zygote have a greater lineage potential than ESCs, defined as totipotent, being able also to generate extra-embryonic tissues including trophectoderm (Fisher and Fisher, 2011).

Self-renewal is the process by which stem cells divide to make more stem cells, perpetuating the stem cell pool throughout life. Self-renewal is division with maintenance of the undifferentiated state. In this process, a stem cell divides asymmetrically or symmetrically to generate one or two daughter stem cells that have a developmental potential similar to the mother cell. Symmetric division generates two identical sister cells whereas during asymmetric division one cell preserves the original phenotype of the mother cell and the second cell acquires a new phenotype. Asymmetric division is the basic mechanism for maintaining cell diversity, but both types of cell division ensure that physiological and morphological properties of the parental cells are transmitted to the next cell generation. The ability to self-renew is essential for stem cells (embryonic and adult) to expand their number during development, to be maintained within adult

tissues, and to restore the stem cell pool after injury. Defects in self-renewal mechanisms can lead to developmental defects, premature aging phenotypes, and cancer (reviewed in (He et al., 2009)).

The self-renewal and pluripotency features of ESCs make them an ideal in vitro tool to study early mammalian development, but it also offers great therapeutic potential within the field of regenerative medicine. As ESCs might represent a potential source for cell and tissue replacement, the molecular and cellular mechanisms controlling pluripotency and differentiation have to be elucidated in order to make these potential clinical applications a reality.

ESCs were successfully derived by explanting blastocysts or ICMs on a layer of “feeder” cells (mitotically inactivated fibroblasts) in medium containing fetal calf serum (Evans and Kaufman, 1981; Martin, 1981). Evans and Kaufman facilitated the derivation of ESCs by using the embryonic diapose property of rodents. Diapause is a condition of embryo arrest at the peri-implantation blastocyst stage, where implantation is prevented by estrogen deprivation. The derivation of mouse ESCs using feeders and serum is inefficient and variable and the genetic background has a major influence on the capacity to give rise to ESCs. For many years, the ESC derivation was poorly understood and it became necessary to refine the culture conditions and define the molecular requirements for efficient generation of ECSs. In 1988, two different studies by Williams and Smith found that the self-renewal support coming from feeder cells arose from cytokine produced by these cells termed leukemia inhibitory factor (LIF) (Smith et al., 1988; Williams et al., 1988). LIF promotes ESC self-renewal by activation of the

transcription factor Stat3 (Matsuda et al., 1999; Niwa et al., 2000). Lately, serum has been replaced by addition of bone morphogenetic factor-4 (BMP4) (Ying et al., 2003).

In 1999, Burdon and colleagues showed that the inhibition of the Erk pathway (also called mitogen activated protein kinase, MAPK) promoted self-renewal of ESCs by blocking differentiation cues provided by it (Burdon et al., 1999). Inhibition of another enzyme, glycogen synthase kinase-3 (GSK3), was also shown to enhance ESC self-renewal (Sato et al., 2004). Recent developments have enabled the derivation of ESCs in defined serum-free medium supplemented with two small-molecule kinase inhibitors (2i) (Ying et al., 2008): PD0325901 blocks differentiation via the MAP kinase pathway and CHIR99021 enhances self-renewal of ESCs by activating Wnt signaling (Wray et al., 2010; Ying et al., 2008). ESCs grown in 2i are more homogeneous in morphology and gene expression than serum ESCs, and are postulated to represent the ground state of pluripotency (reviewed in (Marks and Stunnenberg, 2014)). Recent studies have shown that the epigenome and transcriptome of 2i and serum ESCs are markedly different, suggesting that these ESCs represent two distinct states of pluripotency regulated by different factors and pathways. There is growing evidence that the 2i ESCs closely parallel the early blastocyst cells of the inner cell mass (ICM) or even earlier stages, while serum cells possibly reflect later stages.

Successful derivations have also been reported from morulae and even from isolated eight-cell stage blastomeres, leading to the suggestion that ESCs might represent a very early stage of development (Tesar et al., 2007). Embryo derived stem cells can be derived from pre- and early post-implantation stages of an

embryo. Pluripotent stem cells generated from postimplantation epiblast (E5.5-6.5) are called epiblast stem cells (EpiSCs). These can generate teratocarcinomas but do not contribute effectively to blastocyst chimeras (Hayashi et al., 2011). Embryonic germ (EG) cells are pluripotent stem cells derived from primordial germ cells (PGCs) from early somite-stage embryos (E7.5-13.5) (Matsui et al., 1992). Once established, EG cells are indistinguishable from ESCs apart from a variable degree of imprint erasure. Similar to primordial germ cells, it is possible to convert spermatogonial stem cells into pluripotent stem cells by exposing them to an appropriate regime of in vitro stimuli (Kanatsu-Shinohara et al., 2004) (reviewed in (Nichols and Smith, 2012)).

Somatic cells can acquire the ESC properties trough nuclear reprogramming. Over the last two decades, there have been several approaches towards efficient and successful reprogramming. Nuclear transplantation (NT), also referred to as somatic cell nuclear transfer (SCNT), denotes the introduction of a nucleus from a donor somatic cell into an enucleated oocyte (Wilmut et al., 1997). NT demonstrated that the epigenetic state of terminally differentiated cells is not irreversibly fixed but can be reprogrammed to a pluripotent state that is capable of directing development of a new organism. Another approach of epigenetic reprogramming of somatic nuclei to an undifferentiated state has been demonstrated by fusion of embryonic cells with somatic cells. This method indicated that the pluripotent phenotype is dominant in such fusion products since hybrids between various somatic and embryonic cells shared many features with the parental embryonic cells (Zwaka and Thomson, 2005).

In 2006, Takahashi and Yamanaka achieved a significant breakthrough in

reprogramming somatic cells back to an ES-like state when they successfully reprogrammed mouse embryonic fibroblasts (MEFs) and adult fibroblasts to pluripotent ES-like cells after the forced expression of only four transcription factors Oct4, Sox2, c-Myc, and Klf4 (Takahashi and Yamanaka, 2006). Successful generation of pluripotent cells, named induced pluripotent stem cells (iPSC), using this technology has opened the doors to the disease modeling strategies and cell transplantation studies. iPSC have drawn special attention to both the public and scientific community because they avoid the handling of embryonic material and can be patient tailored (reviewed in (Liang and Zhang, 2013)).

The progression of pluripotent or undifferentiated ES cells to a differentiated phenotype is regulated by changes in gene expression, in which, genes that are responsible for self-renewal are down-regulated while lineage-specific genes are up-regulated. The mechanisms by which ES cells maintain their pluripotency are thought to be orchestrated by several crucial factors: extracellular signaling, transcription factor networks and epigenetic factors.

1.2.1 Extracellular signaling in pluripotency and self-renewal

Several key extracellular signaling pathways have been identified to be crucial in maintenance of pluripotency and self-renewal of ES cells. The extracellular signaling cascades are known to regulate ES cell pluripotency via two different mechanisms: targeting core pluripotency transcription factors and targeting cell cycle progression - related genes. Leukemia inhibitory factor (LIF), a member of

the IL6 family, binds to leukemia inhibitory factor receptor (LIFR) that subsequently heterodimerizes with gp130 receptor forming a trimeric complex, which triggers three different signaling pathways: the JAK (Janus Kinase)/STAT3 (signal transducer and activator of transcription 3), the PI3K (phosphoinositide 3 kinase)/AKT pathway and SHP2 (SH2 domain containing tyrosine phosphatase 2)/MAPK (mitogen activated protein kinase) pathway. These three pathways influence self-renewal, propagation and differentiation, respectively (reviewed in (Burdon, 2002)). Other important signaling cascades involved in ES cells are Wnt/b-catenin signaling, bone morphogenic protein (BMP) signaling, fibroblast growth factor 4 (Fgf4) signaling and TGF-b/Activin signaling.

1.2.2 Transcriptional network to maintain pluripotency

A unique network of inter-related transcription factors characterizes the ESC state. Indeed, a large scale RNAi mediated knockdown study identified 8 genes that are crucial for maintaining the undifferentiated state of ES cells, of which 7 are transcription factors or chromatin associated proteins: Oct4, Nanog, Sox2, Tbx3, Esrrb, Tcl1 and Dppa4 (Ivanova et al., 2006).

Oct4 is one of the key components of the molecular circuitry regulating embryonic stem cell proliferation and differentiation. Oct4 (encoded by the *Pou5f1* gene) belongs to the Pit-Oct-Unc (POU) family of transcription factors that have two DNA binding domains. During mouse embryo development Oct4 is exclusively expressed within the totipotent mouse blastomeres, pluripotent epiblast as well as primodial germ cells (PGCs) (Rosner et al., 1990; Scholer et al., 1990). Sox2 is a member of high mobility group (HMG) box DNA binding domain proteins. It is

expressed within the ICM and extraembryonic ectoderm of pre-implantation blastocysts (Avilion et al., 2003). Importantly, both proteins have critical roles in the establishment and maintenance of pluripotency, as *Pou5f1*- and *Sox2*-null embryos do not form a pluripotent ICM, but rather, differentiate into trophectodermal tissue (Avilion et al., 2003; Masui et al., 2007). This similarity of phenotypes produced by Sox2 and Oct4 loss is attributed to the synergistic action of Oct4/Sox2 in the regulation of various ESC-specific genes, including themselves. Nanog, the third member of the core ESC transcription factors, sustains mESC self-renewal in the absence of leukemia inhibitor factor (LIF) (Mitsui et al., 2003; Wang et al., 2006). Since nanog-null pre-implantation embryos do not possess a pluripotent ICM, it is believed to be necessary the acquisition of pluripotency (Mitsui et al., 2003; Silva et al., 2009). Nanog-null mESCs are pluripotent, although prone to differentiation, making Nanog dispensable once pluripotency is achieved (Chambers et al., 2007; Mitsui et al., 2003) (reviewed in (Yeo and Ng, 2013)).

The accurate regulation of these TFs is crucial, as their over or under-expression would affect ES cell identity and differentiation state. Studies mapping genomic-binding sites of these core ESC factors revealed extensive Oct4, Sox2 and Nanog cobinding at their own promoters, at numerous active, as well as silent genomic target sites (Loh et al., 2006). It was proposed that the core ESC transcription factors serve to establish a pluripotent state by, on one side, activating the expression of other pluripotency-associated factors while simultaneously repressing lineage-specific genes, and on the other side, by activating their own gene expression and that of each other in an interconnected auto-regulatory loop

(reviewed in (Young, 2011)). Importantly, this model may account for how ESCs can sustain pluripotency, while remaining poised for differentiation.

1.2.3 Chromatin organization and epigenetic factors in pluripotency

Studies of gene regulation in pluripotency and self-renewal initially focused on TF network regulation, until the importance of epigenetic and chromatin mediated mechanisms has been highlighted in ESC pluripotency, differentiation and early development (Reik, 2007).

The chromatin of pluripotent stem cells is believed to have unique characteristics, including elevated transcription, an open conformation and a hyperdynamic association of chromatin proteins, reflecting the plasticity of the genome in pluripotent cells (Meshorer and Misteli, 2006) and likely contributing to the maintenance of pluripotency and self-renewal (Jorgensen et al., 2007; Meshorer et al., 2006). The global levels of nascent RNA and mRNA were reported to be almost two-fold higher in ESC than in their differentiated counterparts. Undifferentiated cells transcribe repetitive elements that are normally silenced in somatic cells and intergenic regions, whereas tissue-specific genes are transcribed at very low levels (Efroni et al., 2008). Many of the transcripts residing from intronic or intergenic regions may act as noncoding RNAs that regulate pluripotency (reviewed in (Mattout and Meshorer, 2010b)).

The majority of ESC chromatin is homogeneously dispersed and largely devoid of condensed regions, whereas in differentiated cells chromatin appears heterogeneous with distinct blocks of compaction (Efroni et al., 2008).

Undifferentiated ESCs contain less heterochromatic regions with some chromatin structural proteins (e.g. Heterochromatin protein 1 HP1, histones H2A and H3) binding less tightly compared to lineage-committed cells (Jorgensen et al., 2007). General transcription factors and chromatin remodelling proteins are overexpressed in ESCs compared to ESC-derived lineage- restricted neural progenitors (NPs) (Meshorer et al., 2006). ESC chromatin is transcriptionally permissive, with low-level stochastic transcription of lineage-restricted genes and normally silent DNA repeat regions, increased nuclease sensitivity, and an abundance of histone modifications associated with transcription (e.g. H3K9ac, H3K4me3, H3K36me3). Knockdown of the chromatin remodeler Chd1 in mouse ESCs causes heterochromatin accumulation and skewed differentiation, suggesting that the 'open' chromatin structure of ESCs is functionally relevant (Gaspar-Maia et al., 2009).

The genome of early blastocyst cells of the ICM E3.5 is hyopmethylated with average of CpG methylation levels of ~20%, and only a few days later (E6.5), the genome methylation increases with average levels reaching ~70%. A high similarity has been reported between the hypomethylated E3.5 blastocyst cells and 2i ground state ESCs, whereas serum ESCs resemble hypermethylated E6.5 blastocyst cells (Habibi et al., 2013). During neural induction, several hundred genes, including stem cell specific genes, acquire CpG methylation and become transcriptionally silenced. The observation that most DNA methylation is acquired by ESC-derived neural precursors rather than upon subsequent differentiation to terminal neurons, suggests that changes occur in the transition from pluripotent to lineage-committed progenitors, a concept echoed by studies of adult stem cells (reviewed in (Fisher and Fisher, 2011)). Together, these results paint a broad

picture of chromatin in pluripotent ESCs that is open, transcriptionally permissive and hyperdynamic, with progression to a more compact and transcriptionally repressed state.

Alterations in chromatin organization within the nucleus may also be relevant for gene regulation during differentiation. Using the DamID technique, sequence scale genomic contacts with the nuclear lamina at the periphery (termed LADS) have been mapped in ESCs and differentiated cells (Peric-Hupkes et al., 2010). LADS tend to be gene-poor but contain minimally expressed genes within regions marked by the repressive histone modifications H3K9me2 and H3K27me3. Differentiation of mouse ESCs to multipotent neural progenitors (NPs) then to terminal astrocytes revealed many regions undergo cell type specific relocations, and these movements appear to be orchestrated in a stepwise fashion. Pluripotency genes including Oct4 and Nanog move to the nuclear lamina and are silenced while neural-lineage specific genes disassociate from the lamina and are induced. Genome-wide ChIP analyses have described large organised chromatin domains of H3K9me2 (termed LOCKS) that increase in size and abundance (from 4% to at most 46% genome coverage) from ESCs to differentiated cells (Wen et al., 2009). LOCKS show tissue-specific distributions and inversely correlate with gene expression, suggestive of a ‘locking-down’ of transcription from unneeded genomic regions.

Two of the main residents of constitutive heterochromatin are the major and minor satellite repeat sequences, which are commonly methylated and located in centromeric regions of the genome. Major satellite repeats seem to localize diffusely in ESC nuclei and form well-defined chromocenters in NPCs (Meshorer et al., 2006). Interestingly, major and minor satellite repeats, as well as other

repetitive sequences, which are normally repressed in differentiated cells, are highly transcribed in mouse ESCs and become associated with heterochromatin-related histone modifications after differentiation (reviewed in (Mattout and Meshorer, 2010a)). Along the same lines, telomeric chromatin is associated with increasing levels of H3K9me3 and H4K20me3 and reduced sensitivity to micrococcal nuclease (MNase) digestion during ESC differentiation (Wong et al., 2009). These studies indicate that chromatin organization is profoundly different in ESCs, and that this apparent open configuration may lead to transcriptional activity of heterochromatin domains.

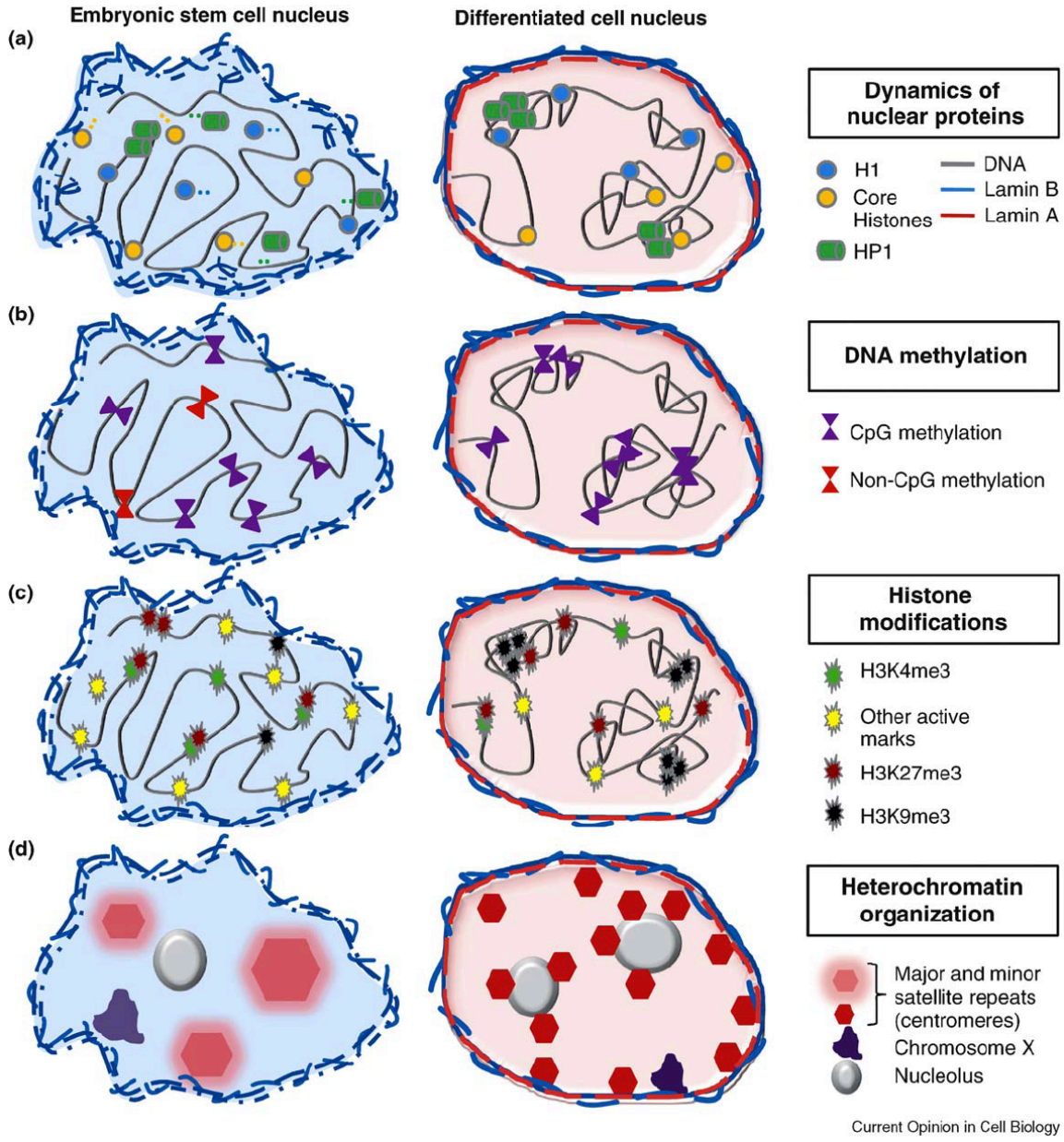

Figure 1. A schematic view of chromatin and genome characteristics in ESCs and in early differentiation. (a) Chromatin protein dynamics. Chromatin proteins such as the linker histone H1 and core histones are more dynamically associated with chromatin in ESCs than in differentiated cells. HP1a and lamin B nuclear proteins also bind more loosely in pluripotent cells. Lamin A expression and localization in the nuclear lamina occur during early differentiation. (b) DNA methylation. In mammalian somatic cells, DNA methylation is present on cytosines in a CpG context. In pluripotent ESCs, 25% of the cytosine methylation sites in the genome are found in a non-CpG context, suggesting that ESCs utilize a unique DNA methylation program. (c) Histone modifications. The global levels of several histone modifications differ between ESCs and differentiated cells. This includes several active marks which are more abundant in ESCs, and repressive marks which are enriched in differentiated

cells, and which accumulate in well-defined foci (H3K9me3). Bivalent marks (H3K4me3 together with H3K27me3) are found on promoters of developmentally regulated genes in ESCs, some of which resolve into a single modification in differentiated cells. (d) Centromeric heterochromatin. Major and minor satellite DNA repeats which are normally found at the heterochromatic centric and pericentric regions, are dispersed in ESCs, but form dense foci upon differentiation. Accordingly, centromeres are redistributed next to nucleoli and the nuclear periphery in differentiated cells. The inactive X chromosome in female somatic cells which is represented in the scheme is also repositioned next to the nuclear envelope. Telomeric chromatin is apparently not displaced in the nucleus, but in ESCs it has a more open structure. Adapted from (Mattout and Meshorer, 2010)

Two key histone modifications that are heavily involved in ESC regulation are H3K4me3 and H3K27me3, which are typically associated with active and repressive chromatin regions, respectively. A major discovery in ESC biology was the co-occupancy of both H3K4me3 and H3K27me3 on large number of promoter sequences (Bernstein et al., 2006; Mikkelsen et al., 2007). These regions are named “bivalent” domains and are thought to silence developmental regulatory genes and prevent premature differentiation by keeping genes in a poised state, ready to be either transcribed or repressed. Upon differentiation, most of the bivalent patterns of histone modification are erased to induce activation of specific lineage developmental genes (retaining of H3K4 methylation) and release of the H3K27me3 repressive mark (reviewed in (Gaspar-Maia et al., 2011)).

1.3 The nucleolus

The most prominent substructure within the nucleus is the nucleolus (from Latin, diminutive of nucleus). Although of small size, the nucleolus is a very productive compartment where ribosome biogenesis takes place. This process includes transcription of hundreds ribosomal RNA (rRNA) genes, rRNA processing, and ribosome subunit assembly. To meet the enormous demand for proteins, growing cells have as many as ten million ribosomes and the nucleolus must have sufficient capacity to fulfill the need for large-scale production of ribosomes at a rapid pace (Olson, 2011). Because of this enormous task, in the past 40-50 years, the major aim of research was to define the components and key steps in the ribosome synthesis and it was not suspected that the nucleolus could do much else. Consequently, the nucleolus managed to keep its other functions undercover for a while (Guetg and Santoro, 2012).

1.3.1 Ribosomal RNA (rRNA) genes

In eukaryotic cells, the most active site of gene transcription is the nucleolus. To produce an elevated number of ribosomes, cells evolved a unique and efficient transcription system by using a specific and efficient RNA polymerase (RNA polymerase I, Pol I) and by amplifying the number of rRNA genes to hundreds or even thousands of copies per genome (Santoro, 2011). Consequently, the presence of many rRNA genes transcribing at high rate has the ability to fulfil the requirement to generate an elevated number of rRNA moieties to meet the enormous demand of ribosome production.

The nucleolus results from the fusion of several nucleolar organizing regions

(Morin et al.), which consist of tandemly repeated ribosomal RNA genes (reviewed in(Santoro, 2005)). In human, the 200 rDNA copies are located in a non-uniform manner between the short arm and the satellite body of the five acrocentric chromosomes 13, 14, 15, 21 and 26, in a telomere-to-centromer orientation (Henderson et al., 1972). In mouse, rDNA repeats are within the centromeric regions of chromosome 12, 15, 16, 18 and 19 (Dev et al., 1977; Henderson et al., 1972; Kurihara et al., 1994a). The positioning of NORs on the short arms of acrocentric chromosomes was proposed to isolate rDNA units from genes transcribed by Pol II and Pol III.

Mammalian rDNA transcription units are large, comprising ~43 kb in humans and ~45 kb in mice (Gonzalez and Sylvester, 1995; Grozdanov et al., 2003). Sequences encoding pre-rRNA (13–14 kb) are separated by long intergenic spacers (IGSs) of approximately 30 kb. Regulatory elements, including gene promoters, spacer promoters, repetitive enhancer elements, and transcription terminators, are located in the IGS (Figure 2). The rDNA promoter has a bipartite structure, consisting of a core promoter element adjacent to the transcription start site and an upstream control element (UCE) approximately 100 nucleotides further upstream (Haltiner et al., 1986; Learned et al., 1986). Mammalian rDNA transcription units are flanked at their 5' and 3' ends by one or more terminator elements that are recognized by TTF-I (transcription termination factor), a specific DNA binding protein that stops elongating Pol I and serves an important role in epigenetic regulation of rRNA genes (Grummt et al., 1986a; Grummt et al., 1985; Henderson and Sollner-Webb, 1986). The major part of the IGS appears to be devoid of regulatory elements, comprising a high density of simple sequence repeats and transposable elements (reviewed in (Sylvester et al., 2004)).

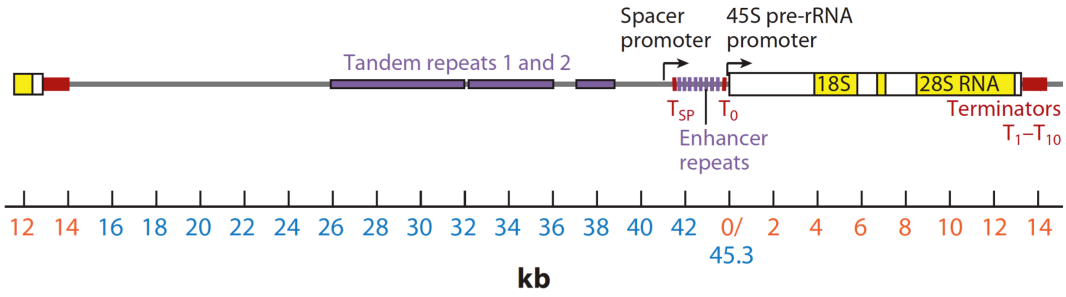

Figure 2. Structural organization of mouse rRNA gene. Graphic of mouse rRNA genes is derived from Genbank accession number BK000964. The sites of transcription initiation of the 45S pre-rRNA and transcripts from the intergenic spacer promoter are indicated by arrows. Scale bars (in kb) are shown below; 0 kb indicates the 5′ end of the pre-rRNA. Terminator elements located downstream of the transcription unit (T1–T10), downstream of the spacer promoter (TSP), and upstream of the gene promoter (T0) are marked by red bars. Repetitive enhancer elements (*purple*) located between the spacer promoter and major gene promoter of the mouse gene promoter are also indicated. Adapted from (McStay and Grummt, 2008).

Transcription of rDNA by Pol I requires the formation of a preinitiation complex on the promoter, including binding of UBF (upstream binding factor) and the promoter selectivity factor, termed SL1 in humans and TIFIB in the mouse (Clos et al., 1986; Grummt, 2003; Moss et al., 2007). UBF affects Pol I transcription at multiple levels, functioning as a transcription activator (Bell et al., 1988; Panov et al., 2006), as an antirepressor (Kuhn and Grummt, 1992; Pelletier et al., 2000) and as a regulator of transcription elongation (Stefanovsky et al., 2006). Promoter specificity is conferred by SL1/TIF-IB, a ~300-kDa protein complex that contains TBP (TATA box binding protein) and at least three Pol I-specific TBP-associated factors (TAFIs), TAFI110/95, TAFI68, and TAFI48 (Comai et al., 1992; Heix et al., 1997; Zomerdijk et al., 1994). TAFIs perform important roles in transcription complex assembly, mediating specific interactions between the rDNA promoter

and Pol I. They interact with UBF and recruit Pol I to rDNA by binding to TIFIA, a basal regulatory factor that is associated with the initiation-competent subpopulation of Pol I (Pol I**β**). Another important Pol I factor is TTF-I (transcription termination factor I), a multifunctional protein that binds to specific terminator elements (T_1 - T_{10}) downstream of the transcription unit and mediates transcription termination and replication fork arrest (Grummt et al., 1986b). A similar sequence element, defined as T_0 is located immediately upstream of the ribosomal gene promoter. The conservation of a binding site for a Pol I transcription terminator protein adjacent to the gene promoter suggested that TTF-I may also exert some essential function in transcription regulation. Indeed, binding of TTF-I to the promoter-proximal terminator was to stimulate *in vitro* transcription of chromatinized rDNA templates by affecting rDNA nucleosomal positioning and occupancy at the rDNA promoter (Henderson and Sollner-Webb, 1986; Langst et al., 1997b). On the other hand, TTF-1 was also shown to bind to and to recruit the repressor protein TIP5 that is a key factor for the establishment of rDNA silencing (see **1.3.4**).

1.3.2 Intergenic ribosomal RNA (IGS-rRNA) transcription

In rats, mice, *Drosophila* and *Xenopus*, the IGS region contains one or more Pol I promoters (spacer promoters) that share sequence homology to the core region of the main rDNA promoter (De Winter and Moss, 1986; Grimaldi and Di Nocera, 1988b; Kuhn and Grummt, 1987; Labhart and Reeder, 1984). Recently, intergenic spacer rRNA transcripts (IGS rRNA) were shown to have a crucial function in rDNA silencing. In mice, intergenic transcripts originating from the spacer promoter that locates approximately 2 kb upstream from the pre-rRNA start site

are processed into a heterogeneous population of 200–250 nucleotide RNAs, dubbed promoter RNA (pRNA) as their sequence matches the rDNA promoter (Mayer et al., 2006). The pRNA associates with nucleolar remodeling complex (NoRC, described in **1.3.4**), thereby maintaining silencing of rDNA chromatin (Santoro et al., 2010b). IGS transcripts are rare, being 1,000-fold less abundant than pre-rRNA. The spacer promoter and the main gene promoter have some sequence homology, binding of TIF-IB/SL1 and the Pol I-associated factor TIF-IA is slightly decreased at the spacer promoter while Pol I is three-fold more abundant at spacer promoter than main gene promoter (Santoro et al., 2010a). The differences in IGS and pre-rRNA levels can be probably ascribed either to stalled Pol I at the spacer promoter or to rapid degradation, as suggested by data showing that binding to NoRC stabilizes pRNA (Mayer et al., 2006). Recent results indicated two additional factors that can lead to low IGS rRNA abundance (Santoro et al., 2010a). IGS rRNA synthesis was shown to occur during a restricted time window of S phase (early) and to originate from a specific set of active and hypomethylated rRNA genes that contain 9 enhancer repeats located between the spacer and the main gene promoter. These spacer transcripts are then processed during mid to late S phase to yield pRNA that is indispensable for establishment of silent rDNA chromatin mediated by NoRC (Santoro et al., 2010a).

The finding that transcripts from the spacer promoter have an indispensable function in epigenetic silencing of rDNA is in apparent disagreement with previous studies showing that spacer promoter enhances transcription from the main rDNA promoter (Caudy and Pikaard, 2002; De Winter and Moss, 1986; Grimaldi and Di Nocera, 1988a; Paalman et al., 1995; Putnam and Pikaard, 1992; Tower et al.,

1989). In the “read-through enhancement” model, it was proposed that Pol I molecules, which are directed by the spacer promoter to transcribe through the enhancer, release rDNA transcription factors from the enhancer and make them available to the gene promoter, thereby stimulating gene promoter transcription (De Winter and Moss, 1987). A corollary of read-through enhancement models is that the spacer promoter must act to somehow amplify or increase the effect exerted by the enhancer repeats alone and that the level of stimulation is proportional to the transcriptional strength of the spacer promoter. However, replacement of mouse spacer promoter by the much more active Chinese hamster spacer promoter did not change the level of gene promoter stimulation (Paalman et al., 1995). According to these results, enhancement of pre-rRNA synthesis does not depend from transcripts originating from spacer promoter and imply that spacer promoter affects the main gene promoter using alternative mechanisms. One possibility is formation of a loop between the spacer promoter and the main gene promoter similar to that one described to occur between rDNA main promoter and terminator regions (Nemeth et al., 2008). The spatial juxtaposition of both promoters might enhance transcription from the main gene promoter by delivering Pol I factors and it would not require IGS rRNA synthesis. Consistent with this, recent results identified binding of CTCF and enrichment of the histone variant H2A.Z at the spacer promoter (van de Nobelen et al., 2010). CTCF is a conserved and ubiquitously expressed protein, which binds DNA and organizes chromatin into loops (Phillips and Corces, 2009) while H2A.Z is a mark associated with “poised” promoters (Fan et al., 2002). Loop formation within the IGS rDNA can be also mediated *via* dimerization of TTF1 bound to terminator elements T0 and T-1, located upstream of the transcription start site of the main

gene promoter and downstream of the spacer promoter, respectively (R.S., unpublished data). Involvement of TTF-1 in a structure mediating interaction between the main gene promoter and the 3'-rDNA region has also been recently proposed (Nemeth et al., 2008). The involvement of TTF-1 in forming the spacer-main gene promoter loop not only suggests that IGS rRNA synthesis is not required but that it might not occur at all. The major obstacle that Pol I would encounter in transcribing IGS rDNA is TTF1 that, if bound to T0 and T-1 elements, might prematurely terminate IGS rRNA transcripts. Thus, when IGS rRNA is synthesized, TTF1 should not be bound to either T0 and/or T-1 elements. As binding of TTF1 to T0 is a prerequisite for 45S pre-rRNA synthesis (Langst et al., 1998), it is unlikely that transcription from spacer promoter enhances the strength of the main gene promoter in the absence of TTF1. Whether and how binding of TTF1 to T0 and T-1 is abrogated during synthesis of IGS rRNA in early S phase, it remains an issue to be investigated. Taken together, all these observations suggest that the dual role of spacer promoter in regulating rRNA transcription can be distinguished by its capacity either to form a loop or to drive IGS rRNA synthesis: in the first case, it stimulates pre-rRNA synthesis; in the second case, it is required for NoRC-mediated rDNA silencing (see also **1.3.4**).

1.3.3 Structure and Epigenetic features of rDNA

One of the earliest and yet still highly informative methods of studying eukaryotic gene expression, is by direct electron microscopic visualization of the transcribing chromatin (Miller and Beatty, 1969). In *S. cerevisiae*, due to their ease of identification, rRNA genes are the most amenable to study in Miller spreads. When spread native rDNA chromatin is visualized, two kinds of rRNA gene units

can be observed: 1- transcribing rRNA genes (active copies) that have a characteristic tree-like appearance (referred as “Christmas tree”), with a DNA "trunk" from which close-packed ribonucleoprotein "branches" of increasing length extend; 2- genes that do not associate with Pol I and are not transcribed (silent copies). Although the genome complexity of higher eukaryotes does not yet allow visualization of rDNA chromatin by Miller spreads, later biochemical studies assessed that the coexistence of active and silent rRNA genes in each cell is not limited to *S.cerevisiae*. Differences in chromatin composition between mammalian active and silent rRNA genes was initially explored by *in vivo* crosslinking analysis of Friend cells using psoralen, an intercalating drug that can introduce crosslinks into DNA sites that are not protected by nucleosomes (Conconi et al., 1989; Sogo et al., 1984). Using this method, it was demonstrated that two distinct types of ribosomal chromatin coexist in each cell. The fraction of rRNA genes inaccessible to psoralen (f-band) contains nucleosomes while the rDNA units accessible to psoralen (s-band) display a chromatin structure free of regularly spaced nucleosomes. The demonstration that nascent rRNA is selectively associated with the heavily psoralen-cross-linked s-band led to the conclusion that the nucleosome-free fraction of rDNA is actively transcribed *in vivo* (active genes) and nucleosomal rDNA fraction corresponds to silent genes (Conconi et al., 1989).

Further studies demonstrated that active and silent rRNA genes are also characterized by different epigenetic marks. CpG methylation, an epigenetic mark associated with heritable gene silencing and heterochromatic structures, was found enriched in the rDNA chromatin fraction inaccessible to psoralen (silent genes) and absent from rDNA units accessible to psoralen (active genes) (Stancheva et al., 1997). Later studies demonstrated a direct role of DNA

methylation in repressing rRNA transcription. Treatment of mouse and human cells with 5-azacytidine, an inhibitor of cytosine methylation, increased 45S pre-rRNA levels, suggesting that lack of DNA methylation alleviates transcriptional repression of the corresponding fraction of silent rRNA genes (Santoro and Grummt, 2001). Notably, methylation-dependent transcriptional silencing could be reproduced *in vitro* but only when methylated rDNA templates were assembled into chromatin. Conversely, transcription on naked rDNA templates was not affected, a finding that implies that CpG methylation operates structural changes on rDNA chromatin that are incompatible for transcription. The repressive action of DNA methylation on rRNA transcription was ascribed to few critical CpGs within the rDNA promoter region. In mouse, methylation of a single CpG within the UCE (upstream control element) of rDNA promoter located at -133 impairs binding of the Pol I transcription factor UBF (upstream binding factor) to rDNA chromatin, thereby preventing initiation complex formation. Consistent with this, methylation of one single HpaII site (CCGG), located in the rat promoter region of silent rDNA chromatin inaccessible to psoralen crosslinking, showed particularly strong correlation with the repressed transcriptional state (Stancheva et al., 1997). The correlation between rDNA methylation and transcriptional silencing is further supported by studies in tumours where rRNA transcription is usually upregulated. Hypomethylation of the rRNA genes has been observed in lung cancer, Wilms tumor and hepatocellular carcinoma (Ghoshal et al., 2004; Powell et al., 2002; Qu et al., 1999; Shiraishi et al., 1999).

The finding that the fraction of silent rRNA genes is enriched in CpG methylated sequences made possible to analyze the composition of silent and active rDNA chromatin in higher eukaryotes and plants. An assay based on chromatin

immunoprecipitation (ChIP) coupled to CpG methylation measurement (ChIP-chop) was developed (Santoro et al., 2002), allowing to identify protein factors, including posttranslational modified histones, that bind either to active (i.e. lack of meCpG) or to silent (i.e. enriched in meCpGs) genes. Using this approach, several studies showed that the promoter of mouse and human active rRNA genes associated with Pol I transcription factors and with histones modified with active marks (i.e. H4Ac and H3K4me2) (Santoro and Grummt, 2005; Santoro et al., 2002). In contrast, silent rRNA genes are associated with the heterochromatin protein 1 (HP1) and with histones modified with silent marks like H3K9me2, H3K27me3, H4K20me3 (Santoro and Grummt, 2001, 2005; Santoro et al., 2002). A similar epigenetic pattern was also described in plants (Lawrence et al., 2004). Thus, active and silent rRNA genes are demarcated both by their pattern of DNA methylation and by specific posttranslational modified histones (**Figure 3**).

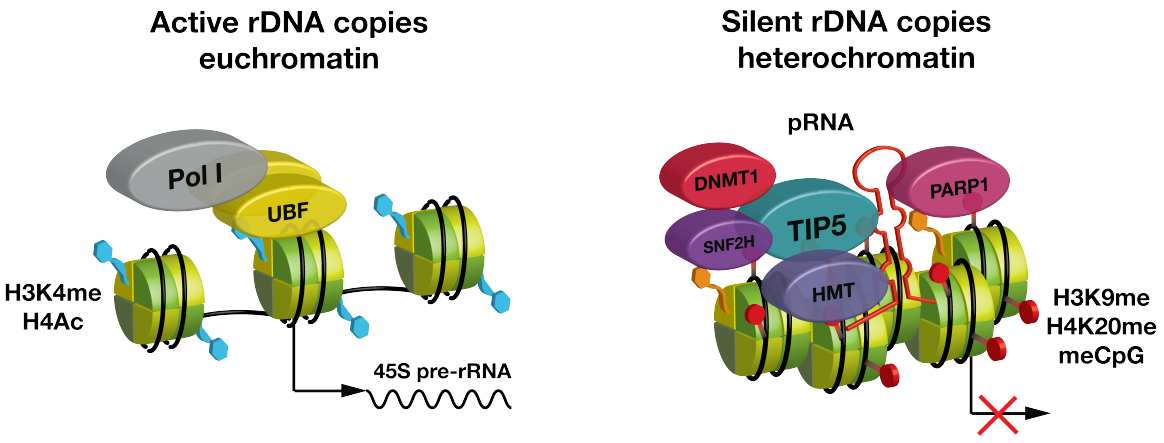

Figure 3. Model: Active and silent rRNA genes

Another important feature that distinguishes active from silent rRNA genes is the replication timing. In mouse and human cells, rRNA genes are replicated in a biphasic manner: the active rRNA genes replicate early, whereas silent rDNA

arrays replicate late (Berger et al., 1997; Li et al., 2005). rDNA replication timing is controlled allelically, with one allele replicating early and one replicating late in almost every cell (Schlesinger et al., 2009). Although the mechanisms of inheritance of active rDNA chromatin remain still elusive, the identification of the nucleolar remodeling complex NoRC led to important advances in the elucidation of the mechanisms controlling maintenance of silent rDNA chromatin in mammals (Santoro et al., 2002; Strohner et al., 2001) (see **1.3.4**).

1.3.4 NoRC complex

A yeast two-hybrid screen searching for TTFI- interacting proteins that have the potential to alter the chromatin structure of the rDNA promoter has identified a chromatin remodeling complex, termed NoRC (nucleolar remodeling complex), which induces nucleosome sliding in an ATP-dependent and a histone H4 tail–dependent fashion (Strohner et al. 2001). NoRC consists of TIP5 (TTF1-interacting protein 5) and the ATPase SNF2h and is the key determinant in setting heterochromatic and silent features at the rDNA locus during cell division (Li et al., 2005; Santoro et al., 2002; Zhou et al., 2002). TIP5, the largest subunit of NoRC, shares a number of important domains with other subunits of known human remodeling complexes like ACF, WCRF, CHRAC and WICH (Bochar et al., 2000; Bozhenok et al., 2002; Ito et al., 1999; LeRoy et al., 1998; Poot et al., 2000). Such shared domains include a bromodomain, a PHD (plant homeodomain) finger, WAKZ motifs, a BAZ1 and a BAZ2 motif as well as AT-hooks (**Figure 4)**. Initial studies showed that NoRC-mediated rDNA transcriptional repression did not occur in the presence of DNA methylation and histone deacetylase inhibitors,

implicating that NoRC acts by inducing DNA methylation and histone deacetylation at rDNA.

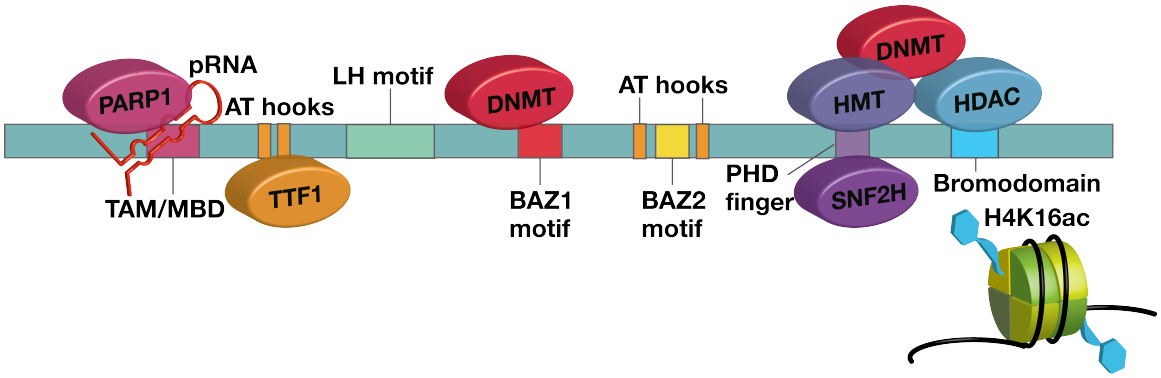

Figure 4. Modular organization and domains of TIP5 (TTF-I-interacting protein 5). Scheme illustrating the modular organization and localization of sequence motifs in TIP5 that have been associated with functions in chromatin structure and function. The domains of TIP5 (*colored boxes*) that interact with proteins involved in the epigenetic control of gene expression are illustrated. The C-terminal part of TIP5 contains a PHD (plant homeodomain) finger that interacts with SNF2h and with histone methyltransferases (HMTs) and a bromodomain that interacts with histone deacetylases (HDAC1 and -2) and with histone H4 acetylated at lysine 16 (H4K16ac). DNA methyltransferases (DNMTs) interact with both the internal and the C-terminal part of TIP5. The MBD (methyl-CpG binding domain)-like TAM (TIP5/ARBD/MBD) domain is required for association with pRNA that in turn mediates the association with the poly(ADP-ribose) polymerase I (PARP1) that is required for NoRC-mediated rDNA heterochromatin formation.

TIP5 was shown to associate with methylated rDNA sequences (Santoro et al., 2002). The association of TIP5 with TTF1 and its dependency on rDNA binding let propose a mechanism of TIP5 targeting to rDNA through DNA-protein recognition, where TTF1 represents the docking protein due to it sequence-specific binding to T0 element (Nemeth et al., 2004; Santoro and Grummt, 2005; Strohner et al., 2001). TIP5 acts as platform for the recruitment of histone-modifying and DNA methylating activities (i.e. HDAC1, SETDB1, SIRT1, MOF, Dnmts) (Santoro and

Grummt, 2005; Santoro et al., 2002; Zhou et al., 2002; Zhou et al., 2009) and represses rRNA transcription. In somatic cells, the association of NoRC with rRNA genes was shown to take place immediately after rDNA replication in late S phase (Li et al., 2005), suggesting a role of NoRC in maintaining the epigenetic and chromatin state of newly duplicated silent rRNA genes. NoRC was shown to position a nucleosome over the rDNA promoter of silent genes (from -132 to +22) (Li et al., 2006). Noteworthy, in this 'inactive' position, the critical CpG dinucleotide at -133, whose methylation prevents binding of UBF, is placed at the 5' boundary of the nucleosome (Santoro and Grummt, 2001). In this position, not hindered by a nucleosome, the CpG-133 would be exposed to methylation mediated by Dnmts associated with NoRC (Santoro et al., 2002). In support of this, impairment of nucleosome remodelling activity of NoRC abrogates transcriptional repression and CpG methylation of an rDNA reporter gene (Santoro and Grummt, 2005).

NoRC function requires the association of TIP5 with the non-coding RNA pRNA (Mayer et al., 2006; Santoro et al., 2010a). Nucleolar retention of TIP5, rDNA methylation and silent histone modifications at rDNA depend on pRNA (Mayer et al., 2006). Importantly, a TIP5 mutant with impaired RNA binding activity (W531G, Y532A) failed to establish rDNA heterochromatin (Mayer et al., 2006). pRNA sequences from nucleotides -127 to -49 in mouse form a conserved hairpin structure that is specifically recognized by the TIP5-TAM domain. Upon pRNA binding, TIP5 undergoes a conformational change that was proposed to facilitate the interaction with other proteins required for rDNA silencing (Mayer et al., 2008). Recently, the poly (ADP-ribose) polymerase I (PARP1) was identified as a TIP5 interacting protein (Guetg et al., 2012). Association of PARP1 with TIP5 is mediated by pRNA and is necessary for the establishment of rDNA

heterochromatic structures. Recruitment of PARP1 occurring at newly synthesized silent rDNA copies and the role of pRNA in this process support the idea that specific non-coding RNA can potentially direct complex patterns of chromatin states at specific genes in a spatially and temporally organized manner.

1.3.5 Nucleolar chromatin

Despite the nucleolus is the most active site of cellular transcription, a shell of highly condensed heterochromatic DNA replicating in mid-late S-phase surrounds the nucleolus of interphase cells (Haaf and Schmid, 1991; Pluta et al., 1995). In mouse, these sequences mainly represent repetitive major satellite (pericentric) and minor satellite (centric) repeats whose maintenance and accurate duplication throughout multiple cell divisions represents a major challenge to ensure genome stability (Guetg et al., 2010). The proximity of these heterochromatic sequences around the nucleolus is partially due to the linear close location next to rRNA repeats. As mentioned, human rRNA genes are located between the short arm and the satellite body of acrocentric chromosomes while mouse rRNA repeats cluster within the centromeric regions of chromosomes 12, 15, 16, 18 and 19 (Dev et al., 1977; Kurihara et al., 1994b). Although the nucleolar proximity of some centromeric heterochromatic repeats can be explained by their linear location close to rRNA repeats (Dev et al., 1977; Kurihara et al., 1994b), other centromeres of chromosomes not containing rRNA genes associate with the nucleolus at a frequency more than that expected for a random distribution (Carvalho et al., 2001), suggesting that the nucleolus might be an attractive compartment of nuclear heterochromatic regions. Similarly, the inactive X-

chromosome was reported to contact the nucleolus during mid-to-late S-phase and this location seems to be required for the duplication of silent chromatin structures(Zhang et al., 2007). The presence of non-nucleolar domains within or close to the nucleolus is also supported by genomic analysis demonstrating that 4% of the entire genome sequences interact with nucleoli of HeLa cells (van Koningsbruggen et al., 2010). These sequences correspond to rDNA, pericentromeric and centromeric repetitive sequences, and to regions with low gene density and significantly enriched in transcriptionally repressed genes (Nemeth et al., 2010; van Koningsbruggen et al., 2010). To note is that lamina associated domains (LADs) that are relatively gene-poor and have a repressive chromatin signature, were also found relocated next to the nucleolus (Kind et al., 2013; Kind and van Steensel, 2010). Therefore, anchoring of heterochromatin at the nucleolus might serve similar functions like the ones described for the nuclear periphery that is responsible for the integrity of mammalian heterochromatin (Pinheiro et al., 2012; Towbin et al., 2012), suggesting interchangeable roles in regulating and maintaining heterochromatic states.

Taken together, these results paint a two-sided picture that represents the nucleolus as the most active site of cellular transcription and, at the same time, the place where heterochromatic repressive structures are retained and most probably maintained.

The coexistence of active and silent rRNA genes might reflect these two opposite functions of the nucleolus. Maintenance of silent rDNA chromatin appears to be necessary for the stability of rRNA genes. In the yeast *S. cerevisiae*, recruitment of the nucleolar protein complexes RENT (regulator of nucleolar silencing and telophase exit) and Cohibin to rDNA suppresses unequal recombination at the

rDNA repeats (Mekhail et al., 2008). This suppression is seemingly linked to the ability of these complexes to induce rDNA silencing. Similarly, segments of rRNA genes and satellite repeat arrays become dispersed in *Drosophila* mutants that are defective in the histone methyltransferase Su(var)3-9, in HP1 (HP1 1, also known as Su(var)2-5) or in several genes involved in the RNA interference (RNAi) pathway (Peng and Karpen, 2007).

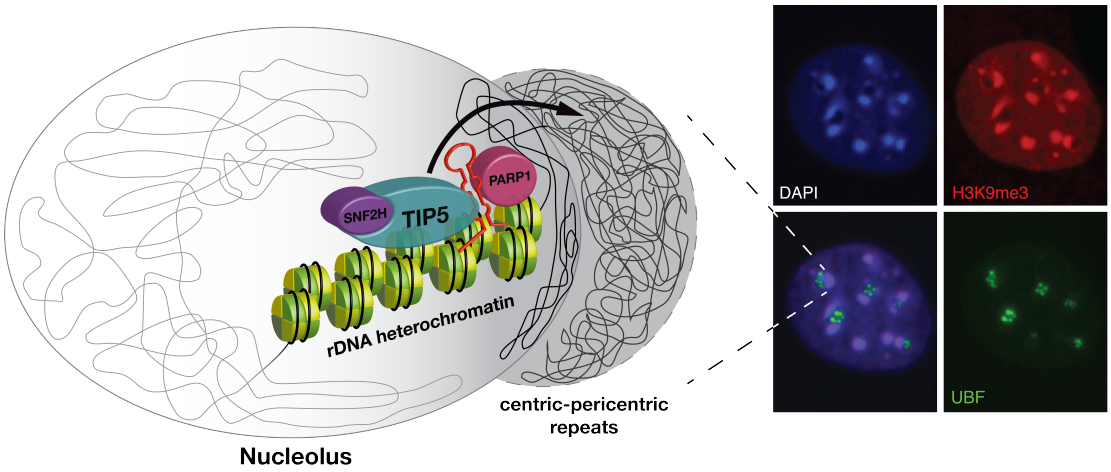

Figure 5. Crosstalk between nucleolar rDNA heterochromatin and nuclear heterochromatin. Right panel. A shell of heterochromatin surrounds the nucleolus. Immunofluorescence of MEF cells showing heterochromatic foci, characterized by H3K9me3 and DAPI staining, located close to nucleoli (visualized by the nucleolar Pol I transcription factor UBF). Left panel. rDNA heterochromatin and its associated components (here shown TIP5, SNF2h, PARP1 and pRNA) influence centric and pericentric heterochromatin located at the nucleolar periphery (Guetg et al., 2010; Guetg et al., 2012). Modified from (Guetg and Santoro, 2012) .

The role of heterochromatic silent rRNA genes seems to go beyond the regulation of rRNA synthesis and rRNA stability by playing important roles at the level of nuclear/nucleolar chromatin architecture. A yeast strain containing a reduced number of rRNA genes that transcribe at high rate to compensate the absence of about 100 copies (143 rRNA repeats in the wild-type strain), yet displays a fraction of 10-20% of silent rDNAs (French et al., 2003; Merz et al., 2008). The

presence of silent rDNA copies in a strain where *bona fide* all rRNA genes should be dedicated to transcription suggests that silent repeats play an indispensable role not necessarily related to transcription. In mouse and human cells, silent rDNA arrays are located in the extranucleolar space, frequently associated with the perinucleolar centromeric heterochromatin (Akhmanova et al., 2000; Mosgöller, 2004), suggesting an intricate relationship between these two types of heterochromatic regions. The establishment of silent rDNA heterochromatin has been recently linked to the formation of centric-pericentric heterochromatin (**Figure 5**). Impairment of the rDNA silencing machinery through depletion of TIP5 denies formation of perinucleolar heterochromatin and decreases heterochromatic marks (i.e. H3K9me3) at major and minor satellite repeats (Guetg et al., 2010). Similarly, overexpression of TIP5 increased H3K9me3 levels at rRNA and centric/pericentric repeats. Also in this case, maintenance of silent rDNA chromatin seems to play an important role for genome stability. TIP5-mediated heterochromatin formation was reported to specifically protect CpG methylated silent rRNA genes from illicit recombination events whereas active genes are not affected. Similarly, genomic instability was also observed at pericentric heterochromatin of cells depleted of TIP5 (Guetg et al., 2010). Centromeric protein CENP-A and major/minor satellites were shown to associate with TIP5 and it was proposed that the spatial and linear closeness of rDNA and satellite sequences may allow TIP5 to interact with centric repeats and aids in establishing heterochromatic structures using similar mechanisms as used to silence the rDNA locus. Alternatively, the influence of TIP5 and silent rRNA genes may affect the centric and pericentric heterochromatin either by spreading mechanisms or by creating a nucleolar/perinucleolar compartment enriched in chromatin repressor

complexes. In both cases, decrease of rDNA silencing after TIP5 depletion would affect the spreading of heterochromatin and reduce the levels of repressor complexes within and nearby the nucleolus. A functional link between rDNA repeats and nuclear heterochromatin could also be observed in *Drosophila*. In this case, rDNA deletions result in reduced heterochromatin-induced gene silencing elsewhere in the genome and the extent of the rDNA deletion correlates with the loss of silencing (Paredes and Maggert, 2009).

2 Aims

Despite sharing the same genome, different cell types from a given organism respond differently to environmental, developmental, or metabolic cues. This variable property is a defining aspect of a cell's identity and is mainly interpreted at the level of epigenetic signature and chromatin structure.

Embryonic stem cells (ESCs) are able to self-renew indefinitely and to differentiate into all cell types of the three germ layers. This dual capacity makes ESCs a potential source for cell and tissue replacement. In order to make these potential clinical applications a reality, intensive research on the mechanisms of pluripotency and ESC differentiation must be carried out.

Chromatin organization and epigenetic signature distinguish pluripotent ESCs from somatic cells. A less compacted chromatin structure and higher levels of euchromatic histone modifications allow ES chromatin to assume a globally more open conformation than in somatic cells. These chromatin properties seem to reflect the plasticity of the genome in ESCs and likely contribute to the maintenance of pluripotency. However, how these changes occur during the ESC differentiation process is not yet clear.

The aim was this work was:

1- to analyze the chromatin and epigenetic signature of rRNA genes in ESCs and during differentiation;
2- to elucidate the mechanisms that control formation of rDNA heterochromatin during stem cell differentiation;
3- to determine whether the epigenetic state of the nucleolus regulates

chromatin plasticity in ESCs and remodelling into heterochromatin upon differentiation.

3 Results

3.1 The epigenetic state of the nucleolus regulates chromatin plasticity and pluripotency of embryonic stem cells

Authors:	Natasa Savic, Dominik Bär, Sergio Leone, Fabienne A. Weber, Eva Vollenweider, Elena Ferrari, Olga Shakhova, Paolo Cinelli, Raffaella Santoro
Journal:	Submitted for publication; under reviewing in Cell Stem Cell
Link:	not yet available
Contribution:	Designing experiments, performance and analysis of the following figures: Fig. 1, Fig. 2A-B, Fig. 3, Fig. 5A-B, Fig. 6, Fig.7, Suppl. Fig. 1, Suppl. Fig. 2, Suppl. Fig. 3B, Suppl. Fig. 5. R.S. supervised the project and wrote the manuscript together with N.S.

3.2 ARTD2 activity is stimulated by RNA

Authors:	Karolin Léger, Dominik Bär, Natasa Savic, Raffaella Santoro and Michael O. Hottiger
Journal:	Nucleic Acids Research 2014 Feb 8. [Epub ahead of print]
Link:	http://nar.oxfordjournals.org/content/early/2014/02/08/nar.gku131.long
Contribution:	Experimental contribution in Figure 4, Analysis of ARTD1 activity by RNA.

3.1 The epigenetic state of the nucleolus regulates chromatin plasticity and pluripotency of embryonic stem cells

Natasa Savic[1,3], Dominik Bär[1], Sergio Leone[1,3], Fabienne A. Weber[2,3], Eva Vollenweider[1,2], Elena Ferrari[1], Olga Shakhova[4], Paolo Cinelli[2,5,6], Raffaella Santoro[1,5*]

[1]Institute of Veterinary Biochemistry and Molecular Biology, University of Zurich [2]Institute of Laboratory Animal Science, University of Zurich [3]Molecular Life Science Program, Life Science Zurich Graduate School, University of Zurich; [4]Cell and Developmental Biology, Institute of Anatomy, University of Zurich, [5]Center for Applied Biotechnology and Molecular Medicine, University of Zurich, Zurich, Switzerland, CH-8057 Zurich; [6]Division of Trauma Surgery, Center for Clinical Research, University Hospital Zurich, CH-8091 Zurich, Switzerland;

*Correspondence: raffaella.santoro@vetbio.uzh.ch

Abstract

Clustering of heterochromatin at nucleoli is a phenomena occurring in many organisms, yet its physiological relevance is poorly understood. Using ncRNA-based strategies to target heterochromatin at nucleoli of embryonic stem cells (ESCs), we investigated whether the nucleolus regulates chromatin plasticity in ESCs and remodelling into heterochromatin upon differentiation. In ESCs, rRNA genes are euchromatic due to the impairment of ncRNA pRNA processing that abrogates recruitment of nucleolar repressor TIP5. Upon differentiation, processing is activated and mature pRNA establishes nucleolar heterochromatin, concurrently with nuclear heterochromatin formation. Tethering heterochromatin at ESC nucleoli through pRNA initiates heterochromatinization of ESC genome, including global H3K9me2 increase and silencing at repetitive sequences like it is found in differentiated cells. Nucleolus-mediated heterochromatic ESCs transcribe differentiation genes and are not longer pluripotent, while inhibition of nucleolar heterochromatin prevents differentiation. Our finding unravelled the nucleolus as a regulator of chromatin plasticity and pluripotency and challenges current view on heterochromatin regulation and function in ESCs.

Introduction

The spatiotemporal organization of the genome in the nucleus is an emerging key player to regulate genome function. The cell nucleus is a highly structured compartment where chromatin is distributed in subdomains based on compaction degree and transcriptional status (Gonzalez-Sandoval et al., 2013; Joffe et al., 2010). Remarkably, transcriptionally silent heterochromatin clusters together at the nuclear periphery and around the nucleolus, suggesting that this spatial distribution may be regulated, and could influence cell activities. ESC chromatin is a global decondensed structure lacking “conventional” constitutive heterochromatin (Efroni et al., 2008; Jorgensen et al., 2007; Melcer et al., 2012; Meshorer et al., 2006). Such a structure correlates with a globally permissive transcriptional state and it has been proposed to contribute to the developmental plasticity and pluripotency of ESC genome that has to have the ability to enter any distinct differentiation pathway (Meshorer and Misteli, 2006). As differentiation advances, large-scale genome silencing takes place and ESC chromatin undergoes structural remodelling toward a highly condensed heterochromatic form (Bhattacharya et al., 2009; Meshorer et al., 2006; Park et al., 2004). Changes in nuclear architecture are characterized by the maturation of centric and pericentric heterochromatin (Aoto et al., 2006; Bartova et al., 2008b; Efroni et al., 2008), formation of large genomic regions enriched in H3K9me2 (LOCKs) (Wen et al., 2009), anchoring of multigene regions at the nuclear periphery (Peric-Hupkes et al., 2010) and clustering of centromeres either at the nucleolus or at the nuclear envelop (Bartova et al., 2008a; Wiblin et al., 2005). However, how ESCs mediate the switch from a lower to a higher order chromatin structure and,

in turn, its spatial distribution within the cell still remains elusive and calls for studies aimed to understand the mechanistic and functional insights of this process.

The nucleolus is the compartment where transcription of hundreds of ribosomal RNA (rRNA) genes, rRNA processing, and ribosome subunit assembly take place (Haaf and Schmid, 1991; Pluta et al., 1995). Clustering of heterochromatin at nucleoli is a phenomenon known to occur in many different organisms and cell types, yet neither the factors involved nor their physiological relevance is understood. Within the nucleolus of somatic cells, a fraction of rRNA genes (about 400 in mouse and human cells) is transcriptionally silent, possesses epigenetic features characteristic of constitutive heterochromatin and is stably inherited independently of cell metabolic activities (Conconi et al., 1989; Santoro and Grummt, 2001; Santoro et al., 2002). In mouse and human cells, silent rDNA arrays are located in the extranucleolar space, frequently associated with centromeric heterochromatin (Akhmanova et al., 2000; Mosgöller, 2004), suggesting an intricate relationship between these two types of heterochromatic regions. TIP5 (TTF1-interacting protein 5), the main subunit of the nucleolar remodeling complex NoRC, establishes rDNA heterochromatin through recruitment of DNA and histone modifier complexes (Guetg et al., 2012; Santoro and Grummt, 2005; Santoro et al., 2002). The activity of TIP5 to form heterochromatin at rDNA requires the association with the long non-coding (lnc)RNA pRNA (Guetg et al., 2012; Mayer et al., 2006; Santoro et al., 2010a). pRNA has been implicated in TIP5 nucleolar retention and the association with rDNA. However, it remains still elusive whether and how pRNA acts as guider for TIP5 recruitment to rDNA.

In this study, we investigated whether the nucleolus is implicated in the open and transcriptional permissive chromatin organization and pluripotency of ESCs and its contribution in the remodelling into heterochromatic structures that occurs upon ESC differentiation. We found that rRNA genes lack heterochromatin in ESCs and acquire epigenetic silent marks upon ESC differentiation, timely coinciding with the maturation of “conventional” constitutive heterochromatic sequences such as centric and pericentric repeats. We determined the mechanistic and functional insights of this process by unravelling an unsuspected role of ncRNA processing in epigenetic and chromatin regulation. We showed that the determinant for the lack of rDNA heterochromatin in ESCs is the impairment of processing of pRNA precursor intergenic spacer (IGS)-rRNA. Upon ESC differentiation processing is activated and produces mature pRNA that has the ability to establish heterochromatin by guiding TIP5 to rDNA through the association of TIP5 with TTF1, which docks the complex at rDNA. In contrast, the unprocessed IGS-rRNA transcript impairs TIP5-TTF1 association and recruitment to rDNA, abolishing formation of rDNA heterochromatin in ESCs. Consistently, addition of mature pRNA in ESCs is sufficient to establish rDNA heterochromatin. Tethering of heterochromatin at nucleoli of ESCs through ectopic mature pRNA initiates structure remodelling of nuclear architecture toward a highly condensed heterochromatic form like it is found in differentiated cells, including a global increase in H3K9me2, transcriptional repression at repetitive sequences, and activation of differentiation genes. Nucleolus-mediated heterochromatic ESC genome is not longer pluripotent, while inhibition of nucleolar heterochromatin through depletion of TIP5 prevents exit from the undifferentiated state. Together the results indicate that the nucleolar chromatin is an important regulator of

nuclear architecture by controlling chromatin plasticity and pluripotency of ESCs. Moreover, the data unravel a further level of complexity of ncRNA regulation and propose RNA processing as a way to modulate distinct and specific features of the same ncRNA.

Results

Establishment of rDNA heterochromatin occurs during ESC differentiation

To determine whether the epigenetic state of the nucleolusis is regulated upon ESC differentiation, we analyzed the rDNA chromatin state during transition of ESCs into neural progenitor cells (NPCs) that are Pax-6 positive and do not express the pluripotency factor Nanog (**Figure 1A**) (Bibel et al., 2004). Previous studies showed that methylation of the two unique CpG dinucleotides at the mouse rDNA promoter is the epigenetic mark that distinguishes active and silent rRNA genes (Santoro and Grummt, 2001). To determine the content of active and silent repeats, we measured CpG methylation at rDNA promoter of ESCs, NPCs and mouse somatic cells from brain tissue using HpaII digestion followed by qPCR, a method that accurately quantifies the amounts of silent, heterochromatic rRNA genes (Santoro et al., 2002). Consistent with a previous bisulfite analysis (Schlesinger et al., 2009), rDNA promoter in ESCs displays very low meCpG levels, confirming the accuracy of our method. After 8 days of differentiation, a fraction of rRNA genes (25-30%) acquired CpG methylation at levels similar to those measured in mouse brain tissue (**Figure 1B**). Similar results were also obtained with a different ESC line and differentiation protocol (**Figure S1A**), suggesting that *de novo* rDNA methylation is a process that takes place during

early ESC differentiation. Consistent with these results, 45S pre-rRNA amounts were lower in NPCs than in ESCs and similar to mouse fibroblast NIH3T3 cells (**Figure1C**). Remarkably, rDNA methylation in induced pluripotent stem cells (iPSC) decreased to about one half when compared to the original fibroblast cells (**Figure 1D**), implying a link between cell pluripotency and rDNA methylation levels. Analysis of heterochromatin-related histone modifications H3K9me2, H3K9me3 and H3K27me3 at rDNA (**Figure 1E, Figure S1B**) revealed that upon differentiation all these histone modifications increased at rDNA promoter and coding regions, indicating that rDNA heterochromatin formation takes place during ESC-NPC transition. Consistent with previous reports showing heterochromatin maturation during ESC differentiation, H3K9me3 levels increased at major and minor satellite repeats (Martens et al., 2005; Meshorer et al., 2006; Wong et al., 2009) while H3K9me2 occupancy was not greatly affected. The increase in heterochromatic marks during ESC-NPC was accompanied by a reduction of transcription levels of major and minor satellites, which are normally repressed in differentiated cells (**Figure S1C**) (Efroni et al., 2008). We conclude that formation of rDNA heterochromatin takes place during ESC-NPC transition and it timely coincides with the switch to a higher condensed heterochromatic form of centric and pericentric repeats.

TIP5 is recruited to rDNA during ESC differentiation

To determine how rDNA heterochromatin is established during ESC differentiation, we measured the association of Pol I upstream binding factor UBF, that exclusively binds to unmethylated active rRNA genes, and of TIP5, which associates with methylated silent rDNA (Santoro and Grummt, 2001; Santoro et

al., 2002). As shown in **Figure 1F**, UBF occupancy at rDNA was lower in NPCs than in ESCs, a further indication that the number of euchromatic active rRNA genes decreases during differentiation. In contrast, TIP5 binds to rDNA only in NPCs but not in ESCs (**Figure 1F**). Similarly, the poly(ADP-ribose)-polymerase-1 (PARP1), previously shown to interact with TIP5 *via* pRNA and implicated in the formation of rDNA heterochromatin (Guetg et al., 2012), increases its association with the rDNA promoter in NPCs. These results indicate that the establishment of rDNA heterochromatin in ESC-NPC transcription is accompanied by a decrease in the association of factors specific to active genes and an increase in the binding of components of the rDNA silencing machinery.

TIP5 protein and mRNA levels were higher in ESCs than in NPCs (**Figure 1G**), implying that the lack of rDNA heterochromatin in ESC and its establishment during ESC differentiation is independent of TIP5 amounts. We then analyzed the cellular localization of TIP5 in mouse embryonic fibroblasts (MEFs), ESCs and NPCs (**Figure 1H**). Consistent with previous results, TIP5 was exclusively localized within nucleoli of somatic MEFs (Strohner et al., 2001). In contrast, the cellular localization of TIP5 in ESCs was predominantly nucleoplasmic and often excluded from the nucleoli. After 8 days of differentiation, TIP5 was drastically reduced in the nucleoplasm and exclusively localized within the nucleoli of NPCs, showing a cellular localization that is characteristic of all somatic cells analyzed so far (**Figure 1H, lower panel**). We conclude that binding of TIP5 to rDNA is impaired in ESCs and its recruitment to rDNA is achieved upon ESC differentiation.

Processing of pRNA mediates formation of rDNA heterochromatin

We reasoned that impairment of TIP5 binding to rDNA might be responsible for the lack of rDNA heterochromatin in ESCs. Previous studies showed that the association of pRNA with TIP5 is required to form rDNA heterochromatin by mediating nucleolar retention of TIP5, the association with rDNA and the interaction with PARP1 (Guetg et al., 2012; Mayer et al., 2006). pRNA is a 250-300 nt transcript complementary to rDNA promoter sequences and derives from the processing of IGS-rRNA whose synthesis is driven by an alternative rDNA promoter that is located 2 kb upstream of the pre-rRNA transcription start site in mouse genome (Mayer et al., 2006; Santoro et al., 2010a) (**Figure 2A**). To analyze whether pRNA is implicated in the lack of rDNA heterochromatin in ESCs, we initially measured pRNA levels in ESCs and at different time points of differentiation by strand specific reverse transcription (RT) (**Figure 2B**). Measurements of pRNA region from -165 to -20 did not reveal remarkable differences between ESCs and NPCs, indicating that formation of rDNA heterochromatin in NPCs does not depend on the amounts of pRNA sequences. Since amplifications of pRNA sequences do not distinguish between IGS-rRNA and mature pRNA, we quantified the levels of unprocessed transcripts by amplifying the 5'- and internal IGS-rRNA regions (**Figure 2B**). Unprocessed transcript levels were higher in ESCs than in NPCs, suggesting that IGS-rRNA processing in ESCs is less efficient than in NPCs. To support these results, we constructed an IGS-rRNA reporter gene plasmid that allows measurements of ectopic IGS-rRNA and pRNA (**Figure 2C, left panel**). We transfected the reporter gene in NIH3T3 cells, previously described to have an efficient IGS-rRNA processing (Santoro et al., 2010a), and in ESCs and measured ectopic pRNA and

IGS-rRNA levels (**Figure 2C**). While ectopic IGS-rRNA was efficiently processed in NIH3T3 cells (80%), maturation of pRNA was strongly reduced in ESCs. Taken together these results indicate that IGS-rRNA is not efficiently processed in ESCs and that it is less abundant in NPCs than in ESCs.

To test whether the lack of IGS-rRNA processing is the determinant that impairs formation of rDNA heterochromatin in ESCs, we transfected *in vitro* synthesized mature pRNA in ESCs and monitored TIP5 cellular localization, rDNA methylation, rRNA transcription, and H3K9me2 and H3K9me3 levels at rDNA (**Figure 3**). In ESCs transfected with pRNA, TIP5 decreased in the nucleoplasm and accumulated within nucleoli, as indicated by the colocalization with the nucleolar protein UBF (**Figure 3A**). Remarkably, ectopic pRNA in ESCs reduced 45S pre-rRNA levels and increased both H3K9me2 and CpG methylation levels at the rDNA promoter (**Figures 3B-D, Figure S2**). The modest increase in CpG methylation (from 1.7% to 4.4%) can be also attributed to the 2i conditions that we used to culture ESCs, recently described to lead to pronounced reduction in DNA methylation due to the downregulation of the *de novo* methyltransferases DNMT3a and DNMT3b (Leitch et al., 2013). Consistent with previous studies showing that TIP5 mediates dimethylation but not trimethylation of H3K9 at rRNA genes (Guetg et al., 2010; Santoro and Grummt, 2005), ectopic pRNA did not increase H3K9me3 levels at rDNA (**Figure 3D**). These results indicate that addition of pRNA in ESCs is sufficient to guide TIP5 to rDNA and to establish rDNA heterochromatin.

To determine how pRNA guides TIP5 to rDNA, we mutated pRNA sequences that were previously implicated in rDNA methylation and TIP5 association in somatic cells (Mayer et al., 2008; Schmitz et al., 2010). First, we transfected ESCs with a

pRNA mutant (pRNAΔT_0) whose sequences corresponding to the T_0 element at the rDNA promoter were replaced with unrelated nucleotides (**Figure 3A**). These sequences were previously described to form dsDNA:RNA triplex, a structure implicated in *de novo* rDNA methylation through recruitment of DNMT3b (Schmitz et al., 2010) and recently proposed as guiding module for TIP5 targeting to rDNA (Bierhoff et al., 2013). However, transfection of pRNAΔT_0 induced recruitment of TIP5 to nucleoli and promoted rDNA methylation as seen in ESCs containing wild-type pRNA (**Figures 3A, B**), indicating that nucleolar targeting of TIP5 and *de novo* rDNA methylation in ESCs is not mediated by rDNA:pRNA triplex. Consistent with these results, replacement of the 5'-pRNA region (Control-pRNA) which includes T_0 element induced TIP5 nucleolar localization (**Figure 3E**). In contrast, replacement of 3'-pRNA sequences (pRNA-Control), previously reported to form a stem-loop structure that is necessary for the association with TIP5 *in vitro* (Mayer et al., 2008), impairs nucleolar localization of TIP5. Remarkably, point mutations that disrupt the stem-loop structure were not efficient in recruiting TIP5 to the nucleoli while a compensatory mutation allowing hairpin formation did it. Together, these results indicate that pRNA guides TIP5 to rDNA in *trans* through the hairpin structure and that addition of mature pRNA in ESCs is sufficient for the establishment of rDNA heterochromatin. We conclude that the impairment of IGS-rRNA processing that abrogates formation of mature pRNA is the major determinant causing the lack of rDNA heterochromatin in ESCs.

TIP5-TTF1 association is mediated by pRNA and impaired by IGS-rRNA

Why is IGS-rRNA unable to promote recruitment of TIP5 to rDNA? We first determined whether TIP5 binds to IGS-rRNA. Recombinant TIP5 was incubated

with nonspecific radiolabeled transcripts (McStay and Grummt), and TIP5/RNA complexes were challenged with increasing amounts of RNA-control, pRNA and IGS-rRNA (**Figure 4A**). Consistent with previous results, pRNA had a higher affinity for TIP5 compared to control RNA (Mayer et al., 2006). Surprisingly, IGS-rRNA not only efficiently competed for TIP5 association but also displayed a higher affinity than pRNA. To determine whether TIP5 has a better binding affinity to other sequences within IGS-rRNA than to pRNA, we compared TIP5 association with pRNA, spacer region and enhancer-repeat RNA. As shown in **Figure S3A**, spacer and enhancer sequences were much less efficiently associated with TIP5 than pRNA, suggesting that TIP5 binds to IGS-rRNA through the pRNA sequences and that upstream sequences might stabilize the complex through weak interactions. Together, these results indicate that TIP5 has the ability to bind to pRNA sequences within IGS-rRNA and suggest that impairment of TIP5 binding to rDNA in ESCs might depend on the context of this interaction.

The experiments described in **Figure 3** showed that TIP5 targeting to rDNA is not mediated by pRNA:rDNA triple helix but depends on the 3'-pRNA region that was previously shown to interact with TIP5 (Mayer et al., 2008). We hypothesized that pRNA binding to TIP5 might favour the association with a docking protein for the recruitment to rDNA promoter sequences and that IGS-rRNA might hinder this process. One important TIP5 interacting protein is the transcription terminator factor TTF1 (Nemeth et al., 2004; Strohner et al., 2001). Indeed, TIP5 was identified with a two-hybrid screen with TTF1 as bait. TTF1 binds to terminator (T) elements, sequences located at the 5'- and 3'-rDNA regions, and is implicated in several rDNA regulatory processes such as transcript termination, replication fork arrest and transcription (Evers and Grummt, 1995; Gerber et al., 1997; Langst et

al., 1997a). The association of TIP5 with TTF1 and its dependency on rDNA binding proposed that TTF1 recruits TIP5 to rDNA (Nemeth et al., 2004; Santoro and Grummt, 2005; Strohner et al., 2001). However, whether and how pRNA is implicated in this process has so far not been investigated. TTF1 binds to RNA (**Figure 4B**), forming high molecular weight complexes that are probably due to the known ability of TTF1 to dimerize (Sander and Grummt, 1997). However, in contrast to TIP5, TTF1 did not display any preferential binding to pRNA sequences (**Figure 4C**). As in ESCs TTF1 is bound to rDNA promoter region (**Figure S3B**), we analyzed whether the association of TIP5 with TTF1 is regulated by pRNA or IGS-rRNA. To do this, we performed pulldown assays using purified RNA-free His-tagged TTF1 (aa.1-210, containing TIP5-interacting region) and GST-tagged-TIP5 (aa. 332-723, comprising the RNA- and TTF1-interacting regions) (**Figure 4D**) (Mayer et al., 2006; Nemeth et al., 2004). In this assay, we first bound GST or GST-TIP5$_{332-723}$ to glutathione beads and then we incubated GST-bound proteins either with no RNA, or with equivalent moles of RNA-control, pRNA or IGS-rRNA. Subsequently, bound GST-TIP5±RNA complexes were assayed for the interaction with His-TTF1$_{1-210}$. In the absence of RNA and in the presence of RNA control, TIP5 and TTF1 did not associate (**Figure 4D**). In contrast, TIP5-pRNA complexes displayed a strong interaction with TTF1, indicating that pRNA is required for TIP5-TTF1 association. Remarkably, TIP5 bound to IGS-rRNA did not interact with TTF1 (**Figure 4D**, left panel). Consistent with the role of 3'-pRNA sequences in TIP5 nucleolar targeting (**Figure 3E**), this region was sufficient for TIP5-TTF1 interaction while the 5'-pRNA region was not (**Figure 4D**, right panel). We conclude that pRNA mediates the association of TIP5 with TTF1 and that unprocessed IGS-rRNA prevents this interaction. Based

on these results, we propose that the impairment of IGS-rRNA processing and the consequent lack of mature pRNA in ESCs abolishes the interaction of TIP5 with TTF1, thus preventing TIP5 targeting to rDNA and inhibiting formation of nucleolar heterochromatin.

The epigenetic state of nucleolar chromatin affects ESC chromatin and pluripotency

Clustering of heterochromatin at nucleoli is a phenomenon known to occur in many different organisms and cell types, yet neither the factors involved nor its physiological relevance is well understood. Recently, we showed that NIH3T3 cells depleted of TIP5 displayed loss of heterochromatin at both rDNA and major and minor satellites, suggesting a crosstalk between nucleolar and nuclear heterochromatin that is mediated by TIP5 (Guetg et al., 2010). Remarkably, somatic cells depleted of TIP5 and ESCs display similar nuclear architecture features such as the enlargement of nucleolar surfaces, the reduction of nucleoli number and the formation of few decondensed heterochromatic foci (**Figure 5A**). To determine whether the epigenetic state of rRNA genes affects the open chromatin structure of ESCs, we analyzed the effects of pRNA-mediated rDNA specific targeting for heterochromatin formation on H3K9me3 and H3K9me2 levels at major and minor satellites, LINE L1 elements and IAP LTR transposons (**Figure 3D, Figure S2**). ESCs+pRNA increased H3K9me2 levels not only at rDNA but also at major and minor repeats and at LINE elements while IAP LTR transposons were not significantly affected. H3K9me3 levels drastically increased at both minor and major satellites while remaining unchanged at rDNA, LINE L1 elements and IAP LTR transposons. Among the four experiments we performed,

we observed an inverse correlation in the enrichment between H3K9me2 and H3K9me3 levels at minor and major repeats (**Figure S2**), suggesting a two-step process that initiates with H3K9me2 (that is the activity brought to rDNA by TIP5 (Santoro and Grummt, 2005)) and which is further completed with the establishment of trimethylation at H3K9. Consistent with this, ESCs+pRNA increased the total amount of H3K9me2 to levels similar to those observed during ESC-NPC transition (**Figure 5B**), a result in agreement with a previous work showing acquisition of large region of the H3K9me2 during differentiation which affects at least 30% of the genome (Wen et al., 2009). In contrast, NPCs and ESCs+pRNA did not alter global H3K9me3 content when compared to ESCs. The increased heterochromatic content of ESCs+pRNA was also accompanied by a reduction of transcript levels of major and minor satellites, while transcription of LINE and IAP elements were not greatly affected (**Figure 5C**). We also observed a strong DAPI staining around and within many of the nucleoli occupied by TIP5 in ESCs+pRNA (**Figure 3A**), suggesting that AT-rich heterochromatin (including major and minor satellite) alters its structural organization upon pRNA-driven formation of rDNA heterochromatin in ESCs. Taken together, these results suggest that pRNA-mediated targeting of heterochromatin at rDNA in ESCs initiates a structural remodelling toward a highly condensed nuclear heterochromatin, a structure that ESCs normally acquire during differentiation.

We next analyzed whether the increased heterochromatic content mediated by pRNA affects ESC properties. Transfection of pRNA in ESCs did not alter important molecular features of the undifferentiated state such as cell proliferation, expression of the pluripotency genes *Oct4* and *Nanog*, cell morphology and alkaline phosphatase (AP) staining (**Figure 6A-C**, and data not shown). To

determine whether addition of pRNA affects pluripotency *in vivo*, we performed teratoma formation assay and assessed for the presence of tissues derived from all three-germ layers (Zhang et al., 2008). As shown in **Figure 6D**, ESCs+pRNA were no longer pluripotent because they lost the capability to form teratoma while control cells displayed teratomas consisting of derivatives of the three germ layers (**Figure S4**). To get insights into the loss of pluripotency, we analyzed transcription profiles of ESCs transfected with RNA-control and pRNA sequences by RNAseq and found upregulation of 529 transcripts and downregulation of 509 transcripts in ESCs+pRNA (**Table S1**). We carried out functional annotation analysis with the DAVID tools (Huang et al., 2009) of transcripts whose levels were altered in ESCs+pRNA (**Figure 6E; Table S1**). The top 8 Gene Ontology (GO) terms were all related to cell developmental and differentiation processes. Enrichment for these processes was particularly evident for transcripts upregulated in ESCs+pRNA when compared to control cells, suggesting that addition of pRNA promotes expression of genes involved in cell differentiation and developmental processes. Together, these results indicate that the elevated heterochromatic content induced by formation of nucleolar heterochromatin through pRNA impairs pluripotency and highlight the role of the nucleolus in the control of ESC chromatin plasticity that is required for the maintenance of the undifferentiated state.

To further explore the role of nucleolar chromatin in ESCs, we analyzed the differentiation capacity of cells depleted of TIP5. ESCs were initially treated with siRNA-Control and siRNA-Tip5 for 3 days, leading to 50% reduction of TIP5 levels (**Figure 7A,B**). ESCs depleted of TIP5 proliferated less when compared to control cells but displayed similar expression levels of the pluripotency markers *Oct4*,

Nanog and *Rex1*, exhibited the typical cell morphology of ESCs and were positive for AP staining (**Figure 7B-E**). Similar results were obtained with other siRNA-TIP5 sequences (data not shown), suggesting that TIP5 might play additional roles in ESCs which are not linked to the nucleolus and to pluripotency, an issue that is currently under investigation in our laboratory. To determine whether TIP5 depletion affects ESC differentiation, we treated again an equal number of siRNA-control and -Tip5 treated ESCs with their respective siRNAs and we induced monolayer differentiation upon withdrawal of 2i and LIF (**Figure 7A**). After 3 days, control cells displayed morphological structures typical of differentiated cells while cells depleted of TIP5 underwent cell death and detached from the plate (**Figure 7F-H**). The majority of the few siRNA-TIP5 cells that remained attached to plates showed ESC-like structures and were positive for AP staining (**Figure 7G,H, Figure S5**). The effects observed with TIP5 depletion were specific for differentiated cells since ESCs double-treated with siRNA-Tip5 and cultured in LIF containing medium did not show any defect in viability (data not shown). These results indicate that TIP5 is required for viability of ESCs induced to differentiate and suggest that the establishment of nucleolar heterochromatin is a required event for early differentiation.

Discussion

In this work, we determined that the epigenetic state of nucleoli, at rRNA genes, in ESCs and during ESC differentiation (1) depends on processing of pRNA-precursor IGS-rRNA, (2) regulates ESC nuclear architecture and chromatin plasticity, and (3) is implicated in the maintenance of pluripotency.

The epigenetic state of nucleolar chromatin regulates nuclear architecture and pluripotency of ESCs

The spatiotemporal organization of genomes in the nucleus is an emerging key player to regulate genome function. For instance, the remodelling of the open and transcriptional permissive chromatin of ESCs toward a highly condensed heterochromatic form characterizes the exit from pluripotency and the progression into differentiated states. We determined here that the nucleolus is not only the place where ribosomes are produced but it also plays a role in nuclear architecture and pluripotency by regulating heterochromatic structures elsewhere in the genome. Using mature pRNA as a means to specifically tether heterochromatin at nucleoli of ESCs, we showed that the formation of heterochromatin within nucleoli, at rRNA genes, has the ability to signal and to initiate the establishment of repressive chromatin structures at regions of the genome located outside of the nucleolus like it is found in differentiated cells. The remodelling into heterochromatic structures induced by ectopic pRNA in ESCs is also evidenced by a global increase in H3K9me2, the maturation of heterochromatin at repetitive sequences and their transcriptional repression, all features characterizing the ESC differentiation process (Efroni et al., 2008; Wen et al., 2009). Although showing some of the molecular outlines of the undifferentiated cells, such heterochromatic ESCs transcribe genes implicated in differentiation processes and are not longer pluripotent, underscoring the role of the euchromatic organization in ESC functions and suggesting that nucleolar chromatin is an important regulator of the pluripotent state. Although we cannot define which is the first event that globally initiates the formation of

heterochromatin at the exit from pluripotency and entry into differentiation, our results place the nucleolus as an important regulator of this process. First, the establishment of rDNA heterochromatin during differentiation coincides with the formation of highly condensed heterochromatic structures and LOCKs (Meshorer and Misteli, 2006; Wen et al., 2009). This was particularly evident for the maturation of constitutive heterochromatin at major and minor satellite repeats, which displayed the same timing of rDNA for the acquisition of histone repressive marks and transcriptional repression upon ESC differentiation. The crosstalk between these repeats is consistent with the positioning of H3K9me3 rich regions and clustering of centromeres around nucleoli, previously described to accompany changes in nuclear architecture during ESC differentiation (Bartova et al., 2008a; Wiblin et al., 2005). Second, targeting of heterochromatin at rDNA in ESCs induces heterochromatic changes and increases global H3K9me2 content at levels similar to those found in somatic cells, and leads to loss of pluripotency. Third, impairing the formation of rDNA heterochromatin by TIP5 knockdown inhibits ESC differentiation, suggesting that the establishment of nucleolar heterochromatin might be a necessary step for the switch from a lower to a higher order chromatin structure and exit from the undifferentiated state.

The crosstalk between rDNA and nuclear repetitive sequences is also in line with recent data showing the loss of heterochromatin at both rDNA and major and minor satellites of somatic cells depleted of TIP5 (Guetg et al., 2010; Postepska-Igielska et al., 2013). Because of the linear proximity of rDNA and centromeric sequences at rDNA-containing chromosomes (Dev et al., 1977; Kurihara et al., 1994b), rDNA chromatin might affect the epigenetic states of centric and pericentric repeats through spreading mechanisms (i.e. from silent rRNA repeats

to adjacent centric-pericentric repeats). However, centromeres of chromosomes not containing rRNA genes were described to associate with the nucleolus at a frequency more than that expected for a random distribution (Carvalho et al., 2001), implying an active anchoring of heterochromatic sequences at nucleoli that is independent on sequence position. In this case, the establishment of rDNA heterochromatin might allow the formation of a nucleolar/perinucleolar compartment enriched in chromatin repressor complexes that becomes attractive for genomic regions that have to be repressed. An important example is provided by the perinucleolar targeting of the inactive X that was implicated for the maintenance of its repressed epigenetic state (Zhang et al., 2007). In line with this, recent high-resolution sequencing of the nucleolus unraveled the presence of regions with low gene density and significantly enriched in transcriptional repressed genes (Nemeth et al., 2010; van Koningsbruggen et al., 2010). Therefore, anchoring of heterochromatin at the nucleolus might serve similar functions like the ones described for the nuclear periphery that is responsible for the integrity of mammalian heterochromatin (Pinheiro et al., 2012; Towbin et al., 2012). Consistent with this, genomic regions localized at the lamina (LADs) after cell division were shown to relocate either at the lamina or at the nucleolus (Kind et al., 2013), suggesting interchangeable roles in regulating and maintaining heterochromatic states.

The results described here also provided evidences that rRNA genes do not only function in synthesizing rRNA for ribosome production. Indeed, accumulating evidences suggested that the major task for the formation of silent rDNA heterochromatin is not to regulate rRNA transcription. Silent rRNA repeats, present in all somatic cells, maintain their chromatin and epigenetic state

independently of transcriptional activity and are stably propagated throughout the cell cycle (Conconi et al., 1989), a result in agreement with the many data showing that rRNA synthesis is regulated by modulating the activity of transcriptionally competent (active) genes and not by changing the number of silent genes (reviewed in (Santoro, 2012)). Our results indicated that the epigenetic state of rRNA genes contributes to nuclear architecture and cellular functions such as pluripotency and ESC differentiation by controlling the balance between heterochromatin and euchromatin. The relationship between nucleolar and nuclear chromatin is also supported by data showing that the maintenance of rDNA heterochromatin is required for genome stability. In the yeast *S. cerevisiae*, *Drosophila* and mouse cells disruption of rDNA heterochromatin instigates genome instability at the rDNA and satellite repeat arrays (Guetg et al., 2010; Mekhail et al., 2008; Peng and Karpen, 2007). In addition, rDNA deletions in *Drosophila* result in reduced heterochromatin-induced gene silencing elsewhere in the genome and the extent of the rDNA deletion correlates with the loss of silencing in much the same manner as mutations in known protein heterochromatin components (Paredes and Maggert, 2009).

RNA processing modulates distinct functions of the same lncRNA

Very little is understood about how specific lncRNAs seek out selective sites in the genome for interaction, and nature of lncRNA-chromatin interactions, and their possible functional roles in lncRNA biology (Rinn and Chang, 2012). This work underlined the role of lncRNA in targeting epigenetic regulatory processes at specific genomic loci leading to the establishment of chromatin conformation patterns that ultimately result in the fine control of genes (Costa, 2008). We

showed that the regulation of pRNA precursor IGS-rRNA processing is a key determinant for the control of the epigenetic state at rDNA and proposed that the processing represents a mean of ncRNA regulation to modulate distinct functions of the same ncRNA. We determined that IGS-rRNA processing is a regulated process and that its impairment in ESCs prevents recruitment of TIP5 to rDNA and formation of rDNA heterochromatin. Although the mechanisms that impair IGS-rRNA processing in ESCs are yet to be determined, our results demonstrated that the lack of mature pRNA abolishes the formation of rDNA heterochromatin in ESCs. Indeed, addition of pRNA in ESCs was sufficient to recruit TIP5 to rDNA and to establish rDNA repressive structures. We unravelled the molecular insights that distinguish the processed from the unprocessed pRNA and showed that while IGS-rRNA abolishes the association of TIP5 with TTF1, pRNA promotes this interaction that serves to guide the complex to rDNA and to establish nucleolar heterochromatin. Thus, the same ncRNA can prevent or promote protein complex assembly and its processing controls the switch to these functions. Although pRNA was recently proposed as an example of guiding of epigenetic regulators to specific genomic loci through RNA-DNA complementarity such as triple helix (Bierhoff et al., 2013; Schmitz et al., 2010), our results do not support this model but favour a pRNA-mediated targeting of TIP5 through DNA-protein recognition rules that is further regulated by processing. Whether triple-helix pRNA is implicated in other physiological processes it remains an issue to be further investigated.

Based on our results describing the mechanistic insights and functional consequences of pRNA processing in epigenetic and chromatin processes, it would not be surprising if processing emerges as a more general mechanism of

lncRNA regulation.

In summary, our data underline the role of lncRNA processing in the regulation of epigenetic-mediated processes and the contribution of chromatin structure in ESC pluripotency and differentiation potential, and indicate that the epigenetic state of nucleolar chromatin is a key regulator of nuclear architecture and chromatin plasticity which serves to control cell pluripotency and lineage commitment.

Experimental Procedures

Experimental Procedures are described in Supplemental Experimental Procedures

Supplemental Information

Supplemental Information includes five figures, two tables, Supplemental Experimental Procedures, and Supplemental References.

Acknowledgments

This work was supported by the Swiss National Science Foundation (SNF 310003A-135801, N.S., S.L. and R.S.; 31003A-118361, P.C.; 323530-133905, F.A.W.), UBS-Promedica Stiftung (E.V., R.S. and O.S.), Forschungskredit of the University of Zurich (N.S.) and the Mäxi Stiftung (D.B and R.S.).

Figure Legends

Figure 1. Establishment of rDNA heterochromatin occurs during ESC differentiation and correlates with the recruitment of TIP5 to rDNA.

(A) qRT-PCR. Nanog and Pax6 mRNA levels in ESCs and NPCs. Data were normalized to Rps12 mRNA.

(B) CpG methylation levels at rDNA promoter in ESCs, NPCs and mouse brain tissues.

(C) 45S pre-rRNA levels in ESCs, NPCs and NIH3T3 cells. rRNA levels were measured by qRT-PCR and normalized to Rps12 mRNA.

(D) CpG methylation levels at rDNA promoter in mouse fibroblasts and iPSCs.

(E) ChIP. H3K9me2, H3K9me3 and H3K27me3 occupancy at rDNA promoter and coding sequences, major and minor satellites and control genes *Evx1*. Data of two independent experiments were normalized to input and rDNA promoter value in ESCs.

(F) ChIP. UBF, TIP5 and PARP1 occupancy at rDNA promoter and coding sequences. *Zfpm2* and *Gapdh* represent control genes. Data of two independent experiments were normalized to input and rDNA promoter values in ESCs.

(G) Tip5 mRNA (qRT-PCR) and protein levels (immunoblot) of ESCs and NPCs. Data were normalized to *Rps12* mRNA or PARP1 protein levels.

(H) TIP5 cellular localization in MEFs, ESCs and NPCs by immunofluorescence. Nucleoli are visualized by UBF signal.

All error bars indicate the SD of two (when indicated) or three independent experiments.

Figure 2. IGS-rRNA is not efficiently processed in ESCs

(A) Schema representing the mouse 5'-rDNA organization: Spacer promoter (grey), intergenic spacer region (blue), rDNA main promoter (Paredes and Maggert), and transcription start sites of IGS-rRNA (-1997) and 45S pre-rRNA (+1). Arrows represent primers used to perform RT (1; -20/-1) and to quantitatively amplify the indicated rDNA sequences (2-7).

(B) Levels of 5'- and internal IGS-rRNA, and pRNA sequences of ESCs and NPCs (from days 2 to 6, from the beginning of differentiation) were measured by qRT-PCR. Data of two independent experiments were normalized to Rps12 mRNA and to ESC values. Amplifications of reactions performed without reverse transcriptase are not shown because out of scale.

(C) Left panel. Schema depicts the IGS-rRNA reporter plasmid. Black arrows represent primers used to perform RT (10) and to amplify plasmid sequences (8 and 9; black lane). Blue and red arrows (2 and 6) indicate primers hybridizing to rRNA sequences as described in (A). Right panel. NIH3T3 and ES cells were transfected with IGS-rRNA reporter plasmid. Data from three experiments are represented as values of amplifications with primers 2 and 8 (IGS-rRNA) normalized to amplifications with primers 6 and 9 (IGS-rRNA+pRNA).

Figure 3. Mature pRNA is required for the establishment of rDNA heterochromatin

(A) Immunofluorescence with anti-TIP5 and anti-UBF antibodies in ESCs transfected with *in vitro* synthesized RNA-control, pRNA and $pRNADT_0$.

(B) rDNA promoter methylation in ESCs transfected with RNA-control, pRNA and $pRNADT_0$. Error bars indicate the SD of three independent experiments.

(C) 45S pre-rRNA levels in ESCs transfected with RNA-control and pRNA. rRNA levels were measured by qRT-PCR and normalized to Rps12 mRNA. Error bars indicate the SD of two independent experiments.

(D) Box-and-whisker plot of four independent ChIP experiments showing H3K9me2 and H3K9me3 association with the rDNA promoter, minor and major satellite repeats, LINE and IAP-gag sequences. Data are represented as bound over input in ESCs+pRNA normalized to values measured in ESCs+RNA-control.

(E) Immunofluorescence with anti-TIP5 and anti-UBF antibodies of ESCs transfected with the indicated pRNA mutants.

Figure 4. pRNA mediates TIP5-TTF1 interaction

(A) TIP5 binds to IGS-rRNA. Increasing equal moles of *in vitro* transcripts corresponding to control, pRNA and IGS-rRNA sequences were used to compete for binding of $TIP5_{332-723}$ to radiolabelled run-off transcripts from pBluescript (MCS-RNA). RNA/protein complexes were analyzed by EMSA.

(B) TTF1 binds to RNA. Increasing equal moles of full length TTF1 and $TIP5_{332-723}$ were incubated with radiolabeled MCS-RNA.

(C) TTF1 does not show preferential binding to pRNA. Increasing equal moles of RNA-control and pRNA were used to compete for binding of full length TTF1 to radiolabeled MCS-RNA.

(D) TIP5-TTF1 interaction is mediated by pRNA and impaired by IGS-rRNA. Upper panel. Schema representing the GST-pull-down strategy used to analyze TIP5-TTF1 interaction in the presence of equivalent moles of RNAs. Lower panel. Pull-down assay. Bound proteins, GST, GST-TIP5 and His-TTF1, were detected with anti-GST and anti-His antibodies, respectively.

Figure 5. Mature pRNA induces global remodelling toward heterochromatic structures

(A) Immunofluorescence representing heterochromatin (DAPI) and nucleoli (UBF) in NIH3T3 cells stably expressing shRNA-control and -Tip5 sequences, and ESCs.

(B) Immunoblot of H3K9me2, H3K9me3 and histone H3 of chromatin fractions of ESCs, NPCs, ESCs+RNA-control and ESCs+pRNA. Values from two independent experiments were normalized to histone H3 levels.

(C) qRT-PCR of major and minor satellite, LINE and IAP retrotrasposon transcripts in ESCs+RNA-control and ESCs+pRNA. Amplifications of reactions performed without reverse transcriptase are not shown because out of scale. Values from two independent experiments were normalized to Rps12 mRNA.

Figure 6. pRNA impairs ESC pluripotency

(A) Nanog and Oct4 mRNA levels in ESCs+RNA-control and ESCs+pRNA (qRT-PCR). Values from two independent experiments were normalized to Rps12 mRNA.

(B) Cell morphology and (C) AP staining of ESCs+RNA-control and ESCs+pRNA.

(D) ESCs+pRNA are not pluripotent. Efficiency of teratoma formation was assessed by number of teratomas generated vs. expected (injections).

(E) Top eight biological process gene ontology terms as determined using DAVID for genes regulated, and up- and downregulated in ESCs+pRNA cells.

Figure 7. Depletion of TIP5 impairs ESC differentiation

(A) Schema showing the experimental strategy for depletion of TIP5 in ESCs.

(B) TIP5, Oct4, Nanog and Rex1 mRNA levels in ESCs depleted of TIP5.

(C) TIP5 knockdown affects ESC proliferation. Data represents relative cell numbers after 3 days of siRNA treatment.

(D) Cell morphology and (E) AP staining of ESCs treated with siRNA-control and -*Tip5*.

(F) Cell morphology and AP staining of cells after 3 days of differentiation. Quantifications are shown respectively in (G) differentiated (+), partially differentiated (+/-) and not differentiated (-) and (H) stained (+), partially stained (+/-) and not stained (-).

(I) Model showing formation of rDNA heterochromatin in ESC differentiation and its influence in nuclear heterochromatin. IGS-rRNA is not processed in ESCs with consequent lack of mature pRNA. The unprocessed transcript impairs the association of TIP5 with TTF1, inhibiting recruitment to rDNA and formation of heterochromatin. Upon differentiation, IGS-rRNA is processed and generates pRNA that allows TIP5 to interact with TTF1 and to be recruited to rDNA. The arrow depicts the influence of rDNA heterochromatin in the formation of nuclear repressive chromatin structures.

References

Akhmanova, A., Verkerk, T., Langeveld, A., Grosveld, F., and Galjart, N. (2000). Characterisation of transcriptionally active and inactive chromatin domains in neurons. J Cell Sci *113 Pt 24*, 4463-4474.

Aoto, T., Saitoh, N., Ichimura, T., Niwa, H., and Nakao, M. (2006). Nuclear and chromatin reorganization in the MHC-Oct3/4 locus at developmental phases of embryonic stem cell differentiation. Dev Biol *298*, 354-367.

Bartova, E., Galiova, G., Krejci, J., Harnicarova, A., Strasak, L., and Kozubek, S. (2008a). Epigenome and chromatin structure in human embryonic stem cells undergoing differentiation. Dev Dyn *237*, 3690-3702.

Bartova, E., Krejci, J., Harnicarova, A., and Kozubek, S. (2008b). Differentiation of human embryonic stem cells induces condensation of chromosome territories and formation of heterochromatin protein 1 foci. Differentiation *76*, 24-32.

Bhattacharya, D., Talwar, S., Mazumder, A., and Shivashankar, G.V. (2009). Spatio-temporal plasticity in chromatin organization in mouse cell differentiation and during Drosophila embryogenesis. Biophys J *96*, 3832-3839.

Bibel, M., Richter, J., Schrenk, K., Tucker, K.L., Staiger, V., Korte, M., Goetz, M., and Barde, Y.A. (2004). Differentiation of mouse embryonic stem cells into a defined neuronal lineage. Nat Neurosci *7*, 1003-1009.

Bierhoff, H., Postepska-Igielska, A., and Grummt, I. (2013). Noisy silence: Non-coding RNA and heterochromatin formation at repetitive elements. Epigenetics *9*.

Carvalho, C., Pereira, H.M., Ferreira, J., Pina, C., Mendonca, D., Rosa, A.C., and Carmo-Fonseca, M. (2001). Chromosomal G-dark bands determine the spatial organization of centromeric heterochromatin in the nucleus. Mol Biol Cell *12*, 3563-3572.

Conconi, A., Widmer, R.M., Koller, T., and Sogo, J.M. (1989). Two different chromatin structures coexist in ribosomal RNA genes throughout the cell cycle. Cell *57*, 753-761.

Costa, F.F. (2008). Non-coding RNAs, epigenetics and complexity. Gene *410*, 9-17.

Dev, V.G., Tantravahi, R., Miller, D.A., and Miller, O.J. (1977). Nucleolus organizers in Mus musculus subspecies and in the RAG mouse cell line. Genetics *86*, 389-398.

Efroni, S., Duttagupta, R., Cheng, J., Dehghani, H., Hoeppner, D.J., Dash, C., Bazett-Jones, D.P., Le Grice, S., McKay, R.D., Buetow, K.H.*, et al.* (2008). Global transcription in pluripotent embryonic stem cells. Cell Stem Cell *2*, 437-447.

Evers, R., and Grummt, I. (1995). Molecular coevolution of mammalian ribosomal gene terminator sequences and the transcription termination factor TTF-I. Proc Natl Acad Sci U S A *92*, 5827-5831.

Gerber, J.K., Gogel, E., Berger, C., Wallisch, M., Muller, F., Grummt, I., and Grummt, F. (1997). Termination of mammalian rDNA replication: polar arrest of replication fork movement by transcription termination factor TTF-I. Cell *90*, 559-567.

Gonzalez-Sandoval, A., Towbin, B.D., and Gasser, S.M. (2013). The formation and sequestration of heterochromatin during development: Delivered on 7 September 2012 at the 37th FEBS Congress in Sevilla, Spain. FEBS J *280*, 3212-3219.

Guetg, C., Lienemann, P., Sirri, V., Grummt, I., Hernandez-Verdun, D., Hottiger, M.O., Fussenegger, M., and Santoro, R. (2010). The NoRC complex mediates the heterochromatin formation and stability of silent rRNA genes and centromeric

repeats. EMBO J *29*, 2135-2146.

Guetg, C., Scheifele, F., Rosenthal, F., Hottiger, M.O., and Santoro, R. (2012). Inheritance of Silent rDNA Chromatin Is Mediated by PARP1 via Noncoding RNA. Mol Cell *45*, 790-800.

Haaf, T., and Schmid, M. (1991). Chromosome topology in mammalian interphase nuclei. Exp Cell Res *192*, 325-332.

Huang, W., Sherman, B.T., and Lempicki, R.A. (2009). Systematic and integrative analysis of large gene lists using DAVID bioinformatics resources. Nat Protoc *4*, 44-57.

Joffe, B., Leonhardt, H., and Solovei, I. (2010). Differentiation and large scale spatial organization of the genome. Curr Opin Genet Dev *20*, 562-569.

Jorgensen, H.F., Azuara, V., Amoils, S., Spivakov, M., Terry, A., Nesterova, T., Cobb, B.S., Ramsahoye, B., Merkenschlager, M., and Fisher, A.G. (2007). The impact of chromatin modifiers on the timing of locus replication in mouse embryonic stem cells. Genome Biol *8*, R169.

Kind, J., Pagie, L., Ortabozkoyun, H., Boyle, S., de Vries, S.S., Janssen, H., Amendola, M., Nolen, L.D., Bickmore, W.A., and van Steensel, B. (2013). Single-cell dynamics of genome-nuclear lamina interactions. Cell *153*, 178-192.

Kurihara, Y., Suh, D.S., Suzuki, H., and Moriwaki, K. (1994). Chromosomal locations of Ag-NORs and clusters of ribosomal DNA in laboratory strains of mice. Mamm Genome *5*, 225-228.

Langst, G., Blank, T.A., Becker, P.B., and Grummt, I. (1997). RNA polymerase I transcription on nucleosomal templates: the transcription termination factor TTF-I induces chromatin remodeling and relieves transcriptional repression. EMBO J *16*, 760-768.

Leitch, H.G., McEwen, K.R., Turp, A., Encheva, V., Carroll, T., Grabole, N., Mansfield, W., Nashun, B., Knezovich, J.G., Smith, A.*, et al.* (2013). Naive pluripotency is associated with global DNA hypomethylation. Nat Struct Mol Biol *20*, 311-316.

Martens, J.H., O'Sullivan, R.J., Braunschweig, U., Opravil, S., Radolf, M., Steinlein, P., and Jenuwein, T. (2005). The profile of repeat-associated histone lysine methylation states in the mouse epigenome. EMBO J *24*, 800-812.

Mayer, C., Neubert, M., and Grummt, I. (2008). The structure of NoRC-associated RNA is crucial for targeting the chromatin remodelling complex NoRC to the nucleolus. EMBO Rep *9*, 774-780.

Mayer, C., Schmitz, K.M., Li, J., Grummt, I., and Santoro, R. (2006). Intergenic transcripts regulate the epigenetic state of rRNA genes. Mol Cell *22*, 351-361.

Mekhail, K., Seebacher, J., Gygi, S.P., and Moazed, D. (2008). Role for perinuclear chromosome tethering in maintenance of genome stability. Nature *456*, 667-670.

Melcer, S., Hezroni, H., Rand, E., Nissim-Rafinia, M., Skoultchi, A., Stewart, C.L., Bustin, M., and Meshorer, E. (2012). Histone modifications and lamin A regulate chromatin protein dynamics in early embryonic stem cell differentiation. Nat Commun *3*, 910.

Meshorer, E., and Misteli, T. (2006). Chromatin in pluripotent embryonic stem cells and differentiation. Nat Rev Mol Cell Biol *7*, 540-546.

Meshorer, E., Yellajoshula, D., George, E., Scambler, P.J., Brown, D.T., and Misteli, T. (2006). Hyperdynamic plasticity of chromatin proteins in pluripotent embryonic stem cells. Dev Cell *10*, 105-116.

Mosgöller, W. (2004). Nucleolar ultrastructure in vertebrates. (New York, Kluwer

Academic/Plenum Publishers).

Nemeth, A., Conesa, A., Santoyo-Lopez, J., Medina, I., Montaner, D., Peterfia, B., Solovei, I., Cremer, T., Dopazo, J., and Langst, G. (2010). Initial genomics of the human nucleolus. PLoS Genet *6*, e1000889.

Nemeth, A., Strohner, R., Grummt, I., and Langst, G. (2004). The chromatin remodeling complex NoRC and TTF-I cooperate in the regulation of the mammalian rRNA genes in vivo. Nucleic Acids Res *32*, 4091-4099.

Paredes, S., and Maggert, K.A. (2009). Ribosomal DNA contributes to global chromatin regulation. Proc Natl Acad Sci U S A *106*, 17829-17834.

Park, S.H., Kook, M.C., Kim, E.Y., Park, S., and Lim, J.H. (2004). Ultrastructure of human embryonic stem cells and spontaneous and retinoic acid-induced differentiating cells. Ultrastruct Pathol *28*, 229-238.

Peng, J.C., and Karpen, G.H. (2007). H3K9 methylation and RNA interference regulate nucleolar organization and repeated DNA stability. Nat Cell Biol *9*, 25-35.

Peric-Hupkes, D., Meuleman, W., Pagie, L., Bruggeman, S.W., Solovei, I., Brugman, W., Graf, S., Flicek, P., Kerkhoven, R.M., van Lohuizen, M.*, et al.* (2010). Molecular maps of the reorganization of genome-nuclear lamina interactions during differentiation. Mol Cell *38*, 603-613.

Pinheiro, I., Margueron, R., Shukeir, N., Eisold, M., Fritzsch, C., Richter, F.M., Mittler, G., Genoud, C., Goyama, S., Kurokawa, M.*, et al.* (2012). Prdm3 and Prdm16 are H3K9me1 methyltransferases required for mammalian heterochromatin integrity. Cell *150*, 948-960.

Pluta, A.F., Mackay, A.M., Ainsztein, A.M., Goldberg, I.G., and Earnshaw, W.C. (1995). The centromere: hub of chromosomal activities. Science *270*, 1591-1594.

Postepska-Igielska, A., Krunic, D., Schmitt, N., Greulich-Bode, K.M., Boukamp,

P., and Grummt, I. (2013). The chromatin remodelling complex NoRC safeguards genome stability by heterochromatin formation at telomeres and centromeres. EMBO Rep *14*, 704-710.

Rinn, J.L., and Chang, H.Y. (2012). Genome regulation by long noncoding RNAs. Annu Rev Biochem *81*, 145-166.

Sander, E.E., and Grummt, I. (1997). Oligomerization of the transcription termination factor TTF-I: implications for the structural organization of ribosomal transcription units. Nucleic Acids Res *25*, 1142-1147.

Santoro, R. (2012). The nucleolus. The epigenetics of the nucleolus : structure and function of active and silent ribosomal RNA genes. In The nucleolus (Olson MOJ) Springer, 57-82.

Santoro, R., and Grummt, I. (2001). Molecular mechanisms mediating methylation-dependent silencing of ribosomal gene transcription. Mol Cell *8*, 719-725.

Santoro, R., and Grummt, I. (2005). Epigenetic mechanism of rRNA gene silencing: temporal order of NoRC-mediated histone modification, chromatin remodeling, and DNA methylation. Mol Cell Biol *25*, 2539-2546.

Santoro, R., Li, J., and Grummt, I. (2002). The nucleolar remodeling complex NoRC mediates heterochromatin formation and silencing of ribosomal gene transcription. Nat Genet *32*, 393-396.

Santoro, R., Schmitz, K.M., Sandoval, J., and Grummt, I. (2010). Intergenic transcripts originating from a subclass of ribosomal DNA repeats silence ribosomal RNA genes in trans. EMBO Rep *11*, 52-58.

Schlesinger, S., Selig, S., Bergman, Y., and Cedar, H. (2009). Allelic inactivation of rDNA loci. Genes Dev *23*, 2437-2447.

Schmitz, K.M., Mayer, C., Postepska, A., and Grummt, I. (2010). Interaction of noncoding RNA with the rDNA promoter mediates recruitment of DNMT3b and silencing of rRNA genes. Genes Dev *24*, 2264-2269.

Strohner, R., Nemeth, A., Jansa, P., Hofmann-Rohrer, U., Santoro, R., Langst, G., and Grummt, I. (2001). NoRC--a novel member of mammalian ISWI-containing chromatin remodeling machines. EMBO J *20*, 4892-4900.

Towbin, B.D., Gonzalez-Aguilera, C., Sack, R., Gaidatzis, D., Kalck, V., Meister, P., Askjaer, P., and Gasser, S.M. (2012). Step-wise methylation of histone H3K9 positions heterochromatin at the nuclear periphery. Cell *150*, 934-947.

van Koningsbruggen, S., Gierlinski, M., Schofield, P., Martin, D., Barton, G.J., Ariyurek, Y., den Dunnen, J.T., and Lamond, A.I. (2010). High-resolution whole-genome sequencing reveals that specific chromatin domains from most human chromosomes associate with nucleoli. Mol Biol Cell *21*, 3735-3748.

Wen, B., Wu, H., Shinkai, Y., Irizarry, R.A., and Feinberg, A.P. (2009). Large histone H3 lysine 9 dimethylated chromatin blocks distinguish differentiated from embryonic stem cells. Nat Genet *41*, 246-250.

Wiblin, A.E., Cui, W., Clark, A.J., and Bickmore, W.A. (2005). Distinctive nuclear organisation of centromeres and regions involved in pluripotency in human embryonic stem cells. J Cell Sci *118*, 3861-3868.

Wong, L.H., Ren, H., Williams, E., McGhie, J., Ahn, S., Sim, M., Tam, A., Earle, E., Anderson, M.A., Mann, J.*, et al.* (2009). Histone H3.3 incorporation provides a unique and functionally essential telomeric chromatin in embryonic stem cells. Genome Res *19*, 404-414.

Zhang, L.F., Huynh, K.D., and Lee, J.T. (2007). Perinucleolar targeting of the inactive X during S phase: evidence for a role in the maintenance of silencing.

Cell *129*, 693-706.

Zhang, W.Y., de Almeida, P.E., and Wu, J.C. (2008). Teratoma formation: A tool for monitoring pluripotency in stem cell research.

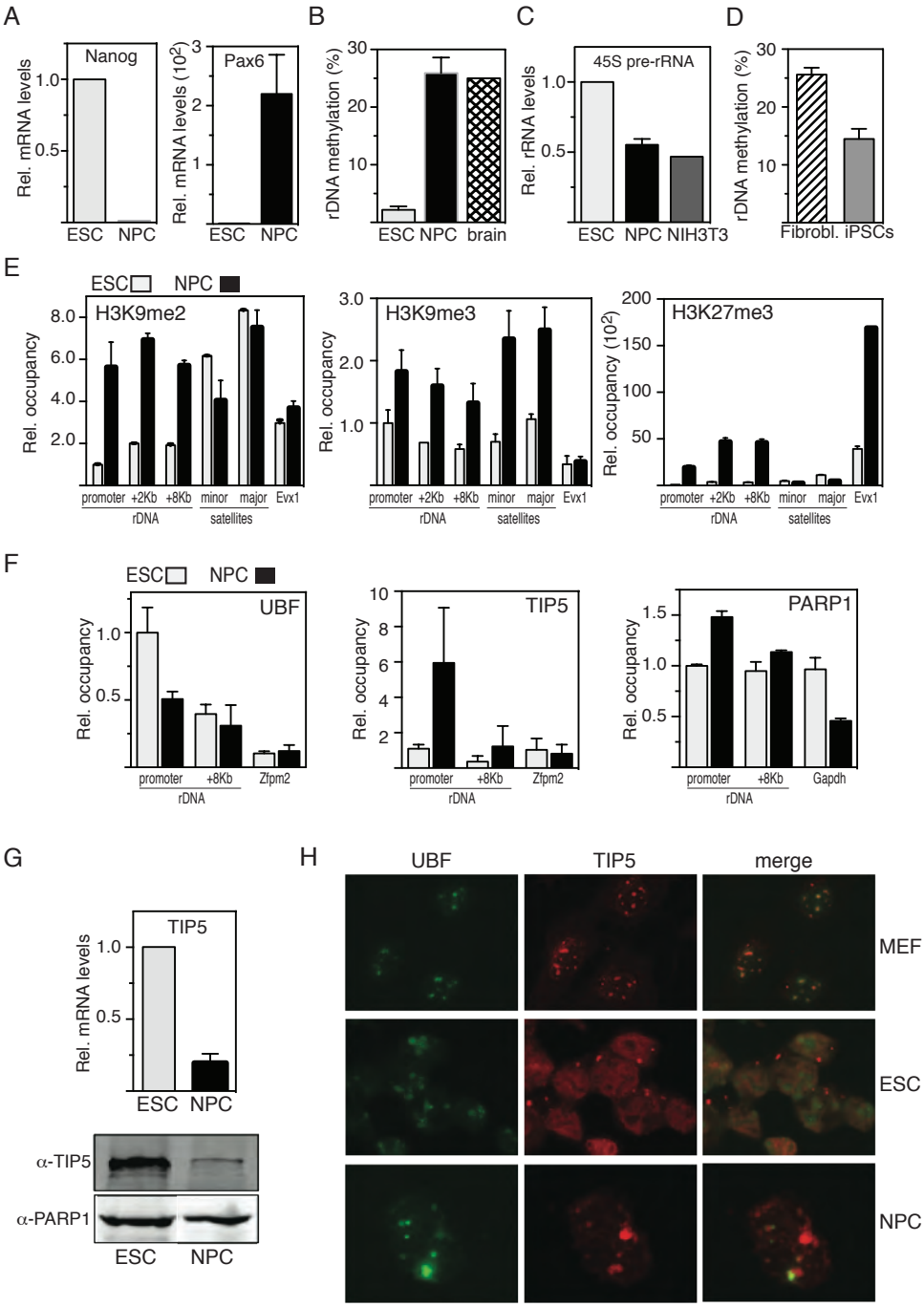
A
Nanog
Rel. mRNA levels
1.0
0.5
ESC NPC
Pax6
Rel. mRNA levels (10²)
3
2
1
ESC NPC
B
rDNA methylation (%)
30
20
10
ESC NPC brain
C
45S pre-rRNA
Rel. rRNA levels
1.0
0.5
ESC NPC NIH3T3
D
rDNA methylation (%)
30
20
10
Fibrobl. iPSCs
E
ESC NPC
H3K9me2
Rel. occupancy
8.0
6.0
4.0
2.0
promoter +2Kb +8Kb minor major Evx1
rDNA satellites
H3K9me3
3.0
2.0
1.0
H3K27me3
Rel. occupancy (10²)
200
150
100
50
F
ESC NPC
UBF
Rel. occupancy
1.0
0.5
promoter +8Kb Zfpm2
rDNA
TIP5
10
8
6
4
2
PARP1
1.5
1.0
0.5
promoter +8Kb Gapdh
G
TIP5
Rel. mRNA levels
1.0
0.5
ESC NPC
α-TIP5
α-PARP1
ESC NPC
H
UBF
TIP5
merge
MEF
ESC
NPC

Figure 1

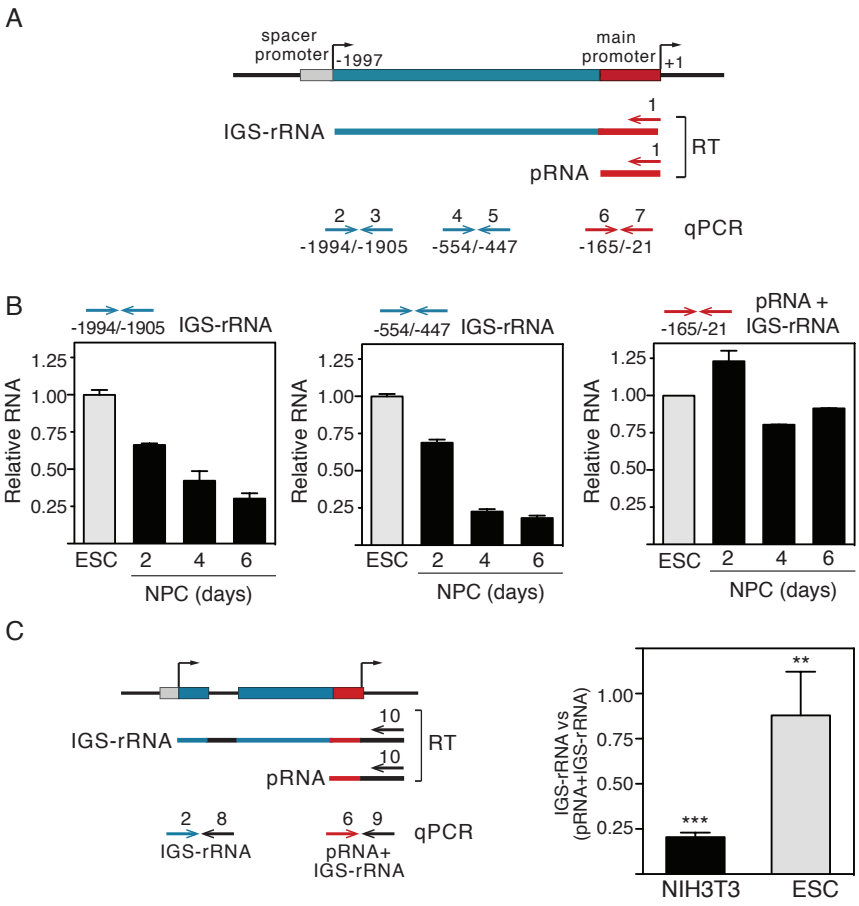
A
spacer promoter
-1997
main promoter
+1
IGS-rRNA
1
1
RT
pRNA
2 3
-1994/-1905
4 5
-554/-447
6 7
-165/-21
qPCR
B
-1994/-1905 IGS-rRNA
-554/-447 IGS-rRNA
-165/-21 pRNA + IGS-rRNA
Relative RNA
1.25
1.00
0.75
0.50
0.25
ESC 2 4 6
NPC (days)
C
IGS-rRNA
10
10
RT
pRNA
2 8
IGS-rRNA
6 9
pRNA+ IGS-rRNA
qPCR
IGS-rRNA vs (pRNA+IGS-rRNA)
**
***
NIH3T3
ESC

Figure 2

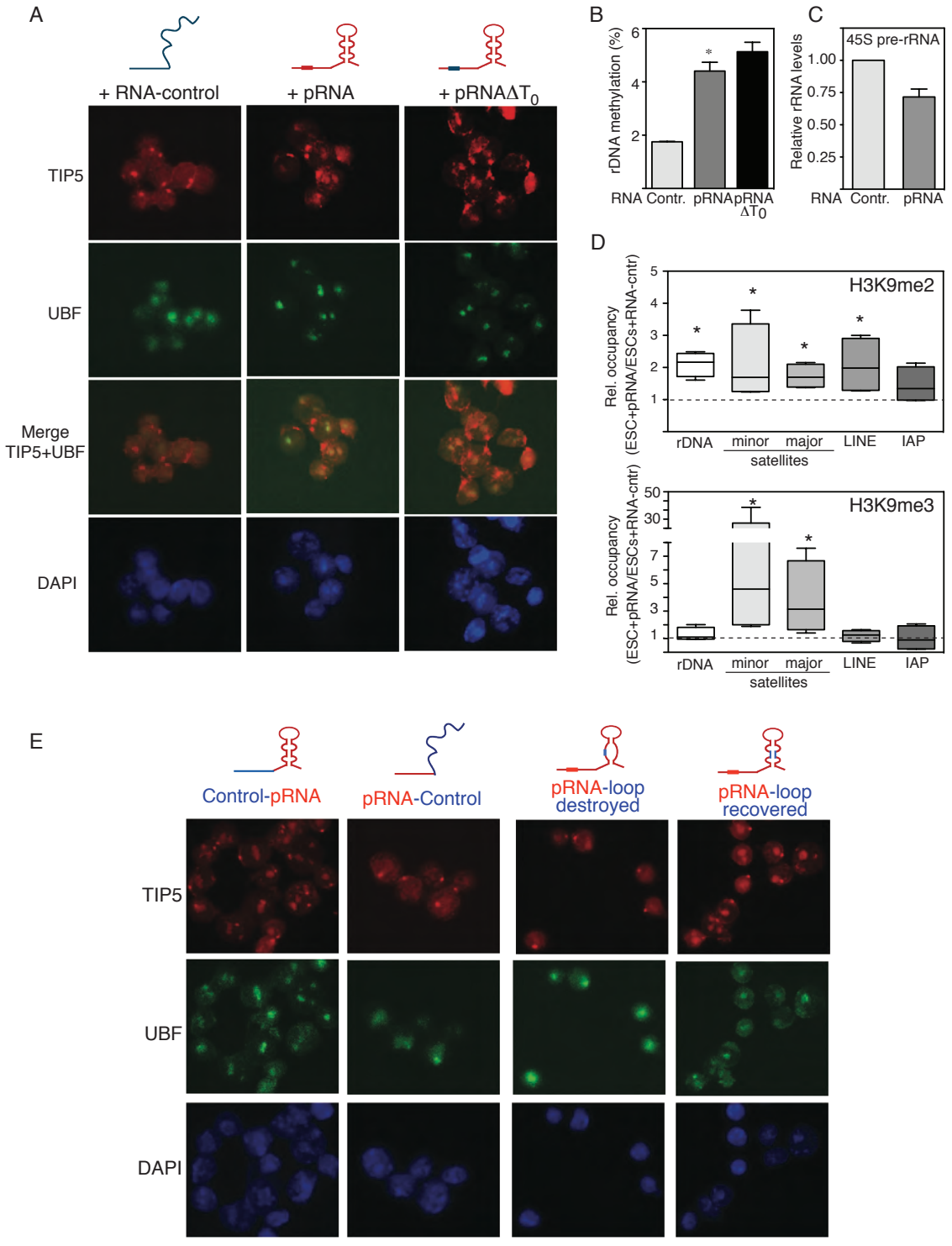
A
+ RNA-control
+ pRNA
+ pRNAΔT0
TIP5
UBF
Merge TIP5+UBF
DAPI
B
rDNA methylation (%)
RNA Contr. pRNA pRNA ΔT0
C
45S pre-rRNA
Relative rRNA levels
RNA Contr. pRNA
D
H3K9me2
Rel. occupancy (ESC+pRNA/ESCs+RNA-cntr)
rDNA minor major satellites LINE IAP
H3K9me3
E
Control-pRNA
pRNA-Control
pRNA-loop destroyed
pRNA-loop recovered
TIP5
UBF
DAPI

Figure 3

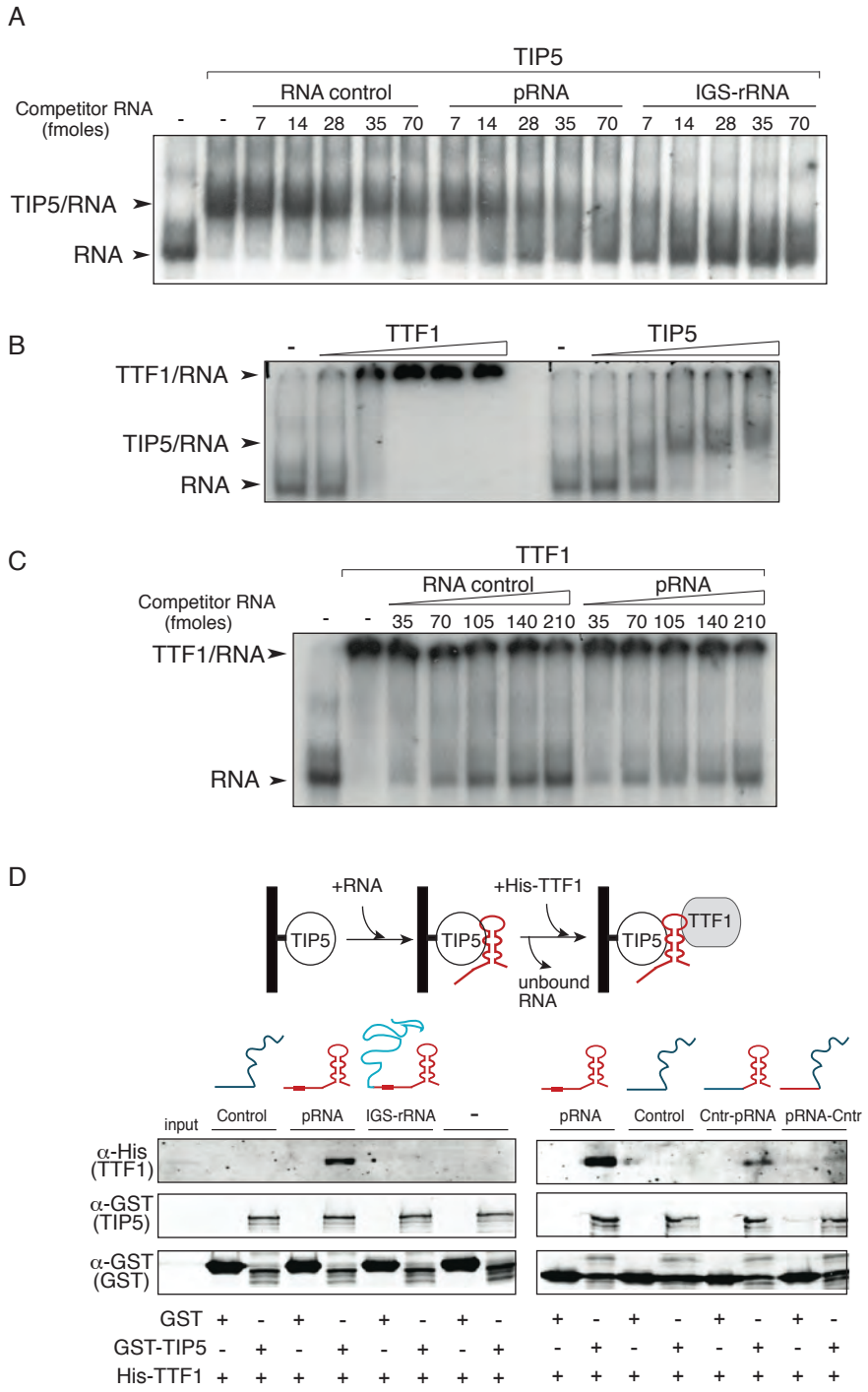
A
TIP5
RNA control
pRNA
IGS-rRNA
Competitor RNA (fmoles)
- - 7 14 28 35 70 7 14 28 35 70 7 14 28 35 70
TIP5/RNA
RNA
B
TTF1
TIP5
TTF1/RNA
TIP5/RNA
RNA
C
TTF1
RNA control
pRNA
Competitor RNA (fmoles)
- - 35 70 105 140 210 35 70 105 140 210
TTF1/RNA
RNA
D
+RNA
+His-TTF1
TIP5
TTF1
unbound RNA
input
Control
pRNA
IGS-rRNA
-
pRNA
Control
Cntr-pRNA
pRNA-Cntr
α-His (TTF1)
α-GST (TIP5)
α-GST (GST)
GST
GST-TIP5
His-TTF1

Figure 4

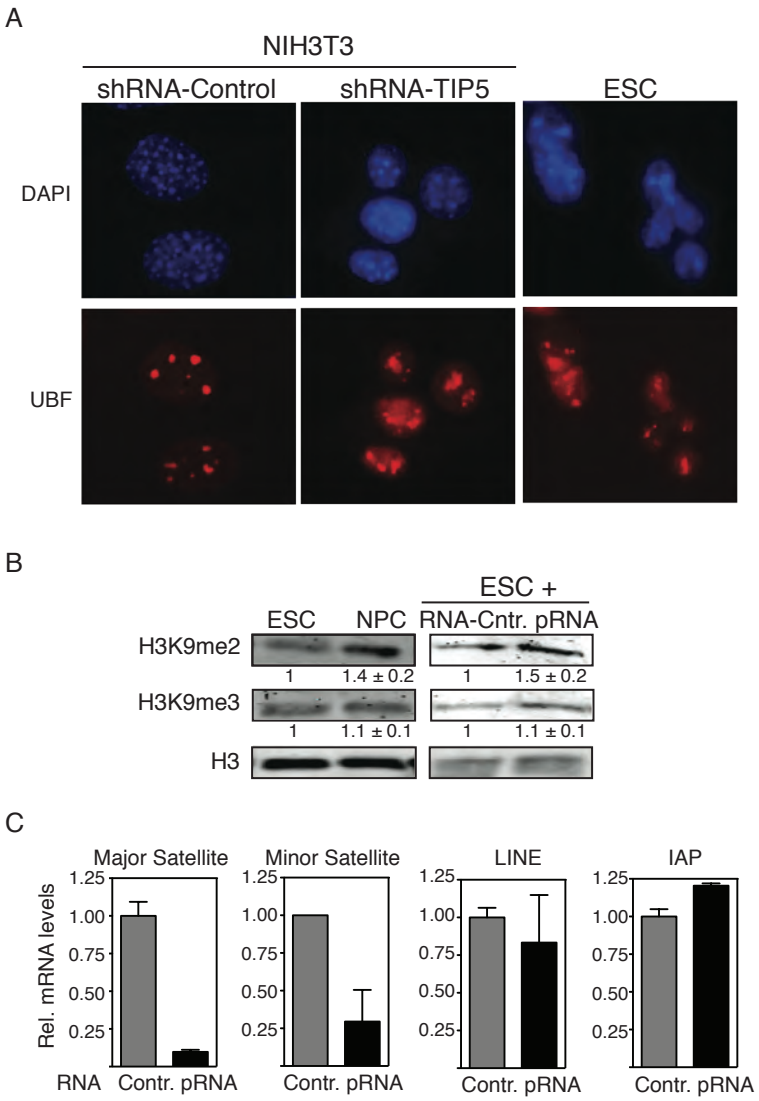
A
NIH3T3
shRNA-Control
shRNA-TIP5
ESC
DAPI
UBF
B
ESC +
ESC
NPC
RNA-Cntr. pRNA
H3K9me2
1
1.4 ± 0.2
1
1.5 ± 0.2
H3K9me3
1
1.1 ± 0.1
1
1.1 ± 0.1
H3
C
Major Satellite
Minor Satellite
LINE
IAP
Rel. mRNA levels
1.25
1.00
0.75
0.50
0.25
RNA
Contr. pRNA

Figure 5

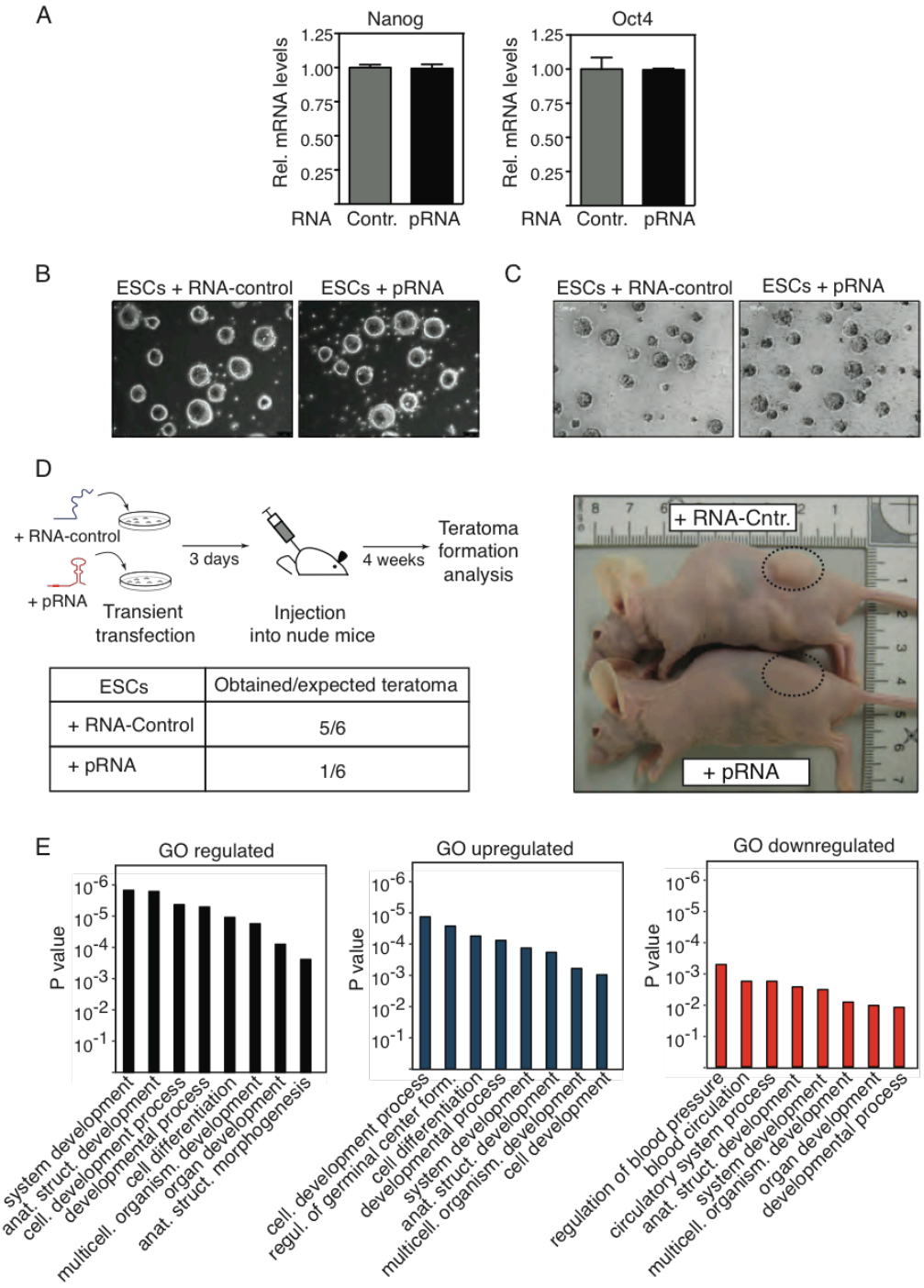

ESCs	Obtained/expected teratoma
+ RNA-Control	5/6
+ pRNA	1/6

Figure 6

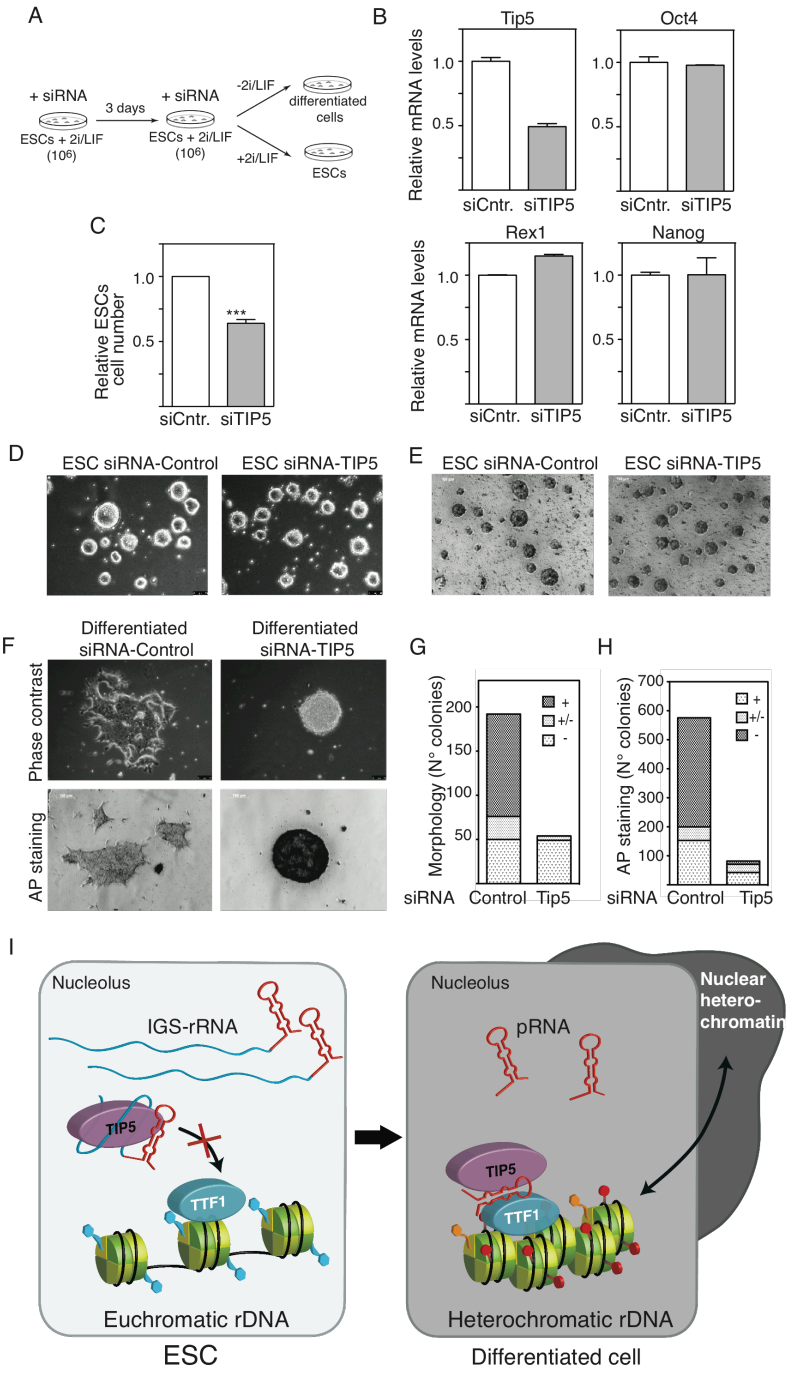
A
+ siRNA
3 days
ESCs + 2i/LIF
(10⁶)
+ siRNA
ESCs + 2i/LIF
(10⁶)
-2i/LIF
differentiated cells
+2i/LIF
ESCs
B
Tip5
Oct4
Relative mRNA levels
1.0
0.5
siCntr.
siTIP5
Rex1
Nanog
C
Relative ESCs cell number
***
D
ESC siRNA-Control
ESC siRNA-TIP5
E
F
Differentiated siRNA-Control
Differentiated siRNA-TIP5
Phase contrast
AP staining
G
Morphology (N° colonies)
+
+/-
-
siRNA
Control
Tip5
H
AP staining (N° colonies)
I
Nucleolus
IGS-rRNA
TIP5
TTF1
Euchromatic rDNA
ESC
pRNA
Nuclear hetero-chromatin
Heterochromatic rDNA
Differentiated cell

Figure 7

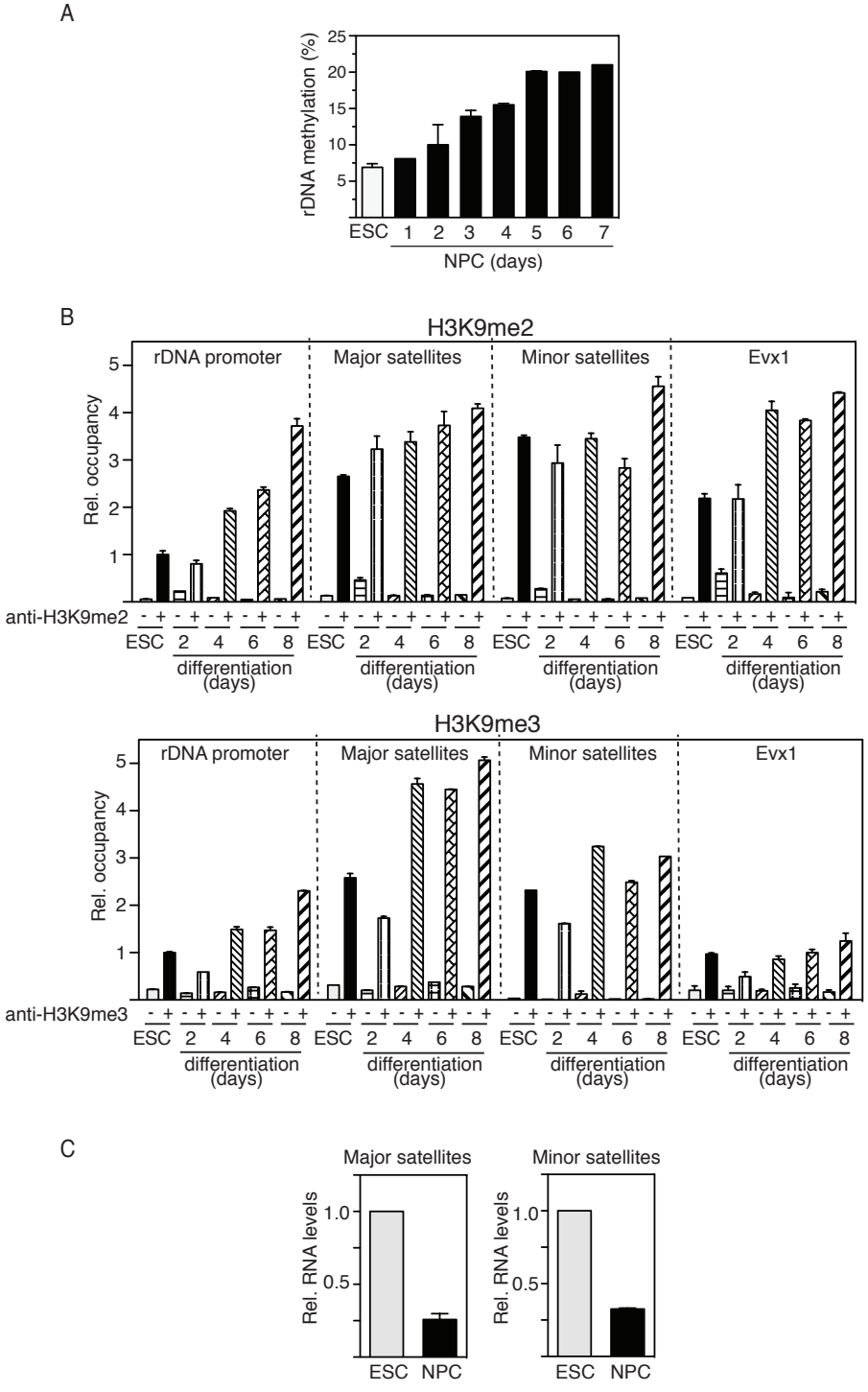

Supplementary Figure S1

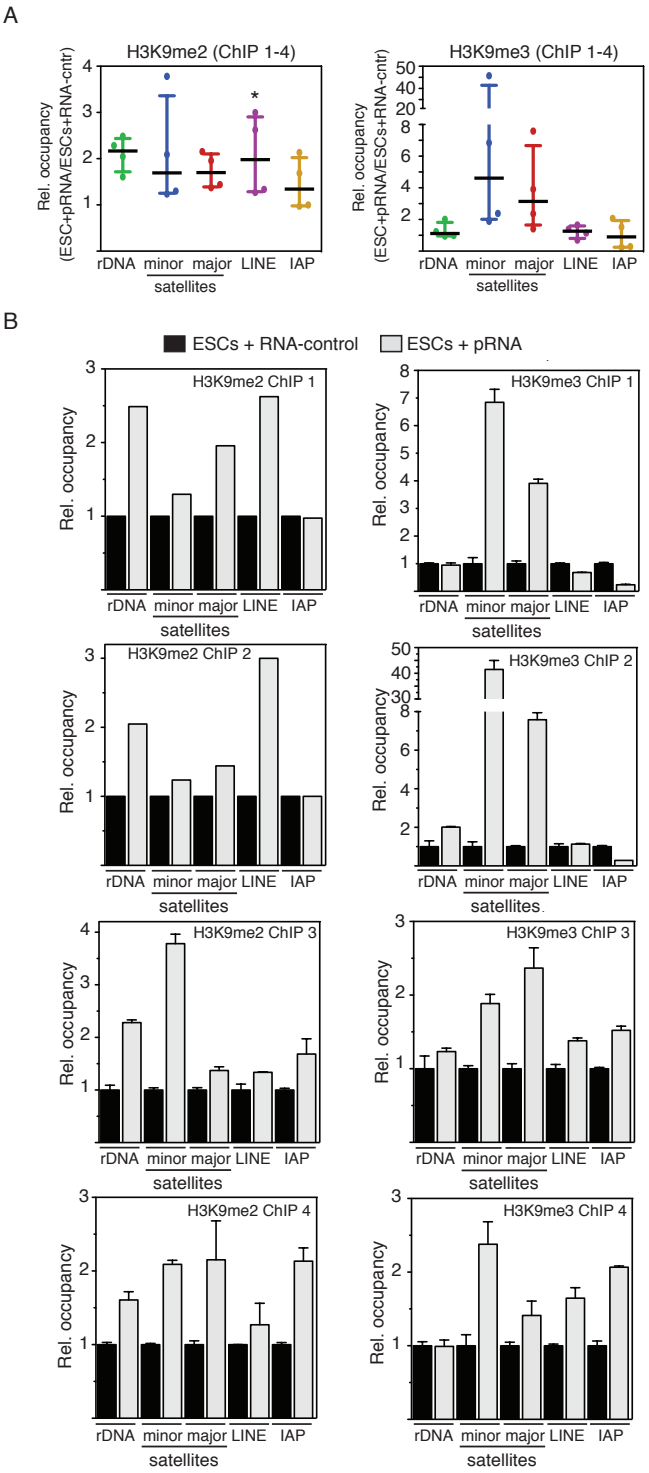

Supplementary Figure S2

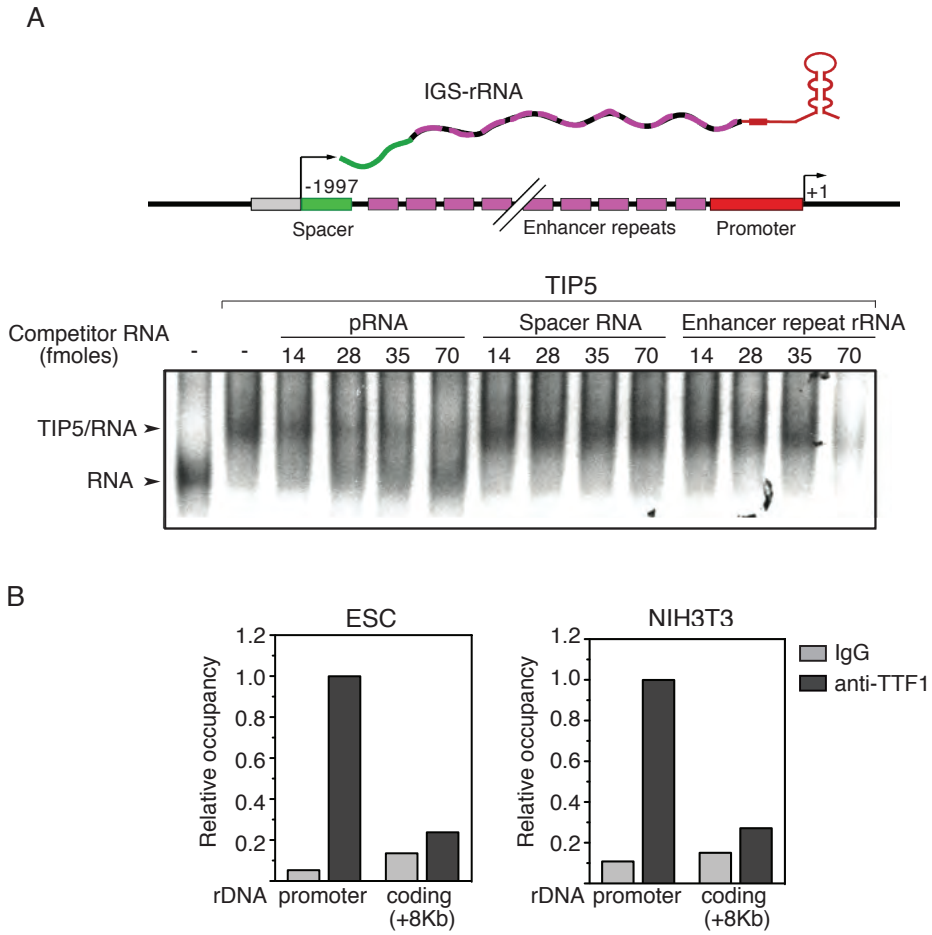

Supplementary Figure S3

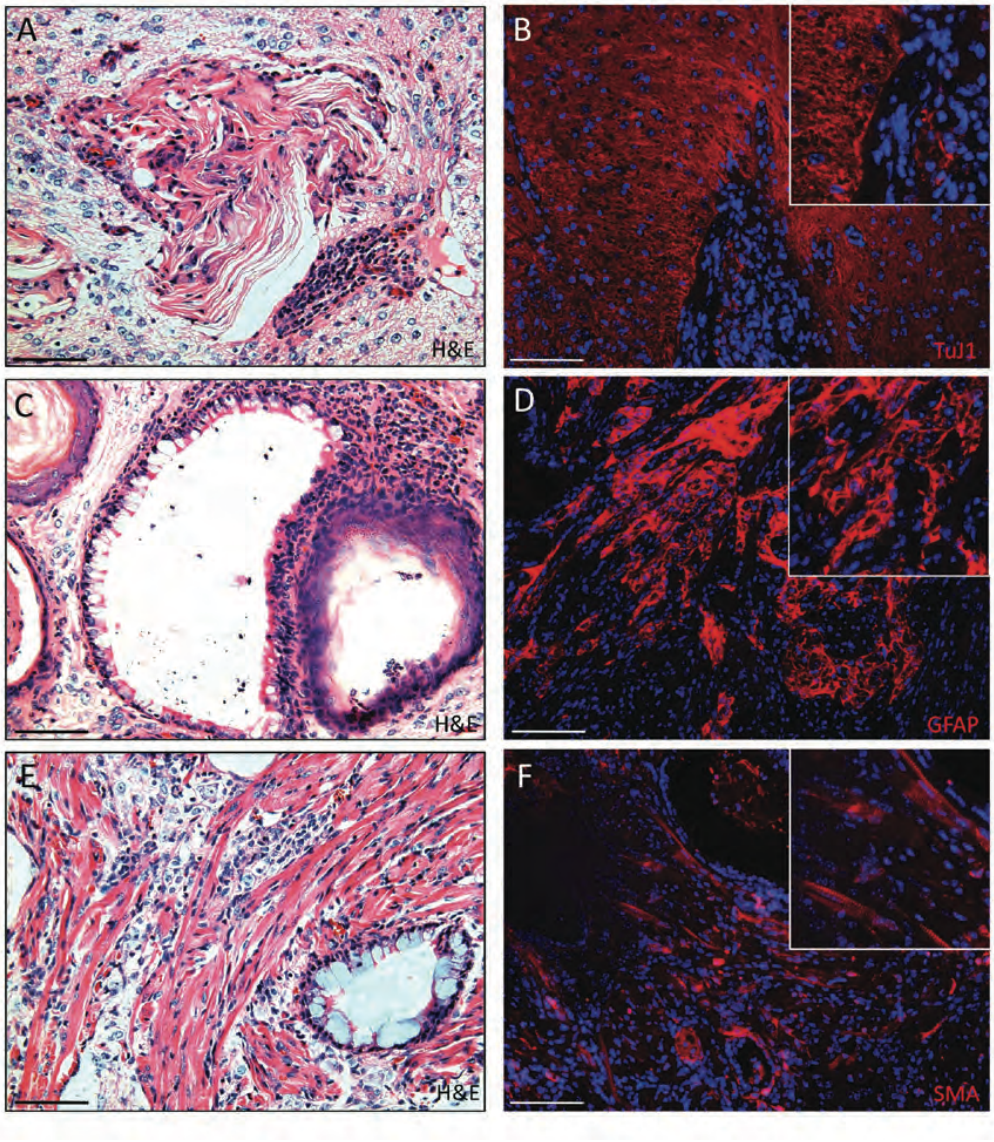

Supplementary Figure S4

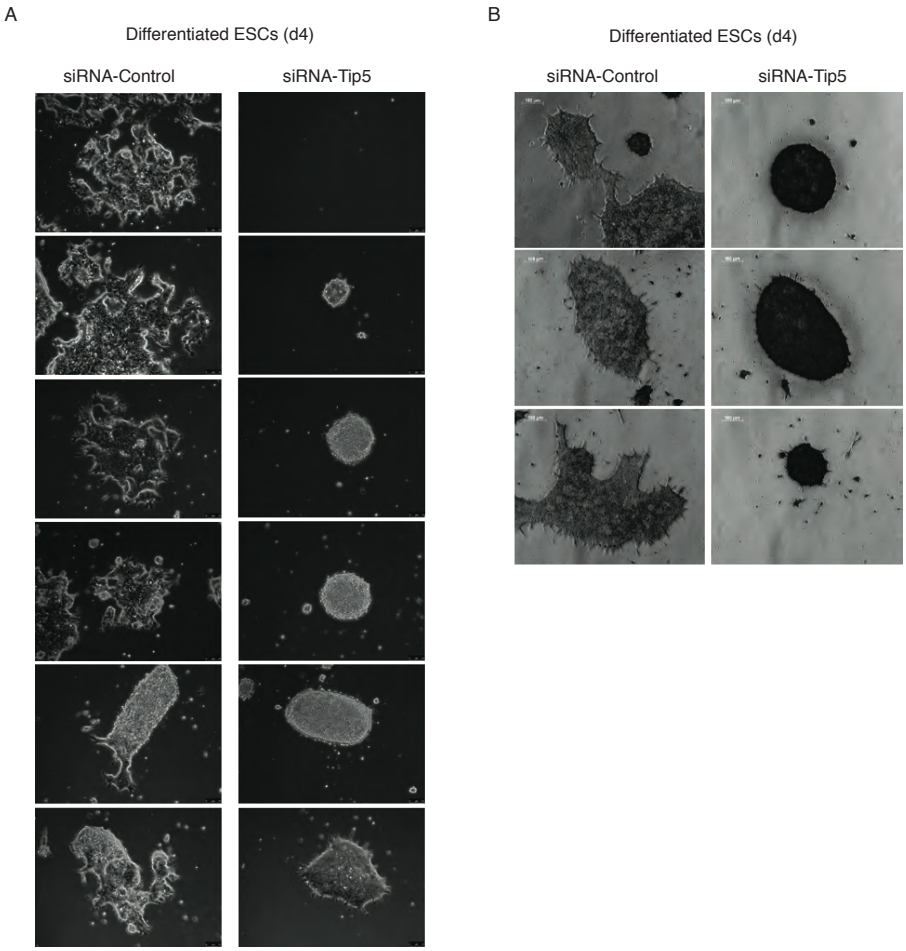

Supplementary Figure S5

The epigenetic state of the nucleolus regulates chromatin plasticity and pluripotency of embryonic stem cells

Savic et al.

Supplemental data

Supplemental Figure legends

Figure S1 (related to Figure 1B, 1E)

(A) CpG methylation levels at rDNA promoter in ESCs (JM8N4) and during differentiation into NPCs. ESCs were cultivated on monolayer and differentiation was induced with N2B27 medium supplemented with RA. Error bars indicate the SD of two independent experiments.

(B) ChIP. H3K9me2 and H3K9me3 occupancy at rDNA promoter and coding sequences, major and minor satellites and control genes *Evx1* monitored during different time points (days) of differentiation. Data were normalized to input and rDNA promoter values in ESCs.

(C) Major and minor satellite transcript levels in ESCs and NPCs were measured by qRT-PCR and normalized to Rps12 mRNA. Error bars indicate the SD of two independent experiments.

Figure S2 (related to Figure 3D)

(A) Scatter plot of the four ChIP experiments shown in Figure 3D.

(B) Results of the single four ChIP experiments showing an inverse correlation in the enrichment between H3K9me2 and H3K9me3 levels at minor and major

repeats in ESCs+pRNA when compared to ESCs+RNA-control. Data are represented as bound over input in ESCs+pRNA normalized to values measured in ESCs+RNA-control.

Figure S3 (related to Figure 4)

(A) TIP5 binds to IGS-rRNA and it has a stronger affinity for pRNA sequences. Increasing equal moles of *in vitro* transcripts corresponding to pRNA, spacer promoter and enhancer repeat RNA were used to compete for binding of $TIP5_{332-723}$ to radiolabelled run-off transcripts from pBluescript (MCS-RNA). RNA/protein complexes were analyzed by EMSA.

(B) TTF1 binds to the rDNA promoter of ESCs. ChIP showing association of TTF1 with rDNA promoter in ESCs and NIH3T3 cells. Data of two independent experiments were normalized to input and rDNA promoter values. The low levels of TTF1 association with +8 Kb rDNA sequences (that do not contain T elements) demonstrated the specificity of the assay.

Figure S4 (related to Figure 6D)

Histological analysis of teratomas revealed that ESCs differentiate into all three germ layers as shown by the presence of ectoderm (A, B, D), endoderm (C) and mesoderm (E,F). A, C, E haematoxylin staining. Immunostaining for bIII tubulin (TuJ1) (B), glial fibrillary acidic protein (GFAP) (D) and smooth muscle actin (SMA) (F). Inserts show higher magnification. Scale bars, 100 μm.

Figure S5 (related to Figure 7F,G)

(A) Cell morphology and (B) AP staining of differentiated ESCs treated with

siRNA-control and -*Tip5*.

Supplemental Table legends

Supplemental Table S1 (related to Figure 6E)

Total RNA of ESCs+Control-RNA and ESCs+pRNA from two biological replicates were purified and analyzed by RNA seq. The table includes the list of genes whose transcript levels were altered in ESCs+pRNA when compared to control cells (defined as regulated, upregulated and downregulated) and gene onthology analysis using DAVID tools.

Supplemental Table S2 (Related to Experimental Procedures)

List of primers used for amplification in ChIP and RT-PCR analyses

Experimental procedures

mESC culture

129 mouse embryonic stem cells (E14 line) were cultured in N2B27 media (D-MEM F12, Neurobasal medium, N2/B27 supplements, 2mM L-glutamine with Pen/Strep, β-Mercaptoethanol) supplemented with recombinant leukemia inhibitory factor, LIF (ESGRO, 1000 U/ml) and MEK and GSK3β inhibitors, 2i (Stemolecule CHIR99021 and PD0325901, 3μM and 1μM respectively). Cells were seeded at a density of 50,000 cells/cm^2 in culture dishes (Corning® CellBIND® surface) treated with 0.1% Gelatine without feeder layer. Propagation of cells was carried out every 2 days using Trypsin 0.5x for enzymatic cell dissociation.

mESC differentiation

mESCs were differentiated to neural progenitor cells according to previously established protocol (Bibel et al., 2004). In brief, differentiation employed a suspension-based embryoid bodies formation (Bacteriological Petri Dishes, Bio-one with vents, Greiner®). The neural differentiation media (D-MEM, 10% FCS, 1xMEM NEAA, 2mM L-glutamine with Pen/Strep, β-Mercaptoethanol) was filtered trough 0.22μm filters and stored at 4°C. During the 8-day differentiation procedure media was exchanged every 2 days. In the last 4 days of differentiation the media was supplemented with 2 μM retinoic acid (RA) to generate neural precursors that are Pax-6-positive radial glial cells.

Transfections

ESCs were seeded at a density of 20,000 cells/cm^2 and transfected with the indicated siRNAs (50 nM siRNA) or synthetic RNAs (1 mg/ml) using Lipofectamine® RNAiMAX (Life Techonlogies) in Opti-MEM® GlutaMAX™ (GIBCO) reduced-serum medium. Analysis of differentiated transfected ESCs was performed using consecutive transfections. Three days after the first transfection, equal amounts of ESCs (e.g. siRNA-control and siTIP5 treated cells) were again transfected and induced to differentiate in complete media (G-MEM, 10%FCS, Sodium Pyruvate 100mM, 1xMEM NEAA, L-Glutamine) by withdrawal of LIF and 2i. Efficiencies of siRNA-mediated depletions and synthetic RNA levels were monitored by qRT-PCR 3-4 days post-transfection.

***In Vitro* Transcription**

The indicated pRNA and control sequences were cloned by PCR into pJET1/2 plasmids. pRNA : mrDNA from -232 to -1; Control-pRNA: control sequences at 5', mrDNA from -140 to -1 at 3'; pRNA-Control: mrDNA from -232 to -140 at 5', control sequences at 3' ; pRNA-loop destroyed: mrDNA from -232 to -1 sequences where GGG (-115/-113) were replaced with AAA; pRNA-loop recovered: mrDNA from -232 to -1 sequences where CCC (-60/-58) were replaced with TTT. All plasmids were verified by sequencing. Synthetic RNAs were synthesized using T7 polymerase and as substrate Xba I linearized pJET1/2 vectors containing the indicated sequences. After treatment with DNase I, transcripts were double purified using TRIzol reagent (Invitrogen) according to the manufacture's protocol.

Indirect immunofluorescence

ESCs or differentiated cells were grown on gelatin-coated coverslips and permeabilized with 0.05% Triton X-100 in 20mMTris-HCl, pH 8, 5mM MgCl2, 0.5mM EDTA, and 25% glycerol. After washing, cells were fixed with cold methanol (7 min) and stained with anti-TIP5 (Diagenode) and anti-UBF (SantaCruz) antibodies and DAPI (Molecular Probes), and immunofluorescent images were digitally recorded.

Chromatin Immunoprecipitation

The chromatin immunoprecipitation (ChIP) protocol was previously described (Santoro, 2014). Briefly, formaldehyde 1% was added to cultured cells to cross-link proteins to DNA. Isolated nuclei were then lysed in 300µl lysis buffer (50 mM Tris-HCl [pH 8.1], 10 mM EDTA, 1% SDS) and sonicated using a Bioruptor ultrasonic cell disruptor to shear genomic DNA to an average fragment size of 200bp. 20 to 40 mg chromatin was diluted tenfold with IP buffer (16.7 mM Tris-HCl [pH 8.1]), 167 mM NaCl, 1.2 mM EDTA, 0.01% SDS, 1.1% Triton X-100) and than immunoprecipitated overnight with ChIP-grade antibodies. After elution and reversion of crosslinks, the precipitated DNA was purified with phenol/chloroform, ethanol precipitated and than quantified by qPCR. rDNA, major and minor satellite sequences were amplified with previously reported primers (Martens et al., 2005) (Martens et al., 2005; Santoro et al., 2002). Primers are listed in Table S2.

RNA Extraction, reverse transcription and quantitative PCR (RT-qPCR)

RNA was purified with Trizol reagent (Life Technologies) . Residual contaminating genomic DNA was removed with Ambion® TURBO™ DNase according to

manufacture's instructions. RNA was primed with random hexamers and reverse-transcribed to first-strand cDNA. Reverse transcription of pRNA and IGS-rRNA was performed using DNA oligo -20/-1 Rev or random primers. qRT-PCR was performed with SensiMix SYBR Hi-ROX Mix (Bioline) on a Rotor-Gene Q (Qiagen). Amplification of samples without reverse transcriptase assured absence of DNA (data not shown). The relative transcription levels were determined by normalizing to Rps12 mRNA levels. Statistical significance (P-values) of the difference in expression levels between genes was calculated using the two-sample paired t-test. Primer sequences used in qRT-PCR are listed in Table S2.

CpG methylation

rDNA CpG methylation was measured as previously described (Santoro, 2014; Santoro et al., 2002)). 2 mg genomic DNA were digested with HpaII (NEB) in the presence of 5 ng of unmethylated pBluescript KS(+) plasmid. rDNA CpG methylation levels were measured by quantitative amplification using primer pairs (-165/-145 Forw and -20/-1 Rev) that flank the restriction sites CCGG at -142 of rDNA promoter or primers that amplify neighbouring sequences lacking HpaII sites (+1/+20 Forw and +111/+130 Rev). Values were obtained using logarithmic dilutions of mouse genomic DNA as standard curve. CpG methylation levels were calculated as resistance to HpaII digestion by normalizing the amounts of rDNA amplified from -165 to -1 to the levels of amplicons from +1 to +130. To verify HpaII digestion efficiency, pBluescript KS(+) plasmid was analyzed by qPCR using one forward primer that is complementary to sequences upstream of the CCGG site of b-lactamase gene (at 2580) and two different reverse primers that map upstream and downstream the HpaII sites (see Table S2). All analyzed

samples displayed 96-98% digestion efficiency.

EMSA

Radiolabeled MCS-RNA was synthesized by T7 RNA polymerase using pBluescript-KS(+)/EcoRI as template. After treatment with DNase I, transcripts were purified and 50,000 cpm of MCS-RNA were incubated for 15 min on ice with 40 ng recombinant TIP5 or TTF1 in EMSA buffer (20 mM Tris-HCl [pH 8.0], 5 mM MgCl2, 100 mM KCl, and 0.2 mM EDTA). Cold competitor RNA was added, and incubation was continued for 30 min. RNA-protein complexes were analyzed by electrophoresis on 6% (w/v) native polyacrylamide gels and visualized by autoradiography.

GST-Pulldown

5 µg of GST-TIP5$_{235-741}$ were incubated with 15µl of GST beads (Glutathione Sepharose 4B, GE Healthcare) in AM100 buffer (100mM KCl, 20mM Tris-HCl pH 8.0, 5mM $MgCl_2$, 0.2mM EDTA, 1X Protease Inhibitor (Roche)) for 12-16 hours at 4°C. After two washes with EMSA buffer containing 3% Glycerol, bound GST-TIP5$_{235-741}$ was incubated with 25 nmoles of the indicated RNAs for 1h at 4°C. After a double wash with AM200 buffer (200mM KCl, 20mM Tris-HCl pH 8.0, 5mM $MgCl_2$, 0.2mM EDTA, 1X Complete Protease Inhibitor Cocktail (Roche)), bound GST-TIP5/RNA complexes were incubated with 0.5 µg of His-TTF1$_{1-210}$ for 2h at 4°C. Samples were then washed three times with EBC buffer (250mM NaCl, 50mM Tris-HCl pH8.0, 0.5% NONIDET P-40, 5mM DTT, 1X cOmplete Protease Inhibitor Cocktail), run on a 12% SDS polyacrylamide gel and analyzed by Western blot with anti-GST and anti-RGS.HIS antibodies.

AP staining

Cells were fixed in 4% paraformaldehyde for 10min, washed with AP Buffer (100mM TrisCl pH 9.5, 100mM NaCl, 50mM MgCl2) and then incubated for 30 min in AP Buffer containing NBT (37 mg/ml) and 3.5µl BCIP (175 mg/ml). The staining was blocked with Tris-EDTA (Sigma) for 10min.

Whole-Transcriptome Shotgun Sequencing (RNA-Seq) and Data Analyses

Total RNA of ESCs+Control-RNA and ESCs+pRNA from two biological replicates were purified and analyzed by RNA seq. 100bp paired-end reads have been sequenced with illumina Hiseq. The reads were quality filtered and submitted to RSEM for expression quantitation (Li and Dewey, 2011). Expression counts were further analyzed with the glm method in the edgeR package to compute the significance of differential expression (Robinson et al., 2010).

Teratoma analysis

Teratoma samples were fixed in 4% buffered paraformaldehyde and embedded in paraffin. For immunostainings, 5 μm thickness paraffin sections were deparaffinized and rehydrated and subsequently subjected to the antigen retrieval (Citrate buffer pH 6.0 for 10 minutes at 110°C in rapid microwave histoprocessor, Milestone, USA). The following primary antibodies were used: anti-bIII tubulin (Sigma), anti-GFAP (DAKO) and anti-SMA (Sigma). Nuclei were stained with DAPI and slides were mounted with Fluorescent Mounting Medium (DAKO) to avoid bleaching. Images were captured with a Leica DMI 6000B Microscope and using LAS AF (Leica Application Suite Advanced Fluorescence) software. Animal

experiments were performed in accordance with Swiss law and have been approved by the veterinary authorities of Zurich.

Antibodies

The following antibodies were used: anti-TIP5 (CS-090-100-Diagenode); anti-UBF (sc-13125), anti-GST (sc-459) and anti-PARP1 (sc-53643) from Santa Cruz; anti-H3K9me2 (17-648), anti-H3K9me3 (17-625), and anti-H3K27me3 (17-622) from Millipore; anti-H3 (ab1791) from Abcam; anti-RGS.HIS (34610) from Qiagen. Anti-TTF1 antibody was produced with Genosphere.

Table S2

List of primers

mouse rDNA CpG methylation primers		
Name	For/Rev	Sequence
rDNA promoter -165/-145	For	GACCAGTTGTTCCTTTGAGG
rDNA promoter -21/-1	Rev	ACCTATCTCCAGGTCCAATAG
rDNA coding +1/+20	For	ACTGACACGCTGTCCTTTCC
rDNA coding +111/+130	Rev	GACAGCTTCAGGCACCGCGA

mouse cDNA primers		
Name	For/Rev	Sequence
Tip5	For	AAGATGTGTGGCTACAATGG
Tip5	Rev	TCTGCACCCATCAGCTCCG
Nanog	For	AAGCAGAAGATGCGGACTGT
Nanog	Rev	ATCTGCTGGAGGCTGAGGTA
Pax6	For	GCACATGCAAACACACATGA
Pax6	Rev	ACTTGGACGGGAACTGACAC
Minor satellites	For	CATGGAAAATGATAAAAACC
Minor satellites	Rev	CATCTAATATGTTCTACAGTGTGG
Major satellites	For	GACGACTTGAAAAATGACGAAATC
Major satellites	Rev	CATATTCCAGGTCCTTCAGTGTGC
rDNA spacer -1994/1975	For	GCAGACCGAGTTGCTGTAC

rDNA spacer -1922/1905	Rev	GGGTAGGACTTAAGCCTT
rDNA enhancer -554/-535	For	GAAGCCCTCTTGTCCCCGTC
rDNA enhancer -466/-447	Rev	GATCCAAAGCTCCAGCTGAC
rDNA promoter -165/-145	For	GACCAGTTGTTCCTTTGAGG
rDNA promoter -21/-1	Rev	ACCTATCTCCAGGTCCAATAG
45S pre-rRNA +550/570	For	CTCTTGTTCTGTGTCTGCC
45S pre-rRNA +745/765	Rev	GCCCGCTGGCAGAACGAGAAG
Line L1 ORF2	For	TTTGGGACACAATGAAAGCA
Line L1 ORF2	Rev	CTGCCGTCTACTCCTCTTGG
IAPgag	For	AGCAGGTGAAGCCACTG
IAPgag	Rev	CTTGCCACACTTAGAGC
Oct-4	For	GGCGTTCGCTTTGGAAAGGTGTTC
Oct-4	Rev	CTCGAACCACATCCTTCTCT
Rex1	For	AGAAAGCAGGATCGCCTCAC
Rex1	Rev	AGGGAACTCGCTTCCAGAAC
Rps12	For	GAAGCTGCCAAAGCCTTAGA
Rps12	Rev	AACTGCAACCAACCACCTTC
Gapdh	For	TGCACCACCAACTGCTTAGC
Gapdh	Rev	GGCATGGACTGTGGTCATGAG

ChIP primers		
Name	For/Rev	Sequence
rDNA promoter -165/-145	For	GACCAGTTGTTCCTTTGAGG
rDNA promoter -21/-1	Rev	ACCTATCTCCAGGTCCAATAG
rDNA coding +2251/70	For	GCATCGGTGTGTCGGCATCG
rDNA coding +2346/65	Rev	CTGAGCAGTCCCACCACACC
rDNA coding +8124/145	For	GCGACCTCAGATCAGACGTGG
rDNA coding +8203/224	Rev	CTGTTCACTCGCCGTTACTGAG
Minor satellites	For	CATGGAAAATGATAAAAACC
Minor satellites	Rev	CATCTAATATGTTCTACAGTGTGG
Major satellites	For	GACGACTTGAAAAATGACGAAATC
Major satellites	Rev	CATATTCCAGGTCCTTCAGTGTGC
Evx1 promoter	For	TACACAGCATCTGGGGAGTG
Evx1 promoter	Rev	GTGTGCTGGGTTAAGGGAGA
Gapdh promoter	For	GGTTGCTGTGTCACTACCGAAGAA
Gapdh promoter	Rev	AAATGGAGAAGTGTGGGTCTCCCT
Line L1 ORF2	For	TTTGGGACACAATGAAAGCA
Line L1 ORF2	Rev	CTGCCGTCTACTCCTCTTGG
IAPgag	For	AGCAGGTGAAGCCACTG
IAPgag	Rev	CTTGCCACACTTAGAGC

References

Bibel, M., Richter, J., Schrenk, K., Tucker, K.L., Staiger, V., Korte, M., Goetz, M., and Barde, Y.A. (2004). Differentiation of mouse embryonic stem cells into a defined neuronal lineage. Nat Neurosci *7*, 1003-1009.

Li, B., and Dewey, C.N. (2011). RSEM: accurate transcript quantification from RNA-Seq data with or without a reference genome. BMC Bioinformatics *12*, 323.

Martens, J.H., O'Sullivan, R.J., Braunschweig, U., Opravil, S., Radolf, M., Steinlein, P., and Jenuwein, T. (2005). The profile of repeat-associated histone lysine methylation states in the mouse epigenome. EMBO J *24*, 800-812.

Robinson, M.D., McCarthy, D.J., and Smyth, G.K. (2010). edgeR: a Bioconductor package for differential expression analysis of digital gene expression data. Bioinformatics *26*, 139-140.

Santoro, R. (2014). Analysis of chromatin composition of repetitive sequences: the ChIP-Chop assay. Methods Mol Biol *1094*, 319-328.

Santoro, R., Li, J., and Grummt, I. (2002). The nucleolar remodeling complex NoRC mediates heterochromatin formation and silencing of ribosomal gene transcription. Nat Genet *32*, 393-396.

Nucleic Acids Research Advance Access published February 8, 2014

Nucleic Acids Research, 2014, 1–11
doi:10.1093/nar/gku131

ARTD2 activity is stimulated by RNA

Karolin Léger[1,2], Dominik Bär[1], Nataša Savić[1,2], Raffaella Santoro[1] and Michael O. Hottiger[1,*]

[1]Institute of Veterinary Biochemistry and Molecular Biology, University of Zurich, Winterthurerstrasse 190, 8057 Zurich, Switzerland and [2]Life Science Zurich Graduate School, University of Zurich, 8057 Zurich, Switzerland

Received April 29, 2013; Revised January 20, 2014; Accepted January 22, 2014

ABSTRACT

ADP-ribosyltransferases (ARTs) are important enzymes that regulate the genotoxic stress response and the maintenance of genome integrity. ARTD1 (PARP1) and ARTD2 (PARP2) are homologous proteins that modify themselves and target proteins by the addition of mono- and poly-ADP-ribose (PAR) moieties. Both enzymes have been described to be involved in the genotoxic stress response. Here, we characterize cellular PAR formation on hydrogen peroxide (H_2O_2) or N-methyl-N′-methyl-nitro-N-nitrosoguanidine (MNNG) stress, in combination with application of the RNA polymerase I inhibitor Actinomycin D (ActD), known to cause accumulation of short RNA polymerase I-dependent rRNA transcripts. Intriguingly, co-treatment with ActD substantially increased H_2O_2- or MNNG-induced PAR formation. In cells, this enhancement was predominantly mediated by ARTD2 and not ARTD1. *In vitro* experiments confirmed that ARTD2 is strongly activated by RNA and that the N-terminal SAP domain is important for the binding to RNA. Thus, our findings identify a new activator of ARTD2-dependent ADP-ribosylation, which has important implications for the future analysis of the biological role of ARTD2 in the nucleus.

INTRODUCTION

Cells have evolved a complex and diverse arsenal of mechanisms to overcome genotoxic stress and to guarantee genome integrity (1). Depending on the type of stress, different response mechanisms are activated to repair damaged DNA or to prevent its inheritance (2,3). In addition to factors that directly bind and replace incorrect bases and repair DNA strand breaks, a variety of proteins are indirectly involved in the genotoxic stress response by regulating the levels and activities of other proteins or by modulating chromatin structure. ADP-ribosyltransferases (ARTs) are prominent members of this group of enzymes.

ARTs use nicotinamide adenine dinucleotide (NAD^+) as a substrate for the synthesis of mono- and poly-ADP-ribose modifications on target proteins (4). The ART protein family is divided into diphtheria toxin-like ARTs (ARTDs) and cholera toxin-like ARTs (ARTCs) (5). In humans, the ARTD (PARP) family currently comprises 18 nuclear and cytoplasmic mono- and poly-ARTs, while ARTCs are mainly extracellular enzymes that only transfer a single ADP-ribose unit to their target proteins (5).

Proteins of the ARTD family have been implicated in a plethora of cellular functions (6,7). Research during the past years has documented numerous functions of ARTD1 (PARP1) and of ADP-ribosylation in general that are not directly linked to DNA repair or the DNA damage response (8,9). The function of ARTD1 in DNA repair is substantiated by the strong activation of ARTD1 activity by DNA *in vitro*, as well as by the strong induction of poly-ADP-ribosylation on treatment of cells with DNA-damaging agents. Nevertheless, a direct involvement of DNA damage in the activation of ARTD1 *in vivo* is still largely based on correlations. PAR formation is dependent on the severity of the genotoxic stress and can even lead to cell death due to depletion of NAD^+ and ATP (10). The functional involvement of ADP-ribosylation in the DNA damage response has provided the incentive to generate PARP inhibitors as antitumor drugs, which are being developed and tested as novel therapies (11–14). The closest homolog of ARTD1 is ARTD2 (PARP2), which too is able to mono- and poly-ADP-ribosylate itself in addition to target proteins. Although ARTD1 has already been discovered several decades ago, ARTD2 was coincidentally discovered much later in the 1990s because of the detection of residual PAR-forming activity in mouse embryonic fibroblasts (MEFs) from ARTD1 knockout mice (15). Like ARTD1, ARTD2 has also been implicated in various cellular functions, which include genome and chromosome stability, heterochromatin integrity, cell death, differentiation and inflammation (16). Mammalian ARTD2 is a 66.2-kDA protein with a C-terminal catalytic domain that is 69% similar to the homologous domain in ARTD1 (15,17). Despite this common domain, ARTD2

*To whom correspondence should be addressed. Tel: +41 44 635 54 74; Fax: +41 44 635 6840; Email: hottiger@vetbio.uzh.ch

is catalytically much less active than ARTD1, suggesting that ARTD2 may become activated by different and as yet unknown stimuli. While the DNA binding domain of ARTD1 contains two Zn fingers and a Zn-binding domain, the DNA binding element of ARTD2 is represented by the SAF-A/B, Acinus and PIAS DNA-binding (SAP) domain. Furthermore, ARTD2 seems to modify different proteins, suggesting that both enzymes might regulate distinct biological functions (18,19). Thus, the identification of such new ARTD2 activators will likely also reveal novel biological phenomena that are regulated specifically by ARTD2.

Nucleoli are sites of ribosomal RNA (rRNA) gene transcription, rRNA maturation and ribosome production, and assemble around the nucleolar organizer regions (20,21). A human diploid cell contains ~400 rRNA genes, which are all organized in head-to-tail tandem repeats on five different chromosomes (21). However, as in highly metabolically active cells, only a subset of these genes is actively transcribed (22,23). The remaining rRNA genes are silenced in a tissue- and cell type-specific manner (24). Active rRNA genes are transcribed by RNA polymerase I (Pol I) to synthesize a 45S pre-rRNA. For the initiation of rRNA transcription, Pol I has to be part of a multi-protein complex that includes factors such as UBF, SL1 and TIF-IA (25). The production of ribosome subunits is heavily influenced by diverse stress stimuli and metabolic changes (26). The cell reacts to nutrient starvation, oxidative stress or inhibition of protein synthesis with a decrease of rRNA transcription, whereas growth factors and proliferation-stimulating agents increase rRNA transcription. Actinomycin D (ActD) inhibits rRNA synthesis already at low concentrations (50 ng/ml), whereas RNA polymerases II (Pol II) and III (Pol III) are inhibited only at higher concentrations (Pol II > 1 μg/ml, Pol III > 5 μg/ml) (27,28). ActD intercalates into CG-rich regions of the DNA, and thus stabilizes covalent topoisomerase I-DNA complexes, preventing progression of RNA polymerase, thereby inhibiting RNA synthesis (29). The intercalation mainly takes place downstream of rDNA transcription start sites, thus inhibiting transcription during elongation, which leads to an immense accumulation of short RNA transcripts over time (30,31). In *Drosophila*, ARTD1 has been reported to regulate ribosomal biogenesis at the posttranscriptional pre-rRNA processing level (32). Furthermore, ARTD1 and ARTD2 have both been shown to co-localize with B23/nucleophosmin and nucleolin, nucleolar proteins involved in several processes including rRNA transcription and elongation, ribosome assembly and rRNA processing (33,34). However, no direct effect of ARTD1 and ARTD2 on Pol I transcription was described in these studies. More recently, ARTD1 has been linked to heterochromatin formation, specifically to silencing of rRNA genes in the nucleolus (35,36).

Here, we characterize the nucleolar function of ARTD2 on different stresses. Hydrogen peroxide (H_2O_2) or N-methyl-N'-methyl-nitro-N-nitrosoguanidine (MNNG) treatment of different cell lines induced PAR formation in the nucleolus. Co-treatment with low doses of ActD enhanced PAR formation. Surprisingly, this co-treatment mainly activated ARTD2. *In vitro* experiments confirmed that ARTD2 is strongly activated by short rRNA and other single-stranded RNAs, but not by double-stranded DNA, through its SAP domain. Thus, our findings reveal a new activator of ARTD2, which opens new possible implications for the future analysis of the biological role of ARTD2.

MATERIALS AND METHODS

Cell culture

T24 bladder tumor cells were cultivated in McCoy's 5 A medium (Gibco, Invitrogen, CA, USA) at 37°C. NIH/3T3, HeLa cells and MEFs were cultivated in Dulbecco's modified Eagle's medium (PAA, Pasching, Austria). MD-MBA-231 cells were cultivated in Roswell Park Memorial Institute medium (Gibco, Invitrogen, CA, USA). All media were supplemented with 1% (v/v) Penicillin/Streptomycin and 10% (v/v) fetal calf serum (Gibco, Invitrogen, CA, USA).

siRNA transfection

Negative control allstars (siMock), human siPARP1 (SI02662996), human siPARP2 (SI02664725), human siPARG (SI00677782), mouse siPARP1 (SI02731428) and mouse siPARP2 (SI02735670) were all obtained from Qiagen (Hilden, Germany). Cells were seeded 1 day before transfection (5×10^5 cells per 6 cm plate) and transfected with 40 nmol siRNA per plate and RNAi MAX lipofectamine (Invitrogen, Carlsbad, CA, USA).

Antibodies

The following antibodies were used: from Santa Cruz Biotechnology, Inc (Dallas, TX, USA): PARP1/ARTD1 (H-250, sc-7150, rabbit), Pol I (RPA 194, H-300, sc-28714, rabbit). From Active motif (Carlsbad, CA, USA): PARP2 (39744, rabbit). From Sigma Aldrich (St. Louis, MO, USA): tubulin (T6199, mouse). From Cell Signaling (Danvers, MA, USA): fibrillarin (C13C3). From Merck-Millipore (Billerica, MA, USA): phosphor-Histone H2A.X (Ser139). From Jackson ImmunoResearch Laboratories (Suffolk, UK): secondary FITC-conjugated AffiniPure goat anti-mouse, secondary Cy3™ - conjugated AffiniPure goat anti-mouse. From Invitrogen (Gibco, Invitrogen, CA, USA): Alexa-Fluor 488 anti-rabbit IgG (A11008). The antibody 10H anti-PAR was used to identify PAR by immunofluorescence (IF).

RNA analysis

RNA was purified using TRIzol® RNA Isolation Reagent (500 μl, Life Technologies, CA, USA) and reverse transcribed according to the supplier's protocol (High Capacity cDNA Reverse Transcription Kit, Applied Biosystems, Foster City, CA, USA). Quantitative real-time polymerase chain reactions (qPCR) were performed with SYBR® green SensiMix SYBR Hi-ROX Kit (Bioline Reagents Ltd., London, UK) and a Rotor-Gene Q 2plex HRM System (Qiagen, Hilden, Germany).

Cell lysis, sodium dodecyl sulfate polyacrylamide gel electrophoresis (SDS-PAGE) and western blot analysis

Whole cell lysis was performed either with trypsinized cells or directly on plates by using RIPA lysis buffer (50 mM Tris, pH 8, 400 mM NaCl, 0.5% NP40, 1% DOC, 0.1% SDS, 1 μg/ml pepstatin, 1 μg/ml bestatin, 1 μg/ml leupeptin, 2 mM PMSF, 10 mM β-Glycerophosphate, 1 mM NaF and 1 mM dithiothreitol; 10 min, 4°C). Proteins were quantified using the Lowry assay and, if not otherwise indicated, 30 μg of protein extract was loaded and separated on a 10 or 12% SDS-polyacrylamide gel (120 V, 2 h). The gel was blotted on a polyvinylidene difluoride membrane and analysed by using protein specific antibodies.

Immunofluorescence microscopy

Cells were seeded on coverslips (10^5 cells per well in a 24-well-plate) and grown overnight. After H_2O_2 (1 mM in FCS-free medium, 10 min), MNNG (500 μM in FCS-free medium, 30 min) or medium-only treatment, cells were fixed (methanol: acetic acid 3:1, 5 min on ice), washed twice with phosphate buffered saline (PBS) and incubated with antibody (1:350) in PBS (containing 5% milk and 0.05% Tween, 1 h at room temperature or overnight at 4°C). When indicated, 4% PFA was used as fixation method (15 min, room temperature). Cells were then incubated with antibody for 1 h at room temperature. After washing with PBS, coverslips were mounted with Vectashield containing 4′,6-diamidino-2-phenylindole (DAPI; Vector Laboratories, Burlingame, CA, USA). Conventional microscopy was carried out using a Leica DMI 6000B light microscope (Leica microsystems GmbH, Wetzlar, Germany). Confocal laser scanning microscopy was carried out with a Leica SP 5 resonant APD system (Leica microsystems GmbH, Wetzlar, Germany).

The mean PAR signal intensity per cell was quantified with ImageJ (37) in at least 100 cells per replicate. The color threshold was set for Max entropy and B&W. According to the intensity of the picture, the threshold was set for each experiment the same way; thus, different replicates were comparable with each other.

Co-localization was quantified with Imaris (Bitplane, Belfast, UK) using the co-loc application. The thresholds were set for all three channels (DAPI, blue; PAR, red; and fibrillarin, green) and kept for the whole analysis. At least 50 cells were analyzed for H_2O_2 treated samples (from three biological replicates) and at least 25 cells were analyzed for H_2O_2 ActD treated samples (from two biological replicates).

In vitro RNA transcription

Linearized vectors containing rRNA sequences (mouse rRNA from −16 to +130 and −232 to −1) and control sequences (36) were used to *in vitro* transcribe RNA using T7 polymerase. After DNase I treatment, transcripts were double purified using TRIzol reagent (Invitrogen, Carlsbad, CA, USA) according to the manufacturer's protocol.

In vitro ARDT1 or ARTD2 activity assay

Ten picomoles of baculovirus-purified MYC-hARTD1(wt)-HIS or purified human ARTD2(fl)-HIS was incubated with NAD^+ in the reaction buffer (250 mM Tris–HCl, pH 8, 20 mM $MgCl_2$, 1.25 mM dithiothreitol, 5 μg/ml P/B/L–proteinase inhibitors, 30°C, 10 min). Five picomoles of EcoRI linker DNA or different concentrations as indicated of short RNA transcripts were added to the reaction. For ADP-ribosylation reactions, radioactive NAD^+ (^{32}P, final concentration 100 nM) and nonradioactive NAD^+ (final concentration 1.6 or 16 μM) were added. Reactions were terminated by adding Laemmli buffer and subsequent boiling of the samples (5 min, 95°C). SDS-PAGE was performed; gels were stained with coomassie, destained and subjected to film exposure. The autoradiography was quantified with the software GelEval (http://www.frogdance.dundee.ac.uk/).

In vitro poly-ADP-ribose-glycohydrolase (PARG) assay

ARTD1 auto-ADP-ribosylation was carried out as described before and the reaction mix was purified over illustra MicroSpin G-50 Columns (GE Healthcare GmbH Europe, Freiburg, Germany). Equal amounts of reaction mix were added to prechilled tubes containing baculo-purified hPARG-(fl) (2 pmol). Reactions were carried out in the presence or absence of the indicated molecules.

Nothern blot and Northwestern analysis

Purified RNA from NIH/3T3 or T24 cells pretreated with ActD (50 ng/ml for 0.5 h, 4 h or 20 h) and rRNA transcripts were monitored by hybridization to a ^{32}P-labeled riboprobe complementary to +1/+130 mouse or human rRNA sequences. Northwestern analysis was performed as described previously (36).

RESULTS

H_2O_2 treatment predominantly induces nucleolar PAR formation

To investigate the localization and molecular mechanism of PAR formation, T24 cells were treated with H_2O_2 (1 mM for 10 min). PAR formation was analysed by IF using a 10H anti-PAR antibody and both conventional and confocal fluorescence microscopy. The PAR signal was localized mainly to regions of the nucleus that were stained weakly with DAPI, indicating that nucleoli are sites of PAR formation (Figure 1A). The PAR signal in T24 cells treated with H_2O_2 co-localized with ARTD1, which suggests that ARTD1 is at least partly responsible for PAR synthesis in response to oxidative stress in T24 cells (Figure 1B). Co-staining with anti-Pol I and anti-fibrillarin antibodies suggested partial co-localization with the PAR signal (Figure 1C and D). Computerized analysis of the acquired images revealed that 60–65% of the fibrillarin co-localized with a strong PAR signal (Figure 1E). Similar levels of co-localization of fibrillarin with PAR signals were observed in H_2O_2-treated NIH/3T3 (Figure 1D and E). H_2O_2-treated HeLa cells and MEFs displayed a similar location of the PAR signal in

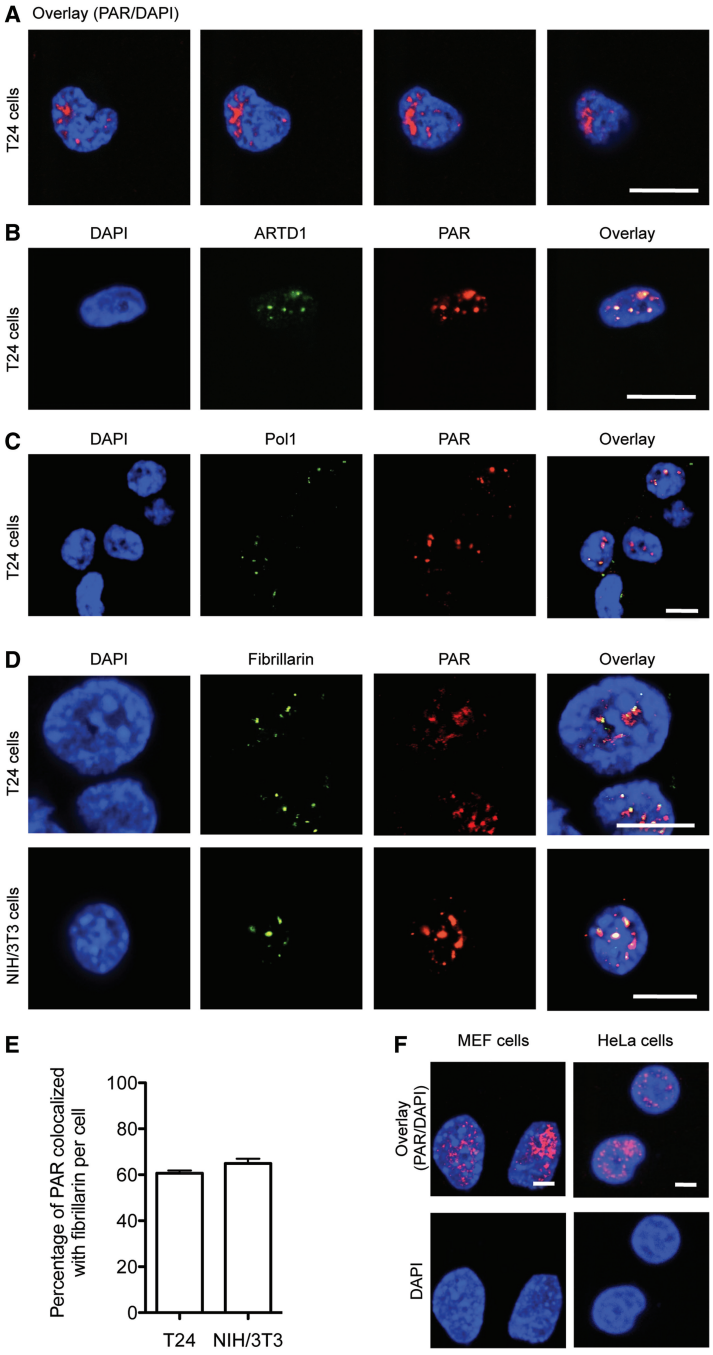

Figure 1. H_2O_2 treatment induces nucleolar poly-ADP-ribose formation. Confocal immunofluorescence microscopy of PAR (red) was performed after H_2O_2 treatment (1 mM, 10 min). (**A**) Z-Stack-resolution of T24 cells, bar = 10 µM. (**B**) Double-staining of T24 cells: PAR (red), ARTD1 (green), bar = 10 µM. (**C**) Double-staining of T24 cells: PAR (red), RNA Pol 1 (green), bar = 10 µM. (**D**) Double staining of T24 (upper row) and 3T3 (lower row) cells after H_2O_2 treatment (1 mM, 10 min): PAR (red) and fibrillarin (green), bar = 10 µM. (**E**) Quantification of the co-localization of the PAR signal and fibrillarin staining in T24 and NIH/3T3 cells. (**F**) Confocal IF microscopy of PAR (red) after H_2O_2 treatment (1 mM, 10 min) was analyzed in MEF and HeLa cells. Bar = 10 µM.

nucleoli (Figure 1F). Taken together, these results indicate that the nucleoli are the main location of cellular PAR formation during oxidative stress.

ActD treatment enhances nucleolar PAR formation on H_2O_2 and MNNG stimulation

Although H_2O_2- and MNNG-induced PAR formation has been attributed to DNA damage, a link between stress-induced PAR synthesis and Pol I-dependent transcription has not been documented previously. To investigate this possibility, we pretreated cells for 20 h with a low dose of ActD (50 ng/ml), which inhibits Pol I-dependent transcription (38), before the exposure to H_2O_2 or MNNG. Intriguingly, pretreatment with ActD followed by exposure to H_2O_2 or MNNG increased both the number of PAR-positive T24 cells and the intensity of the PAR signal in comparison with cells not pretreated with ActD (Figure 2A and B). A similar effect of ActD on the PAR signal was also observed in cells fixed with PFA, thus excluding the possibility that the results obtained by the methanol/acetic acid fixation protocol were an artifact (Supplementary Figure S1A, upper part).

In PFA-fixed cells, PAR formation assessed by confocal microscopy was also localized to DAPI-poor regions (Supplementary Figure S1A, lower part). However, the apparent extent of PAR and fibrillarin co-localization in PFA-fixed cells was less than that in methanol/acetic acid-fixed cells. This discrepancy could be due to PFA fixation leading to masking of the epitope for antibody recognition, an observation that we also made for other nucleolar proteins, which can only be detected in nucleoli when the denaturating action of methanol fixation is used (R.S., unpublished observation). ActD enhanced H_2O_2- or MNNG-induced PAR formation also in NIH/3T3, HeLa and MDA-MB-231 cells (Supplementary Figure S1B–D), indicating that the observed ActD effect is biologically conserved. ActD on its own did not induce PAR formation, indicating that ActD caused increased PAR formation by enhancing the signals induced by H_2O_2 or MMNG. Furthermore, ActD did not alter localization of PAR to nucleoli, as indicated by the unchanged co-staining with fibrillarin (Figure 2C and Supplementary Figure S1D).

To analyze whether ActD-induced PAR formation was due to the induction of cell death, cell viability was monitored. ActD pretreatment with the low concentration of 50 ng/ml did not significantly affect cell viability, while higher ActD concentrations (1 µg/ml) strongly reduced cell viability in T24 cells (Figure 2D). To exclude DNA damage as the stimulus for PAR formation, the levels of histone H2AX phosphorylation (γH2AX), a modification that occurs at sites flanking DNA double-strand breaks (DSBs) (39), were analyzed. Both of the positive controls, the topoisomerase II inhibitor etoposide (50 µM, 16 h), as well as high doses of ActD, induced γH2AX formation in T24 cells (Figure 2E). We thus conclude that the strong PAR signal induced by the pretreatment of T24 cells with the low concentration of ActD (50 ng/ml) was not due to DNA damage or cell death. As PAR formation has previously been reported to occur under replicative stress (40), we also analyzed the PAR signal as well as the γH2AX formation in quiescent (G_0 phase) T24 cells, on combined ActD and H_2O_2, or ActD, etoposide and MNNG treatment (Figure 2E and Supplementary Figure S2A). Comparable with nonarrested cells, quiescent cells treated with the low ActD concentration also displayed PAR formation, but did not show induction of γH2AX, indicating that enhanced PAR formation on ActD treatment does not depend on replicative stress and cell proliferation.

We next tested whether enhanced PAR formation depends on Pol I transcription. The analysis of 45S pre-rRNA levels confirmed that ActD was effective in impairing pre-rRNA synthesis (>90%), while H_2O_2 or MNNG reduced pre-rRNA levels only by 25–40% under the tested conditions (Supplementary Figure S2B). In contrast to ActD, pretreatment with the RNA Pol II inhibitor α-amanitin did not induce PAR formation (Supplementary Figure S2C), indicating that formation of ActD-mediated PAR formation depends on RNA Pol I transcription. Because PAR formation was inhibited by Olaparib, an inhibitor of ARTDs including ARTD1 and ARTD2 [Supplementary Figure S2D, (41)], ARTD1 and/or ARTD2 could potentially be involved in the synergistic effect between stress signaling and the interference of 45S pre-rRNA synthesis for PAR accumulation in the nucleolus.

ARTD2, but not ARTD1, is responsible for the ActD-dependent enhancement of PAR formation after H_2O_2 or MNNG treatment

To investigate whether ActD exerts its synergistic effect through ARTD1 and/or ARTD2, T24 cells were depleted of either ARTD1 or ARTD2 by siRNA (Supplementary Figure S2E), pretreated with ActD as indicated and PAR formation was induced by H_2O_2 or MNNG. PAR formation was quantified by evaluating the mean signal intensity of immunostained cells. PAR levels were more strongly induced after H_2O_2 treatment as compared with MNNG treatment (Figure 3A and B). ActD pretreatment for 4 or 20 h enhanced the mean PAR intensity per cell irrespective of whether H_2O_2 or MNNG was used, while short pretreatment of only 30 min had no effect. This enhancement of PAR formation on ActD treatment was more prominent in MNNG-treated cells as compared with H_2O_2-treated cells under the tested conditions (Figure 3B). Knockdown of ARTD1 almost completely abolished PAR formation in T24 cells treated with H_2O_2, indicating that ARTD1 is responsible for most of the H_2O_2-induced PAR formation (Figure 3C). However, prolonged (4–20 h, 50 ng/ml) pretreatment of ARTD1-silenced cells with ActD strongly enhanced H_2O_2-induced PAR formation, despite the strong sustained reduction of ARTD1 protein levels (Figure 3C). These results indicate that the synergistic effect between oxidative stress and the inhibition of 45S pre-rRNA synthesis on PAR accumulation in the nucleolus is not mediated by ARTD1. In contrast, compared with siMOCK-treated cells, no additional increase in PAR formation was observed after 4–20 h of ActD pretreatment in ARTD2-depleted T24 cells (Figure 3C), indicating

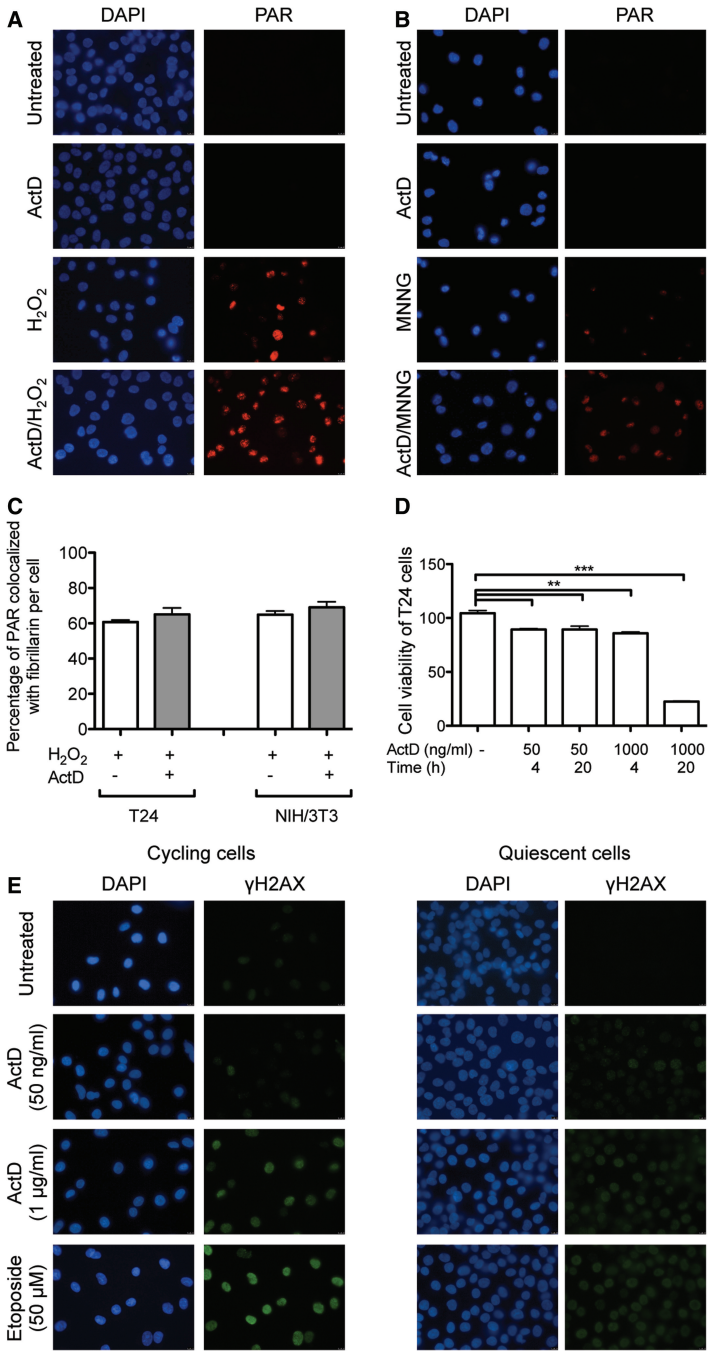

Figure 2. ActD treatment increases nuclear poly-ADP-ribose formation on H_2O_2 and MNNG stimulation. (**A**) Immunofluorescence microscopy of T24 cells was examined after H_2O_2 (1 mM, 10 min) and/or ActD treatment (50 ng/ml, 20 h) and stained for PAR formation (red). (**B**) Immunofluorescence microscopy of T24 cells after MNNG (500 μM, 30 min) and/or ActD treatment (50 ng/ml, 20 h) was examined. (**C**) Quantification of the co-localization of the PAR signal and fibrillarin staining in T24 and NIH/3T3 cells pretreated with ActD. (**D**) Viability assay (Alamar blue assay) of T24 cells treated with ActD (50 and 1000 ng/ml) for 4 h or 20 h [$n = 3$, one-way analysis of variance (ANOVA), followed by Tukey's post hoc test]. (**E**) Immunofluorescence microscopy of T24 cells stained for γ-H2AX after ActD treatment (50 and 1000 ng/ml for 20 h) and etoposide (50 μM for 16 h), either in cycling or in quiescent T24 cells.

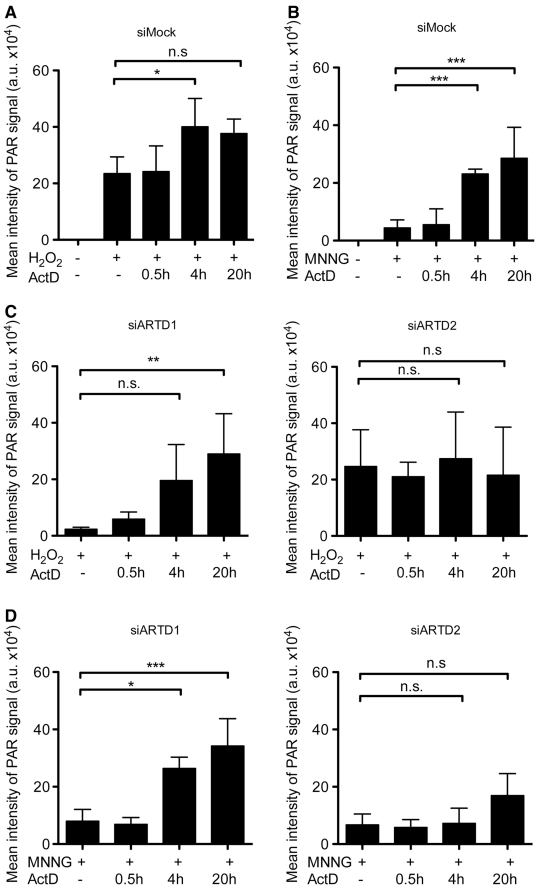

Figure 3. ARTD2 is responsible for the ActD-dependent increase in poly-ADP-ribose formation. Quantitative PAR analysis of siMock-, siARTD1- and siARTD2-treated T24 cells was performed after treatment with ActD (50 ng/ml for 0.5, 4 and 20 h) and H_2O_2 (1 mM, 10 min) or MNNG treatment (500 µM, 30 min). At least 100 cells were analyzed per replicate (for 0.5 h; $n = 2$ for siARDT1 and siARTD2 samples, for other conditions $n = 3$–5, one-way ANOVA with Tukey's post hoc test was performed). (**A**) siMock T24 cells were treated with H_2O_2. (**B**) siMock T24 cells were treated with MNNG. (**C**) H_2O_2 treated siARTD1 (left) and siARTD2 (right) T24 cells. (**D**) MNNG-treated siARTD1 (left) and siARTD2 (right) T24 cells. n.s.: $P > 0.05$; $^*P \leq 0.05$; $^{**}P \leq 0.01$; $^{***}P \leq 0.001$.

that the stimulatory ActD effect on H_2O_2-induced PAR formation was mainly regulated by ARTD2. The presence of ARTD2, but not of ARTD1, also seemed to be responsible for the increased PAR formation observed after co-treatment of ActD and MNNG in T24 cells after 4 h (Figure 3D). The slight, but not significant, increase of the PAR signal in cells pretreated with ActD for 20 h and co-treated with MNNG may hint at the delayed and attenuated stimulation of ARTD1, or an additional ARTD family member that catalyzes additional PAR formation under these conditions. H_2O_2 or MNNG treatment in combination with ActD in NIH/3T3 cells and subsequent quantification of the PAR formation by IF or visualization by western blot further confirmed that ARTD2 is responsible for the stimulatory ActD effect also in mouse cells (Supplementary Figure S3A–H for H_2O_2 or Supplementary Figure S4A and B for MNNG). Together, these results indicate that ARTD2 is involved in PAR formation in response to H_2O_2- or MNNG-treatment in combination with ActD in T24 and NIH/3T3 cells.

ARTD2 activity is stimulated by rRNA *in vitro*

The described synergistic effect between ActD and H_2O_2/MNNG on PAR formation could either be due to an inhibition of PAR degradation or a stimulation of PAR synthesis. The former was studied by determining whether ActD affects activity of the PARG, the primary enzyme responsible for degrading protein-bound poly-ADP-ribose (Figure 4A). *In vitro* ^{32}P-labeled PARylated ARTD1 was incubated with PARG in the presence of ActD or rRNA, and PARylated ARTD1 levels were monitored by autoradiography. Treatment with ActD or rRNA did not prevent degradation of PAR moieties of ARTD1, indicating that neither ActD nor rRNA affects PARG activity.

The results described above indicate that H_2O_2 induces PAR formation in the nucleoli (Figure 1). ActD impairs 45S pre-rRNA synthesis by preventing Pol I elongation through the rDNA coding region and leads to an accumulation of short RNA transcripts corresponding to sequences immediately downstream of the transcription start site (+1/+130), as detected by northern blotting (Figure 4B and Supplementary Figure S5A) (30,31). We described above that only prolonged treatment with ActD (4 and 20 h) enhanced formation of PAR in cells treated with H_2O_2 or MNNG (Figure 3). Because PAR formation correlated with the inhibition of 45S pre-rRNA synthesis (Supplementary Figure S5B), we hypothesized that the production of short rRNA transcripts induced by ActD treatment might stimulate ARTD2 activity. To test this hypothesis, we investigated the *in vitro* ARTD2 automodification in the presence of *in vitro* synthesized rRNA transcripts (corresponding to rDNA sequences from −16 to +130 bp) using P^{32}-labeled NAD^+ to monitor ADP-ribosylation (Figure 4C). Densitrometric analysis of the incorporated radiolabeled ADP-ribose revealed that the automodification of ARTD2 was stimulated by rRNA 3.4-fold stronger in comparison with double-stranded DNA, while rRNA stimulated ARTD1 only 0.7-fold compared with the stimulation with double-stranded DNA (Figure 4C). This effect did not seem to be mediated by specific rRNA sequences, as other nonnucleolar RNA transcripts were able to stimulate ARTD2 activity to a similar extent (Supplementary Figure S5C). In contrast to ARTD2, ARTD1 was strongly activated by double-stranded DNA and, as previously described (36), only exhibited 60% of its activity in the presence of RNA as compared with DNA (Figure 4C).

Because the ActD effect was only observed in the presence of genotoxic stress, we tested whether the activation of ARTD2 by RNA depends on double-stranded DNA. Addition of DNA did not enhance the stimulatory

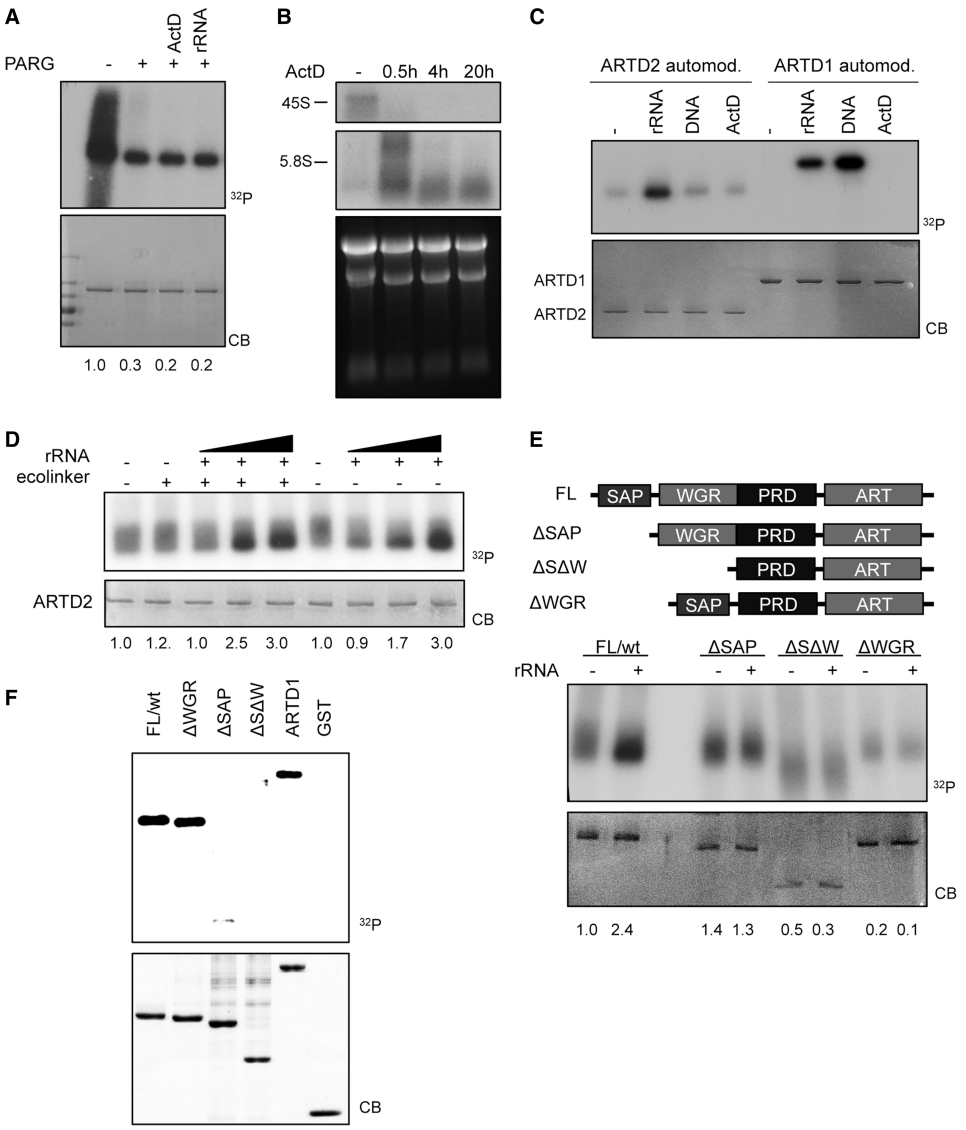

Figure 4. ARTD2 activity is stimulated by rRNA *in vitro* and binds to RNA via the SAP domain (**A**) *In vitro* radioactive PARG assay carried out with *in vitro* modified ARTD1. PARG was added to each reaction in combination with pretreatment of ActD (50 ng/ml) or rRNA (146 nt). The PARG reaction was performed for 15 min at 4 °C. Upper panel shows the autoradiography (^{32}P) and the lower panel the corresponding coomassie blue–stained gel (CB) of a representative experiment. Densitometric analysis of the radioactive signals was performed as described in M&M, and values obtained are indicated at the bottom of the panel. The PARG untreated value was arbitrarily set to 1. (**B**) Northern blot analysis of NIH/3T3 cells treated with ActD (50 ng/ml for 0.5, 4 and 20 h). Hybridization was performed with a riboprobe corresponding to +1/+130 mouse rRNA sequences. The lower panel shows 28S and 18S rRNA stained with ethidium bromide. (**C**) *In vitro* radioactive ARTD2 and ARTD1 activity assay was performed with 100 ng NAD^+ (^{32}P) in the presence of *in vitro* transcribed rRNA piece (146 nt), DNA linker or ActD (50 ng/ml). CB = coomassie blot. Densitometric analysis of the radioactive signals was performed as described in M&M and values obtained are included in the result section. (**D**) *In vitro* radioactive ARTD2 activity assay was performed with 1.6 μM NAD^+ (^{32}P) and *in vitro* transcribed rRNA fragment (146 nt) of different amounts (0.5, 5 and 10 pmol) and in presence or absence of 0.5 pmol DNA linker. Reaction was carried out at 30 °C, 10 min. Densitometric analysis of the radioactive signals was performed as in panel A and values obtained are indicated at the bottom of the panel. The untreated sample was arbitrarily set to 1. (**E**) *In vitro* radioactive ARTD2 activity assay with ARTD2 mutants was performed with 1.6 μM NAD^+ (^{32}P) in presence or absence of 5 pmol rRNA fragment (146 nt). FL/wt = full-length human ARTD2, ARDT2 ΔSAP mutant 95–583 aa, ARTD2 ΔSΔW mutant 231–583 aa, ARTD2 ΔWGR mutant without WGR domain (deleted aa 116–193). Densitometric analysis of the radioactive signals was performed as in panel (A) and values indicated at the bottom of the panel. The untreated wild-type sample was arbitrary set 1. (**F**) ARTD2 binds to RNA via the SAP domain. Northwestern analysis. Membrane-bound recombinant wild type and the indicated ARTD2 mutants as well as ARTD1 (see coomassie-stained gel, CB) were incubated with radiolabeled rRNA (−16 to +130) and bound RNA was visualized by autoradiography (^{32}P).

effect of RNA on ARTD2, confirming that RNA stimulates ARTD2 independent of DNA (Figure 4D).

ARTD2 binds to RNA through its SAP domain

To define which domain of ARTD2 is responsible for the RNA-mediated activation, we compared the effect of RNA on the activities of human $ARTD2_{FL}$ (full length) and $ARTD2_{\Delta SAP}$ (aa 95–583), a mutant that lacks the SAP domain and displays similar basal activity as $ARTD2_{FL}$. Although $ARTD2_{FL}$ was stimulated by RNA, the deletion of the SAP domain impaired RNA-mediated activation (Figure 4E). In addition to the loss of the stimulation by RNA, the additional deletion of the WGR domain (aa 231–583, $ARTD2_{\Delta S\Delta W}$), or removal of the WGR domain alone (deletion of aa 116–193, $ARTD2_{\Delta WGR}$) resulted in a strong reduction of the general ARTD2 activity (Figure 4E). RNA-binding experiments with these proteins confirmed that the SAP domain is responsible for the binding of ARTD2 to RNA. Together, these results suggest that RNA is a potent activator of ARTD2 enzymatic activity predominantly through the SAP domain, and that the WGR domain is an important structural element for the overall activity of the enzyme.

DISCUSSION

ADP-ribosylation has been implicated in several nucleolar processes such as ribosome biogenesis, formation of rDNA heterochromatin and stress sensing (32,34,36,42–44). Here, we show that H_2O_2 or MNNG induces PAR formation in the nucleoli of both mouse and human cells. This is in agreement with previous studies that found ARTD1 and ARTD2 to localize to nucleoli (34). The combination of H_2O_2 or MNNG treatment with low doses of ActD revealed a synergistic effect on PAR formation that is mediated by ARTD2. It was well-known before that ActD treatment leads to the accumulation of short rRNA transcripts, which might be responsible for the enhancement of PAR formation. Short rRNA transcripts were able to strongly stimulate ARTD2 activity via the SAP/WGR domain, while double-stranded DNA did not exhibit this effect. Our findings thus reveal a new activator for ARTD2-dependent ADP-ribosylation, which has important implications for the future analysis of the biological role of ARTD2 in the nucleus.

ADP-ribosylation and in particular the homologous enzymes ARTD1 and ARTD2 have been traditionally implicated in the response to DNA damage. An important cornerstone for this model is the strong *in vitro* activation of ARTD1 by double-stranded or nicked DNA, as well as the detection of PAR on treatment of cells with genotoxic compounds. In these DNA damage-dependent processes, ARTD2 displays much less activity than ARTD1, raising the question whether molecules other than activators of ARTD1 activate ARTD2. Our results strongly suggest that instead of binding to sites of DNA damage, ARTD2 associates with RNA in the nucleolus, providing an alternative cue to identify and respond to DNA damage. In support of this, recent data have implicated site-specific Dicer and Drosha RNA moieties in the control of DNA damage (45). Furthermore, the activation of ARTD2 by RNA may also be part of an intricate network of RNA surveillance and repair mechanisms to preserve RNA quality (46–48). The identification of ARTD2 activation by RNA is a new and unexpected result that may indicate an additional mean for monitoring not only genome integrity, but also other processes specific for ARTD2. Genetic disruption of ARTD2, but not of ARTD1, affects various differentiation processes in mice, including spermatogenesis (49), adipogenesis (50) and the survival of thymocytes (51).

Interestingly, the stimulation of ARTD2 *in vivo* was dependent on the co-stimulation with ActD and H_2O_2 or MNNG, indicating that additional signals induced by H2O2 or MNNG are required for the activation of ARTD2 by RNA. These signals might include the damage of RNA, as oxidative damage in RNA is usually higher than in DNA (52). However, our experiments with H_2O_2-pretreated RNA did not strengthen this hypothesis (data not shown). Alternatively, the treatment of cells with H_2O_2 or MNNG might induce signaling cascades that lead to the posttranslational modification of ARTD2, which is required for the stimulation with RNA, besides damaging the DNA. Future studies of the nucleolar ADP-ribose acceptors and the effect of ADP-ribosylation on the response to RNA damage are needed to reveal and define these functions in detail. Interestingly, the ActD effect was observed in both human and mouse cells, suggesting that the stimulation of ARTD2 is a biologically conserved effect.

Under the study conditions described here, cellular PAR formation on H_2O_2/MNNG treatment occurred to a large portion within nucleoli. Growing evidence indicates that the nucleolus plays a key role in monitoring and responding to cellular stress. After exposure to extra- or intracellular stress, signal pathways induce rapid downregulation of 45S pre-rRNA synthesis that is followed by perturbation of nucleolar structure, cell cycle arrest and stabilization of p53 (53). The formation of high levels of PAR in nucleoli under genotoxic stress conditions might be part of this nucleolus-dependent signaling. Whether PAR formation is due to a high accessibility of nucleolar DNA and RNA to chemical agents and how this occurs remains to be investigated.

Previous studies have shown that RNA is a key regulator of ARTD1 in the nucleolus [(36) and Figure 4D/F]. Nucleolar localization of ARTD1 is dependent on RNA and ARTD1 binds *in vivo* and *in vitro* to the nucleolar noncoding pRNA, an intergenic transcript implicated in the establishment of rDNA heterochromatin (54). pRNA associates with the zinc finger DNA binding domain of ARTD1 and stimulates ARTD1 activity, although to a lesser degree than double-stranded DNA [(36) and Figure 4D].

In this work, we provide evidence that RNA is a key regulator of ARTD2 enzymatic activity. The nucleolar localization of overexpressed ARTD2 has already been described (34) and the currently available antibodies do not permit a direct immunofluorescent localization of endogenous ARTD2 or determination of how RNA affects nucleolar occupancy of ARTD2. However, we

could demonstrate that RNA strongly activates ARTD2 activity. In contrast to ARTD1, double-stranded DNA did not activate ARTD2. These findings suggest that the structure and nature of nucleic acid is an important determinant for the regulation of ARTD2 function. Consistent with this, recent analyses with several DNA structures mimicking intermediates of different DNA metabolizing processes revealed that ARTD2 activation efficiency did not correlate with K(d) values for DNA (55). ARTD2 displayed the highest affinity for flap-containing DNA, but was more efficiently activated by 5′-overhang DNA, suggesting that single-stranded nucleic acids might be a general stimulator of ARTD2. The stimulation did not seem to be sequence-specific, as other RNAs tested were also able to strongly stimulate ARTD2 (36). We have identified SAP to be the main domain responsible for the stimulation by RNA. The SAP motif (after SAF-A/B, Acinus and PIAS) is a putative DNA/RNA binding domain found in diverse nuclear and cytoplasmic proteins (56,57). Based on the presented findings, it is thus possible that other proteins with a SAP motif similarly may bind RNA and be regulated by this binding. Interestingly, deleting the WGR domain only abolished the stimulation by RNA, but also the overall activity of ARTD2, indicating that the structural arrangement of the SAP and the CAT motif is functionally relevant.

Together, the strong activation of ARTD2 by RNA through the SAP domain is a likely underlying cause for the distinct and complementary functions mediated by this homolog as compared with ARTD1. The fact that RNA stimulates PAR formation by ARTD2 has not only mechanistic implications but also sheds new light on how ARTD2 and poly-ADP-ribosylation function during the genotoxic stress response.

SUPPLEMENTARY DATA

Supplementary Data are available at NAR Online.

ACKNOWLEDGEMENTS

P.O. Hassa is acknowledged for providing the 10H antibody and M. Stucki (University of Zurich, Switzerland) is acknowledged for providing the T24 cell line. Confocal microscopy was performed at the Center for Microscopy and Image Analysis of the University of Zurich. M. Fey is acknowledged for technical support. Florian Freimoser and Stephan Christen (University of Zurich, Switzerland) provided editorial assistance and critical input during the writing. K.L. designed and performed experiments; D.B. performed Northwestern analysis; N.S. produced synthetic RNA; R.S. and M.O.H. supervised the work and M.O.H. wrote the manuscript.

FUNDING

Forschungskredit of the University of Zurich (to K.L. and N.S.); Swiss National Science Foundation [310003A-135801 to R.S., 310030B_138667 and PDMFP3_127315 to M.O.H.]; Kanton of Zurich (to M.O.H.). Funding for open access charge: Swiss National Science Foundation.

Conflict of interest statement. None declared.

REFERENCES

1. Harper,J.W. and Elledge,S.J. (2007) The DNA damage response: ten years after. *Mol. Cell*, **28**, 739–745.
2. Zhou,B.B. and Elledge,S.J. (2000) The DNA damage response: putting checkpoints in perspective. *Nature*, **408**, 433–439.
3. Dianov,G.L. and Hubscher,U. (2013) Mammalian base excision repair: the forgotten archangel. *Nucleic Acids Res.*, **41**, 3483–3490.
4. Hassa,P.O., Haenni,S., Elser,M. and Hottiger,M.O. (2006) Nuclear ADP-ribosylation reactions in mammalian cells: where are we today and where are we going? *Microbiol. Mol. Bio.l Rev.*, **70**, 789–829.
5. Hottiger,M.O., Hassa,P.O., Lüscher,B., Schüler,H. and Koch-Nolte,F. (2010) Toward a unified nomenclature for mammalian ADP-ribosyltransferases. *Trends Biochem. Sci.*, **35**, 208–219.
6. Luo,X. and Kraus,W.L. (2012) On PAR with PARP: cellular stress signaling through poly(ADP-ribose) and PARP-1. *Genes Dev.*, **26**, 417–432.
7. Schreiber,V., Dantzer,F., Ame,J.-C. and De Murcia,G. (2006) Poly(ADP-ribose): novel functions for an old molecule. *Nat. Rev. Mol. Cell Biol.*, **7**, 517–528.
8. Hassa,P.O. and Hottiger,M.O. (2008) The diverse biological roles of mammalian PARPs, a small but powerful family of poly-ADP-ribose polymerases. *Front. Biosci.*, **13**, 3046–3082.
9. Kraus,W.L. and Hottiger,M.O. (2013) PARP-1 and gene regulation: Progress and puzzles. *Mol. Aspects Med.*, **34**, 1109–1123.
10. David,K.K., Andrabi,S.A., Dawson,T.M. and Dawson,V.L. (2009) Parthanatos, a messenger of death. *Front. Biosci.*, **14**, 1116–1128.
11. Banerjee,S. and Kaye,S. (2011) PARP inhibitors in BRCA gene-mutated ovarian cancer and beyond. *Curr. Oncol. Rep.*, **13**, 442–449.
12. Bryant,H., Schultz,N., Thomas,H., Parker,K., Flower,D., Lopez,E., Kyle,S., Meuth,M., Curtin,N. and Helleday,T. (2005) Specific killing of BRCA2-deficient tumours with inhibitors of poly(ADP-ribose) polymerase. *Nature*, **434**, 913–917.
13. Telli,M.L. (2011) PARP inhibitors in cancer: moving beyond BRCA. *Lancet Oncol.*, **12**, 827–828.
14. Underhill,C., Toulmonde,M. and Bonnefoi,H. (2010) A review of PARP inhibitors: from bench to bedside. *Ann. Oncol.*, **22**, 268–279.
15. Amé,J., Rolli,V., Schreiber,V., Niedergang,C., Apiou,F., Decker,P., Muller,S., Höger,T., Ménissier-de Murcia,J. and de Murcia,G. (1999) PARP-2, a novel mammalian DNA damage-dependent poly(ADP-ribose) polymerase. *J. Biol. Chem.*, **274**, 17860–17868.
16. Yelamos,J., Schreiber,V. and Dantzer,F. (2008) Toward specific functions of poly(ADP-ribose) polymerase-2. *Trends Mol. Med.*, **14**, 169–178.
17. Oliver,A.W., Ame,J.C., Roe,S.M., Good,V., de Murcia,G. and Pearl,L.H. (2004) Crystal structure of the catalytic fragment of murine poly(ADP-ribose) polymerase-2. *Nucleic Acids Res.*, **32**, 456–464.
18. Yelamos,J., Farres,J., Llacuna,L., Ampurdanes,C. and Martin-Caballero,J. (2011) PARP-1 and PARP-2: New players in tumour development. *Am. J. Cancer Res.*, **1**, 328–346.
19. Troiani,S., Lupi,R., Perego,R., Depaolini,S.R., Thieffine,S., Bosotti,R. and Rusconi,L. (2011) Identification of candidate substrates for poly(ADP-ribose) polymerase-2 (PARP2) in the absence of DNA damage using high-density protein microarrays. *FEBS J.*, **278**, 3676–3687.
20. Brown,D.D. and Gurdon,J.B. (1964) Absence of ribosomal RNA synthesis in the anucleolate mutant of Xenopus laevis. *Proc. Natl Acad. Sci. USA*, **51**, 139–146.

21. Hadjiolov,A.A. (1985) In: Beerman,A.M., Goldstein,L., Portrer,K.R. and Sitte,P. (eds), *Cell Biology Monographs*. Springer, New York, pp. 1–263.
22. Santoro,R. (2005) The silence of the ribosomal RNA genes. *Cell Mol. Life Sci.*, **62**, 2067–2079.
23. Santoro,R. (2011) In: Olson,M.J. (ed.), *The Nucleolus*. Springer, Basel, Switzerland, pp. 57–82.
24. Haaf,T., Hayman,D.L. and Schmid,M. (1991) Quantitative determination of rDNA transcription units in vertebrate cells. *Exp. Cell Res.*, **193**, 78–86.
25. Drygin,D., Rice,W.G. and Grummt,I. (2010) The RNA polymerase I transcription machinery: an emerging target for the treatment of cancer. *Annu. Rev. Pharmacol. Toxicol.*, **50**, 131–156.
26. Olson,M.O. (2004) Sensing cellular stress: another new function for the nucleolus? *Sci. STKE*, **2004**, pe10.
27. Perry,R.P. and Kelley,D.E. (1970) Inhibition of RNA synthesis by actinomycin D: characteristic dose-response of different RNA species. *J. Cell Physiol.*, **76**, 127–139.
28. Sobell,H.M. (1985) Actinomycin and DNA transcription. *Proc. Natl Acad. Sci. USA*, **82**, 5328–5331.
29. Trask,D.K. and Muller,M.T. (1988) Stabilization of type I topoisomerase-DNA covalent complexes by actinomycin D. *Proc. Natl Acad. Sci. USA*, **85**, 1417–1421.
30. Sentenac,A., Simon,E.J. and Fromageot,P. (1968) Initiation of chains by RNA polymerase and the effects of inhibitors studied by a direct filtration technique. *Biochim. Biophys. Acta*, **161**, 299–308.
31. Hadjiolova,K.V., Hadjiolov,A.A. and Bachellerie,J.P. (1995) Actinomycin D stimulates the transcription of rRNA minigenes transfected into mouse cells. Implications for the *in vivo* hypersensitivity of rRNA gene transcription. *Eur. J. Biochem.*, **228**, 605–615.
32. Boamah,E.K., Kotova,E., Garabedian,M., Jarnik,M. and Tulin,A.V. (2012) Poly(ADP-Ribose) polymerase 1 (PARP-1) regulates ribosomal biogenesis in *Drosophila* nucleoli. *PLoS Genet.*, **8**, e1002442.
33. Leitinger,N. and Wesierska-Gadek,J. (1993) ADP-ribosylation of nucleolar proteins in HeLa tumor cells. *J. Cell Biochem.*, **52**, 153–158.
34. Meder,V.S., Boeglin,M., de Murcia,G. and Schreiber,V. (2005) PARP-1 and PARP-2 interact with nucleophosmin/B23 and accumulate in transcriptionally active nucleoli. *J. Cell Sci.*, **118**, 211–222.
35. Guetg,C. and Santoro,R. (2012) Formation of nuclear heterochromatin: the nucleolar point of view. *Epigenetics*, **7**, 811–814.
36. Guetg,C., Scheifele,F., Rosenthal,F., Hottiger,M.O. and Santoro,R. (2012) Inheritance of silent rDNA chromatin is mediated by PARP1 via noncoding RNA. *Mol. Cell*, **45**, 790–800.
37. Schneider,C.A., Rasband,W.S. and Eliceiri,K.W. (2012) NIH Image to ImageJ: 25 years of image analysis. *Nat. Methods*, **9**, 671–675.
38. Bensaude,O. (2011) Inhibiting eukaryotic transcription: Which compound to choose? How to evaluate its activity? *Transcription*, **2**, 103–108.
39. Rogakou,E.P., Pilch,D.R., Orr,A.H., Ivanova,V.S. and Bonner,W.M. (1998) DNA double-stranded breaks induce histone H2AX phosphorylation on serine 139. *J. Biol. Chem.*, **273**, 5858–5868.
40. Ray Chaudhuri,A., Hashimoto,Y., Herrador,R., Neelsen,K.J., Fachinetti,D., Bermejo,R., Cocito,A., Costanzo,V. and Lopes,M. (2012) Topoisomerase I poisoning results in PARP-mediated replication fork reversal. *Nat. Struct. Mol. Biol.*, **19**, 417–423.
41. Wahlberg,E., Karlberg,T., Kouznetsova,E., Markova,N., Macchiarulo,A., Thorsell,A.G., Pol,E., Frostell,A., Ekblad,T., Oncu,D. *et al.* (2012) Family-wide chemical profiling and structural analysis of PARP and tankyrase inhibitors. *Nat. Biotechnol.*, **30**, 283–288.
42. Tulin,A., Stewart,D. and Spradling,A. (2002) The *Drosophila* heterochromatic gene encoding poly(ADP-ribose) polymerase (PARP) is required to modulate chromatin structure during development. *Genes Dev.*, **16**, 2108–2119.
43. Guerrero,P.A. and Maggert,K.A. (2011) The CCCTC-binding factor (CTCF) of *Drosophila* contributes to the regulation of the ribosomal DNA and nucleolar stability. *PLoS One*, **6**, e16401.
44. Rancourt,A. and Satoh,M.S. (2009) Delocalization of nucleolar poly(ADP-ribose) polymerase-1 to the nucleoplasm and its novel link to cellular sensitivity to DNA damage. *DNA Repair (Amst.)*, **8**, 286–297.
45. Francia,S., Michelini,F., Saxena,A., Tang,D., de Hoon,M., Anelli,V., Mione,M., Carninci,P. and d'Adda di Fagagna,F. (2012) Site-specific DICER and DROSHA RNA products control the DNA-damage response. *Nature*, **488**, 231–235.
46. Wurtmann,E.J. and Wolin,S.L. (2009) RNA under attack: cellular handling of RNA damage. *Crit. Rev. Biochem. Mol. Biol.*, **44**, 34–49.
47. Li,Z., Wu,J. and Deleo,C.J. (2006) RNA damage and surveillance under oxidative stress. *IUBMB Life*, **58**, 581–588.
48. Aas,P.A., Otterlei,M., Falnes,P.O., Vagbo,C.B., Skorpen,F., Akbari,M., Sundheim,O., Bjoras,M., Slupphaug,G., Seeberg,E. *et al.* (2003) Human and bacterial oxidative demethylases repair alkylation damage in both RNA and DNA. *Nature*, **421**, 859–863.
49. Dantzer,F., Mark,M., Quenet,D., Scherthan,H., Huber,A., Liebe,B., Monaco,L., Chicheportiche,A., Sassone-Corsi,P., de Murcia,G. *et al.* (2006) Poly(ADP-ribose) polymerase-2 contributes to the fidelity of male meiosis I and spermiogenesis. *Proc. Natl Acad. Sci. USA*, **103**, 14854–14859.
50. Bai,P., Houten,S.M., Huber,A., Schreiber,V., Watanabe,M., Kiss,B., de Murcia,G., Auwerx,J. and Menissier-de Murcia,J. (2007) Poly(ADP-ribose) polymerase-2 [corrected] controls adipocyte differentiation and adipose tissue function through the regulation of the activity of the retinoid X receptor/peroxisome proliferator-activated receptor-gamma [corrected] heterodimer. *J. Biol. Chem.*, **282**, 37738–37746.
51. Yelamos,J., Monreal,Y., Saenz,L., Aguado,E., Schreiber,V., Mota,R., Fuente,T., Minguela,A., Parrilla,P., de Murcia,G. *et al.* (2006) PARP-2 deficiency affects the survival of CD4+CD8+ double-positive thymocytes. *EMBO J.*, **25**, 4350–4360.
52. Hofer,T., Badouard,C., Bajak,E., Ravanat,J.L., Mattsson,A. and Cotgreave,I.A. (2005) Hydrogen peroxide causes greater oxidation in cellular RNA than in DNA. *Biol. Chem.*, **386**, 333–337.
53. Boulon,S., Westman,B.J., Hutten,S., Boisvert,F.M. and Lamond,A.I. (2010) The nucleolus under stress. *Mol. Cell*, **40**, 216–227.
54. Mayer,C., Schmitz,K.M., Li,J., Grummt,I. and Santoro,R. (2006) Intergenic transcripts regulate the epigenetic state of rRNA genes. *Mol. Cell*, **22**, 351–361.
55. Kutuzov,M.M., Khodyreva,S.N., Ame,J.C., Ilina,E.S., Sukhanova,M.V., Schreiber,V. and Lavrik,O.I. (2013) Interaction of PARP-2 with DNA structures mimicking DNA repair intermediates and consequences on activity of base excision repair proteins. *Biochimie*, **95**, 1208–1215.
56. Aravind,L. and Koonin,E.V. (2000) SAP - a putative DNA-binding motif involved in chromosomal organization. *Trends Biochem. Sci.*, **25**, 112–114.
57. Iida,T., Kawaguchi,R. and Nakayama,J. (2006) Conserved ribonuclease, Eri1, negatively regulates heterochromatin assembly in fission yeast. *Curr. Biol.*, **16**, 1459–1464.

4 Discussion

The epigenetic state of the nucleolus regulates chromatin plasticity and pluripotency of embryonic stem cells

The aim of this work was to elucidate the mechanisms that control formation of nucleolar heterochromatin during stem cell differentiation. Furthermore, we investigated whether the nucleolus is implicated in the open chromatin and pluripotent state of ESCs and its contribution in establishing heterochromatic structures during differentiation. The data of this work unravelled that nucleolar rRNA genes acquire heterochromatic structures upon ESC differentiation, timely coinciding with the maturation of heterochromatin at centric and pericentric repeats. This work led to the discovery that lack of nucleolar heterochromatin in ESCs is caused by the impairment of intergenic-spacer (IGS)-rRNA processing that abolishes the nucleolar repressor TIP5 association with TTF1 and its docking to rDNA. Moreover, we showed the epigenetic state of the nucleolus to be a key regulator of ESC nuclear architecture and chromatin plasticity that serves to control pluripotency and commitment.

4.1 RNA processing modulates distinct functions of the same ncRNA

lncRNAs have been implicated in a variety of epigenetic regulatory processes leading to the establishment of chromatin conformation patterns that ultimately result in the fine control of genes (Costa, 2008). Understanding how lncRNAs are regulated is an important challenge aimed to build complex regulatory scripts out of lncRNAs.

lncRNA encompasses different classes of RNA transcripts, including enhancer RNAs, small nucleolar RNA (snoRNA) hosts, intergenic transcripts, and transcripts overlapping other transcripts in either sense or antisense orientation. The widespread use of these transcripts by eukaryotic cells led to propose that they would be the main molecular advance in higher organisms to coordinate complex molecular network (Mattick, 2007).

A common emerging theme of lncRNAs is that they form ribonucleic acid-protein interactions, acting as scaffold to join several proteins together in a complex. An example of this is the lncRNA HOTAIR, which can simultaneously bind both the PRC2 (Polycomb Repressive Complex 2 that promotes H3K27me3) and the LSD1-CoREST complex (Lysine specific demethylase 1-Corepressor to REST that demethylates H3K4me2) via specific domains of the RNA structure (Tsai et al., 2010). This combination of interactions coordinates H3K27 methylation and H3K4me2 demethylation, ensuring gene silencing. The scaffold action is also supported by recent results showing that approximately a third of lncRNAs associate with chromatin-modifying complexes (Khalil et al., 2009).

In this work, we showed a novel way in which lncRNA might act in the regulation

of epigenetic states. We showed that the regulation of IGS-rRNA processing is a key determinant for the control of the epigenetic state at rDNA and propose that processing represents a mean of lncRNA regulation to modulate distinct functions of the same lncRNA. We determined that IGS-rRNA processing is a regulated process and that impairment of IGS-rRNA processing in ESCs prevents recruitment of TIP5 to rDNA and formation of rDNA heterochromatin. Although the mechanisms that prevent IGS-rRNA processing in ESCs are yet to be determined, our results demonstrated that the lack of mature pRNA impairs formation of rDNA heterochromatin in ESCs. Indeed, addition of pRNA in ESCs is sufficient to recruit TIP5 to rDNA and to establish rDNA repressive structures. The results showed that while IGS-rRNA abolishes the association of TIP5 with TTF1, pRNA promotes this association that serves to dock the complex at rDNA and to establish nucleolar heterochromatin. Thus, the same ncRNA can prevent or promote protein complex assembly and its processing controls the switch to these functions. Based on these results, it would not be surprising if processing emerges as a more general mechanism of lncRNA regulation.

The potential of RNA to bind to complementary DNA sequences has led many to hypothesize that lncRNAs may serve as molecular guides to target chromatin-modifying enzymes without the need of adaptor proteins. An example of this is pRNA. Although pRNA sequences greatly deviate from the common purin motif required for Hoogsteen configurations (Buske et al., 2011), they were recently highlighted as an example of RNA-DNA recognition rules because of their ability to recruit DNMT3b through triple helix formation with rDNA (Schmitz et al., 2010). The requirement of pRNA to retain TIP5 at rDNA and within nucleoli has led to the

hypothesis that pRNA guides TIP5 to rDNA (Mayer et al., 2008; Mayer et al., 2006) and that triple-helix might mediate this process (Bierhoff et al., 2013). However, a mechanism of TIP5 targeting through DNA-protein recognition rules was previously suggested based on the association of TIP5 with TTF1 and its dependency on rDNA binding (Nemeth et al., 2004; Santoro and Grummt, 2005; Strohner et al., 2001). Our results joined the two proposed models in one same pathway by showing that pRNA guides TIP5 to rDNA in *trans* and that TIP5-TTF1 association is mediated by pRNA and impaired by IGS-rRNA. The data strongly support a model where pRNA mediates TIP5 targeting to rDNA through DNA-protein recognition rules and that the establishment of rDNA heterochromatin in ESCs does not depend on triple-helix formation. Indeed, pRNA hairpin loop region was sufficient for TIP5 recruitment to rDNA, the association with TTF1 and the formation of rDNA heterochromatin. Whether triple-helix pRNA is implicated in other physiological processes it remains an issue to be further investigated.

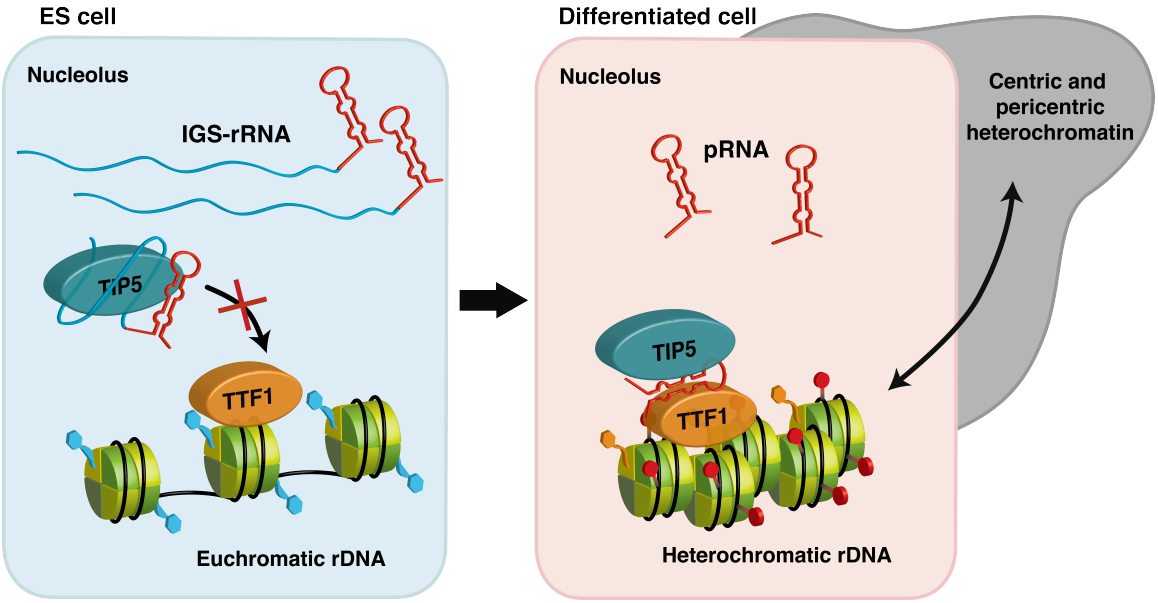

Figure 6. Model showing the formation of rDNA heterochromatin in ESC differentiation and its influence in nuclear heterochromatin. IGS-rRNA is not processed in ESCs with consequent lack of mature pRNA. The unprocessed transcript impairs the association of TIP5 with TTF1, inhibiting recruitment to rDNA and formation of heterochromatin. Upon differentiation, IGS-rRNA is processed and generates pRNA that allows TIP5 to interact with TTF1 and to be recruited to rDNA. The arrow depicts the influence of rDNA heterochromatin in the formation of nuclear repressive chromatin structures.

4.2 The epigenetic state of nucleolar chromatin regulates nuclear architecture and pluripotency of ESCs

The spatiotemporal organization of genomes in the nucleus is an emerging key player to regulate genome function. For instance, the remodelling of the open and transcriptional permissive chromatin of ESCs toward a highly condensed heterochromatic form characterizes the exit from pluripotency and the progression into differentiated states. We determined here that the nucleolus is not only the place where ribosomes are produced but it also plays a role in nuclear architecture and pluripotency by regulating heterochromatic structures elsewhere in the genome. The formation of heterochromatin within nucleoli, at rRNA genes, represents an important step for the establishment of repressive chromatin structures at regions of the genome located outside of the nucleolus.

We determined that rRNA genes acquire heterochromatic structures upon ESC differentiation, timely coinciding with the maturation of heterochromatin at centric and pericentric repeats. We showed that these two classes of heterochromatic sequences are tightly linked. Indeed, specific targeting of heterochromatin at rRNA genes in ESCs through pRNA promotes the maturation of centric and pericentric heterochromatin and a global increase in H3K9me2 amounts to levels similar to those found in differentiated cells. The crosstalk between rDNA and nuclear repetitive sequences is also in line with recent data from our and other labs showing loss of heterochromatin at both rDNA and major and minor satellites of somatic cells depleted of TIP5 (Guetg et al., 2010; Postepska-Igielska et al., 2013). Establishment of repressive structures at non-nucleolar regions by rDNA heterochromatin might occur either through spreading mechanisms (i.e. from

silent rRNA repeats to adjacent centric-pericentric repeats) and/or formation of a nucleolar/perinucleolar compartment enriched in chromatin repressor complexes, which becomes attractive for genomic regions that have to be repressed. An important example is provided by the perinucleolar targeting of the inactive X that was implicated for the maintenance of its repressed epigenetic state (Zhang et al., 2007). In line with this, recent high-resolution sequencing of the nucleolus unraveled the presence of regions with low gene density and significantly enriched in transcriptional repressed genes (Nemeth et al., 2010; van Koningsbruggen et al., 2010). Therefore, anchoring of heterochromatin at the nucleolus might serve similar functions like the ones described for the nuclear periphery that is responsible for the integrity of mammalian heterochromatin (Pinheiro et al., 2012; Towbin et al., 2012). Consistent with this, genomic regions localized at the lamina (LADs) after cell division were shown to relocate either at the lamina or at the nucleolus (Kind et al., 2013), suggesting interchangeable roles in regulating and maintaining heterochromatic states.

The results described here suggested that the task of rRNA genes is not only to synthesize rRNA. Indeed, accumulating evidences indicated that formation of silent rDNA heterochromatin is not implicated in rRNA transcription regulation. Silent rRNA repeats, present in all somatic cells, maintain their chromatin and epigenetic state independently of transcriptional activity and are stably propagated throughout the cell cycle (Conconi et al., 1989), a result in agreement with the many data showing that rRNA synthesis is regulated by modulating the activity of transcriptionally competent (active) genes and not by changing the number of silent genes (reviewed in (Santoro, 2012)). Our results indicated that the

epigenetic state of rRNA genes contributes to nuclear architecture and cellular functions such as pluripotency and ESC differentiation by controlling the balance between heterochromatin and euchromatin. The relationship between nucleolar and nuclear chromatin is also supported by data showing that the maintenance of rDNA heterochromatin is required for genome stability. In the yeast *S. cerevisiae*, *Drosophila* and mouse cells disruption of rDNA heterochromatin instigates genome instability at the rDNA and satellite repeat arrays (Guetg et al., 2010; Mekhail et al., 2008; Peng and Karpen, 2007). In addition, rDNA deletions in *Drosophila* result in reduced heterochromatin-induced gene silencing elsewhere in the genome and the extent of the rDNA deletion correlates with the loss of silencing in much the same manner as mutations in known protein heterochromatin components (Paredes and Maggert, 2009).

The increased heterochromatic content induced by pRNA in ESCs and the consequent loss of pluripotency underscore the role of the open chromatin of ESCs and suggest that nucleolar chromatin is an important regulator of the pluripotent state. As the open chromatin of ESCs has been proposed to contribute to the developmental plasticity or pluripotency (Efroni et al., 2008; Gaspar-Maia et al., 2009; Melcer et al., 2012; Meshorer et al., 2006), remodelling into rigid heterochromatic structures has also to be considered as part of a cell program aimed to restrict chromatin plasticity, to influence defined gene expression profiles and to drive cells into specific lineages. Positioning of H3K9me3 rich regions and clustering of centromeres around nucleoli were previously described to accompany changes in nuclear architecture during ESC differentiation (Bartova et al., 2008a; Wiblin et al., 2005). Although we cannot pinpoint which is the first

event that starts remodelling of nuclear architecture toward a highly condensed heterochromatic form during differentiation, our results place the nucleolus as an important regulator of this process. First, the establishment of rDNA heterochromatin during differentiation coincides with the formation of highly condensed heterochromatic form such as maturation of centric and pericentric heterochromatin and formation of LOCKs (Meshorer and Misteli, 2006; Wen et al., 2009). Second, we showed that targeting of heterochromatin at rDNA in ESCs induced heterochromatic changes similar to those found in somatic cells and leads to loss of pluripotency. Third, impairing the formation of rDNA heterochromatin by TIP5 knockdown inhibits ESC differentiation, suggesting that the establishment of nucleolar heterochromatin might be a necessary step for the switch from a lower to a higher order chromatin structure and exit from the undifferentiated state.

In summary, our data underline the importance of chromatin structure in ESC pluripotency and differentiation potential and indicate that the epigenetic state of nucleolar chromatin is a key regulator of nuclear architecture and chromatin plasticity which serves to control cell pluripotency and commitment.

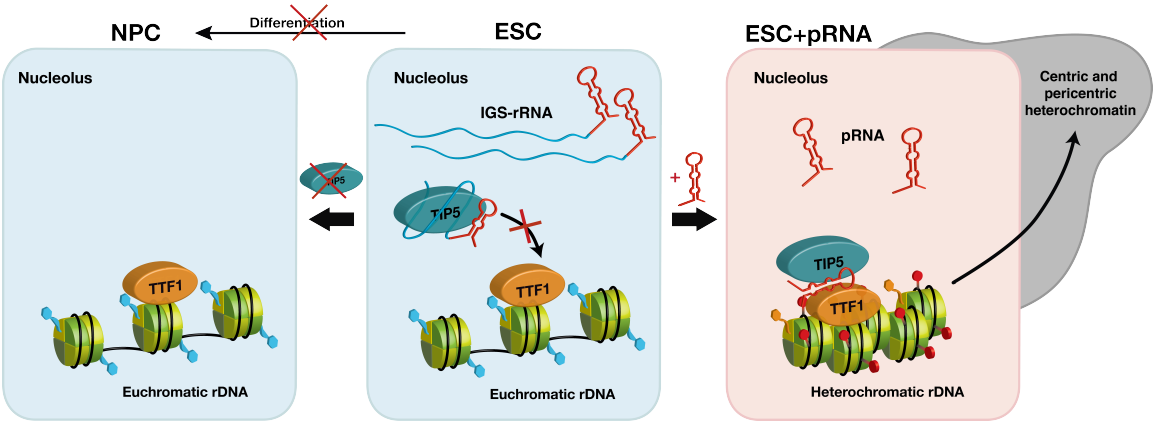

Figure 7. Model showing how the addition of pRNA to ESCs establishes nucleolar and nuclear heterochromatin while depletion of TIP5 impairs differentiation. The unprocessed IGS-rRNA transcript present in ESC impairs the association of TIP5 with TTF1, inhibiting recruitment to rDNA and formation of heterochromatin (middle panel). Addition of pRNA to ESCs, that allows TIP5 to interact with TTF1 and to be recruited to rDNA, is sufficient to establish nucleolar and nuclear heterochromatin like that one found in somatic cells and leads to loss of pluripotency (right panel). Tip5 depleted ESCs are impaired in differentiation probably due to their inability to form nucleolar heterochromatin (left panel).

Bibliography

Akhmanova, A., Verkerk, T., Langeveld, A., Grosveld, F., and Galjart, N. (2000). Characterisation of transcriptionally active and inactive chromatin domains in neurons. J Cell Sci *113 Pt 24*, 4463-4474.

Allfrey, V.G., Faulkner, R., and Mirsky, A.E. (1964). Acetylation and Methylation of Histones and Their Possible Role in the Regulation of Rna Synthesis. Proc Natl Acad Sci U S A *51*, 786-794.

Aoto, T., Saitoh, N., Ichimura, T., Niwa, H., and Nakao, M. (2006). Nuclear and chromatin reorganization in the MHC-Oct3/4 locus at developmental phases of embryonic stem cell differentiation. Dev Biol *298*, 354-367.

Avilion, A.A., Nicolis, S.K., Pevny, L.H., Perez, L., Vivian, N., and Lovell-Badge, R. (2003). Multipotent cell lineages in early mouse development depend on SOX2 function. Genes Dev *17*, 126-140.

Bannister, A.J., and Kouzarides, T. (2011). Regulation of chromatin by histone modifications. Cell Res *21*, 381-395.

Bannister, A.J., Zegerman, P., Partridge, J.F., Miska, E.A., Thomas, J.O., Allshire, R.C., and Kouzarides, T. (2001). Selective recognition of methylated lysine 9 on histone H3 by the HP1 chromo domain. Nature *410*, 120-124.

Bartova, E., Galiova, G., Krejci, J., Harnicarova, A., Strasak, L., and Kozubek, S. (2008a). Epigenome and chromatin structure in human embryonic stem cells undergoing differentiation. Dev Dyn *237*, 3690-3702.

Bartova, E., Krejci, J., Harnicarova, A., and Kozubek, S. (2008b). Differentiation of human embryonic stem cells induces condensation of chromosome territories and formation of heterochromatin protein 1 foci. Differentiation *76*, 24-32.

Bell, S.P., Learned, R.M., Jantzen, H.M., and Tjian, R. (1988). Functional cooperativity between transcription factors UBF1 and SL1 mediates human ribosomal RNA synthesis. Science *241*, 1192-1197.

Berger, C., Horlebein, A., Gogel, E., and Grummt, F. (1997). Temporal order of replication of mouse ribosomal RNA genes during the cell cycle. Chromosoma *106*, 479-484.

Bernstein, B.E., Mikkelsen, T.S., Xie, X., Kamal, M., Huebert, D.J., Cuff, J., Fry, B., Meissner, A., Wernig, M., Plath, K.*, et al.* (2006). A bivalent chromatin structure marks key developmental genes in embryonic stem cells. Cell *125*, 315-326.

Bhattacharya, D., Talwar, S., Mazumder, A., and Shivashankar, G.V. (2009). Spatio-temporal plasticity in chromatin organization in mouse cell differentiation and during Drosophila embryogenesis. Biophys J *96*, 3832-3839.

Bibel, M., Richter, J., Schrenk, K., Tucker, K.L., Staiger, V., Korte, M., Goetz, M., and Barde, Y.A. (2004). Differentiation of mouse embryonic stem cells into a defined neuronal lineage. Nat Neurosci *7*, 1003-1009.

Bierhoff, H., Postepska-Igielska, A., and Grummt, I. (2013). Noisy silence: Non-coding RNA and heterochromatin formation at repetitive elements. Epigenetics *9*.

Bochar, D.A., Savard, J., Wang, W., Lafleur, D.W., Moore, P., Cote, J., and Shiekhattar, R. (2000). A family of chromatin remodeling factors related to Williams syndrome transcription factor. Proc Natl Acad Sci U S A *97*, 1038-1043.

Bozhenok, L., Wade, P.A., and Varga-Weisz, P. (2002). WSTF-ISWI chromatin remodeling complex targets heterochromatic replication foci. Embo J *21*, 2231-2241.

Burdon, S., Savatier (2002). Signalling, cell cycle and pluripotency in embryonic stem cells. Trends Cell Biol *12*, 432-438.

Burdon, T., Stracey, C., Chambers, I., Nichols, J., and Smith, A. (1999). Suppression of SHP-2 and ERK signalling promotes self-renewal of mouse embryonic stem cells. Dev Biol *210*, 30-43.

Buske, F.A., Mattick, J.S., and Bailey, T.L. (2011). Potential in vivo roles of nucleic acid triple-helices. RNA Biol *8*, 427-439.

Cao, R., Wang, L., Wang, H., Xia, L., Erdjument-Bromage, H., Tempst, P., Jones, R.S., and Zhang, Y. (2002). Role of histone H3 lysine 27 methylation in Polycomb-group silencing. Science *298*, 1039-1043.

Carvalho, C., Pereira, H.M., Ferreira, J., Pina, C., Mendonca, D., Rosa, A.C., and Carmo-Fonseca, M. (2001). Chromosomal G-dark bands determine the spatial organization of centromeric heterochromatin in the nucleus. Mol Biol Cell *12*, 3563-3572.

Caudy, A.A., and Pikaard, C.S. (2002). Xenopus ribosomal RNA gene intergenic spacer elements conferring transcriptional enhancement and nucleolar dominance-like competition in oocytes. J Biol Chem *277*, 31577-31584.

Chambers, I., Silva, J., Colby, D., Nichols, J., Nijmeijer, B., Robertson, M., Vrana, J., Jones, K., Grotewold, L., and Smith, A. (2007). Nanog safeguards pluripotency and mediates germline development. Nature *450*, 1230-1234.

Chen, R.Z., Pettersson, U., Beard, C., Jackson-Grusby, L., and Jaenisch, R. (1998). DNA hypomethylation leads to elevated mutation rates. Nature *395*, 89-93.

Clark, S.J., Harrison, J., and Molloy, P.L. (1997). Sp1 binding is inhibited by (m)Cp(m)CpG methylation. Gene *195*, 67-71.

Clos, J., Buttgereit, D., and Grummt, I. (1986). A purified transcription factor (TIF-IB) binds to essential sequences of the mouse rDNA promoter. Proc Natl Acad Sci U S A *83*, 604-608.

Comai, L., Tanese, N., and Tjian, R. (1992). The TATA-binding protein and associated factors are integral components of the RNA polymerase I transcription factor, SL1. Cell *68*, 965-976.

Conconi, A., Widmer, R.M., Koller, T., and Sogo, J.M. (1989). Two different chromatin structures coexist in ribosomal RNA genes throughout the cell cycle. Cell *57*, 753-761.

Costa, F.F. (2008). Non-coding RNAs, epigenetics and complexity. Gene *410*, 9-

17.

Daujat, S., Weiss, T., Mohn, F., Lange, U.C., Ziegler-Birling, C., Zeissler, U., Lappe, M., Schubeler, D., Torres-Padilla, M.E., and Schneider, R. (2009). H3K64 trimethylation marks heterochromatin and is dynamically remodeled during developmental reprogramming. Nat Struct Mol Biol *16*, 777-781.

De Winter, R.F., and Moss, T. (1986). Spacer promoters are essential for efficient enhancement of X. laevis ribosomal transcription. Cell *44*, 313-318.

De Winter, R.F., and Moss, T. (1987). A complex array of sequences enhances ribosomal transcription in Xenopus laevis. J Mol Biol *196*, 813-827.

Defossez, P.A., and Stancheva, I. (2011). Biological functions of methyl-CpG-binding proteins. Prog Mol Biol Transl Sci *101*, 377-398.

Dev, V.G., Tantravahi, R., Miller, D.A., and Miller, O.J. (1977). Nucleolus organizers in Mus musculus subspecies and in the RAG mouse cell line. Genetics *86*, 389-398.

Dillon, N., and Festenstein, R. (2002). Unravelling heterochromatin: competition between positive and negative factors regulates accessibility. Trends Genet *18*, 252-258.

Efroni, S., Duttagupta, R., Cheng, J., Dehghani, H., Hoeppner, D.J., Dash, C., Bazett-Jones, D.P., Le Grice, S., McKay, R.D., Buetow, K.H.*, et al.* (2008). Global transcription in pluripotent embryonic stem cells. Cell Stem Cell *2*, 437-447.

Evans, M.J., and Kaufman, M.H. (1981). Establishment in culture of pluripotential cells from mouse embryos. Nature *292*, 154-156.

Evers, R., and Grummt, I. (1995). Molecular coevolution of mammalian ribosomal gene terminator sequences and the transcription termination factor TTF-I. Proc Natl Acad Sci U S A *92*, 5827-5831.

Fan, J.Y., Gordon, F., Luger, K., Hansen, J.C., and Tremethick, D.J. (2002). The essential histone variant H2A.Z regulates the equilibrium between different chromatin conformational states. Nat Struct Biol *9*, 172-176.

Felsenfeld, G., and Groudine, M. (2003). Controlling the double helix. Nature *421*, 448-453.

Fisher, C.L., and Fisher, A.G. (2011). Chromatin states in pluripotent, differentiated, and reprogrammed cells. Curr Opin Genet Dev *21*, 140-146.

Fransz, P., Soppe, W., and Schubert, I. (2003). Heterochromatin in interphase nuclei of Arabidopsis thaliana. Chromosome Res *11*, 227-240.

French, S.L., Osheim, Y.N., Cioci, F., Nomura, M., and Beyer, A.L. (2003). In exponentially growing Saccharomyces cerevisiae cells, rRNA synthesis is determined by the summed RNA polymerase I loading rate rather than by the number of active genes. Mol Cell Biol *23*, 1558-1568.

Gaspar-Maia, A., Alajem, A., Meshorer, E., and Ramalho-Santos, M. (2011). Open chromatin in pluripotency and reprogramming. Nature reviews Molecular cell biology *12*, 36-47.

Gaspar-Maia, A., Alajem, A., Polesso, F., Sridharan, R., Mason, M.J., Heidersbach, A., Ramalho-Santos, J., McManus, M.T., Plath, K., Meshorer, E.*, et al.* (2009). Chd1 regulates open chromatin and pluripotency of embryonic stem cells. Nature *460*, 863-868.

Gerber, J.K., Gogel, E., Berger, C., Wallisch, M., Muller, F., Grummt, I., and Grummt, F. (1997). Termination of mammalian rDNA replication: polar arrest of replication fork movement by transcription termination factor TTF-I. Cell *90*, 559-567.

Ghoshal, K., Majumder, S., Datta, J., Motiwala, T., Bai, S., Sharma, S.M., Frankel, W., and Jacob, S.T. (2004). Role of human ribosomal RNA (rRNA) promoter methylation and of methyl-CpG-binding protein MBD2 in the suppression of rRNA gene expression. J Biol Chem *279*, 6783-6793.

Gonzalez, I.L., and Sylvester, J.E. (1995). Complete sequence of the 43-kb human ribosomal DNA repeat: analysis of the intergenic spacer. Genomics *27*, 320-328.

Gonzalez-Sandoval, A., Towbin, B.D., and Gasser, S.M. (2013). The formation and sequestration of heterochromatin during development: Delivered on 7 September 2012 at the 37th FEBS Congress in Sevilla, Spain. FEBS J *280*, 3212-3219.

Grewal, S.I., and Elgin, S.C. (2007). Transcription and RNA interference in the formation of heterochromatin. Nature *447*, 399-406.

Grimaldi, G., and Di Nocera, P.P. (1988a). Multiple repeated units in Drosophila melanogaster ribosomal DNA spacer stimulate rRNA precursor transcription. Proc Natl Acad Sci U S A *85*, 5502-5506.

Grimaldi, G., and Di Nocera, P.P. (1988b). Multiple repeated units in Drosophila melanogaster ribosomal DNA spacer stimulate rRNA precursor transcription. Proc Natl Acad Sci U S A *85*, 5502-5506.

Grozdanov, P., Georgiev, O., and Karagyozov, L. (2003). Complete sequence of the 45-kb mouse ribosomal DNA repeat: analysis of the intergenic spacer. Genomics *82*, 637-643.

Grummt, I. (2003). Life on a planet of its own: regulation of RNA polymerase I transcription in the nucleolus. Genes Dev *17*, 1691-1702.

Grummt, I., Kuhn, A., Bartsch, I., and Rosenbauer, H. (1986a). A transcription terminator located upstream of the mouse rDNA initiation site affects rRNA synthesis. Cell *47*, 901-911.

Grummt, I., Maier, U., Ohrlein, A., Hassouna, N., and Bachellerie, J.P. (1985). Transcription of mouse rDNA terminates downstream of the 3' end of 28S RNA and involves interaction of factors with repeated sequences in the 3' spacer. Cell *43*, 801-810.

Grummt, I., Rosenbauer, H., Niedermeyer, I., Maier, U., and Ohrlein, A. (1986b). A repeated 18 bp sequence motif in the mouse rDNA spacer mediates binding of a nuclear factor and transcription termination. Cell *45*, 837-846.

Guetg, C., Lienemann, P., Sirri, V., Grummt, I., Hernandez-Verdun, D., Hottiger,

M.O., Fussenegger, M., and Santoro, R. (2010). The NoRC complex mediates the heterochromatin formation and stability of silent rRNA genes and centromeric repeats. EMBO J *29*, 2135-2146.

Guetg, C., and Santoro, R. (2012). Formation of nuclear heterochromatin: The nucleolar point of view. Epigenetics *7*, 811-814.

Guetg, C., Scheifele, F., Rosenthal, F., Hottiger, M.O., and Santoro, R. (2012). Inheritance of Silent rDNA Chromatin Is Mediated by PARP1 via Noncoding RNA. Mol Cell *45*, 790-800.

Haaf, T., and Schmid, M. (1991). Chromosome topology in mammalian interphase nuclei. Exp Cell Res *192*, 325-332.

Habibi, E., Brinkman, A.B., Arand, J., Kroeze, L.I., Kerstens, H.H., Matarese, F., Lepikhov, K., Gut, M., Brun-Heath, I., Hubner, N.C.*, et al.* (2013). Whole-genome bisulfite sequencing of two distinct interconvertible DNA methylomes of mouse embryonic stem cells. Cell Stem Cell *13*, 360-369.

Haltiner, M.M., Smale, S.T., and Tjian, R. (1986). Two distinct promoter elements in the human rRNA gene identified by linker scanning mutagenesis. Mol Cell Biol *6*, 227-235.

Hayashi, K., Ohta, H., Kurimoto, K., Aramaki, S., and Saitou, M. (2011). Reconstitution of the mouse germ cell specification pathway in culture by pluripotent stem cells. Cell *146*, 519-532.

He, S., Nakada, D., and Morrison, S.J. (2009). Mechanisms of stem cell self-renewal. Annu Rev Cell Dev Biol *25*, 377-406.

Heix, J., Zomerdijk, J.C., Ravanpay, A., Tjian, R., and Grummt, I. (1997). Cloning of murine RNA polymerase I-specific TAF factors: conserved interactions between the subunits of the species-specific transcription initiation factor TIF-IB/SL1. Proc Natl Acad Sci U S A *94*, 1733-1738.

Henderson, A.S., Warburton, D., and Atwood, K.C. (1972). Location of ribosomal DNA in the human chromosome complement. Proc Natl Acad Sci U S A *69*, 3394-

3398.

Henderson, S., and Sollner-Webb, B. (1986). A transcriptional terminator is a novel element of the promoter of the mouse ribosomal RNA gene. Cell *47*, 891-900.

Huang, W., Sherman, B.T., and Lempicki, R.A. (2009). Systematic and integrative analysis of large gene lists using DAVID bioinformatics resources. Nat Protoc *4*, 44-57.

Hubner, M.R., Eckersley-Maslin, M.A., and Spector, D.L. (2013). Chromatin organization and transcriptional regulation. Curr Opin Genet Dev *23*, 89-95.

Ito, T., Levenstein, M.E., Fyodorov, D.V., Kutach, A.K., Kobayashi, R., and Kadonaga, J.T. (1999). ACF consists of two subunits, Acf1 and ISWI, that function cooperatively in the ATP-dependent catalysis of chromatin assembly. Genes Dev *13*, 1529-1539.

Ivanova, N., Dobrin, R., Lu, R., Kotenko, I., Levorse, J., DeCoste, C., Schafer, X., Lun, Y., and Lemischka, I.R. (2006). Dissecting self-renewal in stem cells with RNA interference. Nature *442*, 533-538.

Jackson, J.P., Johnson, L., Jasencakova, Z., Zhang, X., PerezBurgos, L., Singh, P.B., Cheng, X., Schubert, I., Jenuwein, T., and Jacobsen, S.E. (2004). Dimethylation of histone H3 lysine 9 is a critical mark for DNA methylation and gene silencing in Arabidopsis thaliana. Chromosoma *112*, 308-315.

Jeltsch, A. (2006). Molecular enzymology of mammalian DNA methyltransferases. Curr Top Microbiol Immunol *301*, 203-225.

Jenuwein, T., and Allis, C.D. (2001). Translating the histone code. Science *293*, 1074-1080.

Joffe, B., Leonhardt, H., and Solovei, I. (2010). Differentiation and large scale spatial organization of the genome. Curr Opin Genet Dev *20*, 562-569.

Jorgensen, H.F., Azuara, V., Amoils, S., Spivakov, M., Terry, A., Nesterova, T., Cobb, B.S., Ramsahoye, B., Merkenschlager, M., and Fisher, A.G. (2007). The

impact of chromatin modifiers on the timing of locus replication in mouse embryonic stem cells. Genome Biol *8*, R169.

Kanatsu-Shinohara, M., Inoue, K., Lee, J., Yoshimoto, M., Ogonuki, N., Miki, H., Baba, S., Kato, T., Kazuki, Y., Toyokuni, S.*, et al.* (2004). Generation of pluripotent stem cells from neonatal mouse testis. Cell *119*, 1001-1012.

Khalil, A.M., Guttman, M., Huarte, M., Garber, M., Raj, A., Rivea Morales, D., Thomas, K., Presser, A., Bernstein, B.E., van Oudenaarden, A.*, et al.* (2009). Many human large intergenic noncoding RNAs associate with chromatin-modifying complexes and affect gene expression. Proc Natl Acad Sci U S A *106*, 11667-11672.

Kind, J., Pagie, L., Ortabozkoyun, H., Boyle, S., de Vries, S.S., Janssen, H., Amendola, M., Nolen, L.D., Bickmore, W.A., and van Steensel, B. (2013). Single-cell dynamics of genome-nuclear lamina interactions. Cell *153*, 178-192.

Kind, J., and van Steensel, B. (2010). Genome-nuclear lamina interactions and gene regulation. Curr Opin Cell Biol *22*, 320-325.

Kuhn, A., and Grummt, I. (1987). A novel promoter in the mouse rDNA spacer is active in vivo and in vitro. Embo J *6*, 3487-3492.

Kuhn, A., and Grummt, I. (1992). Dual role of the nucleolar transcription factor UBF: trans-activator and antirepressor. Proc Natl Acad Sci U S A *89*, 7340-7344.

Kurihara, Y., Suh, D.S., Suzuki, H., and Moriwaki, K. (1994a). Chromosomal locations of Ag-NORs and clusters of ribosomal DNA in laboratory strains of mice. Mamm Genome *5*, 225-228.

Kurihara, Y., Suh, D.S., Suzuki, H., and Moriwaki, K. (1994b). Chromosomal locations of Ag-NORs and clusters of ribosomal DNA in laboratory strains of mice. Mamm Genome *5*, 225-228.

Labhart, P., and Reeder, R.H. (1984). Enhancer-like properties of the 60/81 bp elements in the ribosomal gene spacer of Xenopus laevis. Cell *37*, 285-289.

Lachner, M., and Jenuwein, T. (2002). The many faces of histone lysine

methylation. Curr Opin Cell Biol *14*, 286-298.

Lachner, M., O'Carroll, D., Rea, S., Mechtler, K., and Jenuwein, T. (2001). Methylation of histone H3 lysine 9 creates a binding site for HP1 proteins. Nature *410*, 116-120.

Langst, G., Becker, P.B., and Grummt, I. (1998). TTF-I determines the chromatin architecture of the active rDNA promoter. Embo J *17*, 3135-3145.

Langst, G., Blank, T.A., Becker, P.B., and Grummt, I. (1997a). RNA polymerase I transcription on nucleosomal templates: the transcription termination factor TTF-I induces chromatin remodeling and relieves transcriptional repression. EMBO J *16*, 760-768.

Langst, G., Blank, T.A., Becker, P.B., and Grummt, I. (1997b). RNA polymerase I transcription on nucleosomal templates: the transcription termination factor TTF-I induces chromatin remodeling and relieves transcriptional repression. Embo J *16*, 760-768.

Lawrence, R.J., Earley, K., Pontes, O., Silva, M., Chen, Z.J., Neves, N., Viegas, W., and Pikaard, C.S. (2004). A concerted DNA methylation/histone methylation switch regulates rRNA gene dosage control and nucleolar dominance. Mol Cell *13*, 599-609.

Learned, R.M., Learned, T.K., Haltiner, M.M., and Tjian, R.T. (1986). Human rRNA transcription is modulated by the coordinate binding of two factors to an upstream control element. Cell *45*, 847-857.

Leitch, H.G., McEwen, K.R., Turp, A., Encheva, V., Carroll, T., Grabole, N., Mansfield, W., Nashun, B., Knezovich, J.G., Smith, A.*, et al.* (2013). Naive pluripotency is associated with global DNA hypomethylation. Nat Struct Mol Biol *20*, 311-316.

LeRoy, G., Orphanides, G., Lane, W.S., and Reinberg, D. (1998). Requirement of RSF and FACT for transcription of chromatin templates in vitro. Science *282*, 1900-1904.

Levine, S.S., King, I.F., and Kingston, R.E. (2004). Division of labor in polycomb group repression. Trends Biochem Sci *29*, 478-485.

Li, B., and Dewey, C.N. (2011). RSEM: accurate transcript quantification from RNA-Seq data with or without a reference genome. BMC Bioinformatics *12*, 323.

Li, E., Bestor, T.H., and Jaenisch, R. (1992). Targeted mutation of the DNA methyltransferase gene results in embryonic lethality. Cell *69*, 915-926.

Li, J., Langst, G., and Grummt, I. (2006). NoRC-dependent nucleosome positioning silences rRNA genes. Embo J *25*, 5735-5741.

Li, J., Santoro, R., Koberna, K., and Grummt, I. (2005). The chromatin remodeling complex NoRC controls replication timing of rRNA genes. EMBO J *24*, 120-127.

Liang, G., and Zhang, Y. (2013). Embryonic stem cell and induced pluripotent stem cell: an epigenetic perspective. Cell Res *23*, 49-69.

Lodish, H. (2013). Molecular Cell Biology, 7th Edition (New York).

Loh, Y.H., Wu, Q., Chew, J.L., Vega, V.B., Zhang, W., Chen, X., Bourque, G., George, J., Leong, B., Liu, J.*, et al.* (2006). The Oct4 and Nanog transcription network regulates pluripotency in mouse embryonic stem cells. Nat Genet *38*, 431-440.

Marks, H., and Stunnenberg, H.G. (2014). Transcription regulation and chromatin structure in the pluripotent ground state. Biochim Biophys Acta *1839*, 129-137.

Martens, J.H., O'Sullivan, R.J., Braunschweig, U., Opravil, S., Radolf, M., Steinlein, P., and Jenuwein, T. (2005). The profile of repeat-associated histone lysine methylation states in the mouse epigenome. Embo J *24*, 800-812.

Martin, G.R. (1981). Isolation of a pluripotent cell line from early mouse embryos cultured in medium conditioned by teratocarcinoma stem cells. Proc Natl Acad Sci U S A *78*, 7634-7638.

Masui, S., Nakatake, Y., Toyooka, Y., Shimosato, D., Yagi, R., Takahashi, K., Okochi, H., Okuda, A., Matoba, R., Sharov, A.A.*, et al.* (2007). Pluripotency

governed by Sox2 via regulation of Oct3/4 expression in mouse embryonic stem cells. Nat Cell Biol *9*, 625-635.

Matsuda, T., Nakamura, T., Nakao, K., Arai, T., Katsuki, M., Heike, T., and Yokota, T. (1999). STAT3 activation is sufficient to maintain an undifferentiated state of mouse embryonic stem cells. Embo J *18*, 4261-4269.

Matsui, Y., Zsebo, K., and Hogan, B.L. (1992). Derivation of pluripotential embryonic stem cells from murine primordial germ cells in culture. Cell *70*, 841-847.

Mattick, J.S. (2007). A new paradigm for developmental biology. J Exp Biol *210*, 1526-1547.

Mattout, A., and Meshorer, E. (2010a). Chromatin plasticity and genome organization in pluripotent embryonic stem cells. Curr Opin Cell Biol *22*, 334-341.

Mattout, A., and Meshorer, E. (2010b). Chromatin plasticity and genome organization in pluripotent embryonic stem cells. Curr Opin Cell Biol *22*, 334-341.

Mayer, C., Neubert, M., and Grummt, I. (2008). The structure of NoRC-associated RNA is crucial for targeting the chromatin remodelling complex NoRC to the nucleolus. EMBO Rep *9*, 774-780.

Mayer, C., Schmitz, K.M., Li, J., Grummt, I., and Santoro, R. (2006). Intergenic transcripts regulate the epigenetic state of rRNA genes. Mol Cell *22*, 351-361.

McStay, B., and Grummt, I. (2008). The epigenetics of rRNA genes: from molecular to chromosome biology. Annu Rev Cell Dev Biol *24*, 131-157.

Meister, P., and Taddei, A. (2013). Building silent compartments at the nuclear periphery: a recurrent theme. Curr Opin Genet Dev *23*, 96-103.

Meister, P., Towbin, B.D., Pike, B.L., Ponti, A., and Gasser, S.M. (2010). The spatial dynamics of tissue-specific promoters during C. elegans development. Genes Dev *24*, 766-782.

Mekhail, K., Seebacher, J., Gygi, S.P., and Moazed, D. (2008). Role for

perinuclear chromosome tethering in maintenance of genome stability. Nature *456*, 667-670.

Melcer, S., Hezroni, H., Rand, E., Nissim-Rafinia, M., Skoultchi, A., Stewart, C.L., Bustin, M., and Meshorer, E. (2012). Histone modifications and lamin A regulate chromatin protein dynamics in early embryonic stem cell differentiation. Nat Commun *3*, 910.

Merz, K., Hondele, M., Goetze, H., Gmelch, K., Stoeckl, U., and Griesenbeck, J. (2008). Actively transcribed rRNA genes in S. cerevisiae are organized in a specialized chromatin associated with the high-mobility group protein Hmo1 and are largely devoid of histone molecules. Genes Dev *22*, 1190-1204.

Meshorer, E., and Misteli, T. (2006). Chromatin in pluripotent embryonic stem cells and differentiation. Nat Rev Mol Cell Biol *7*, 540-546.

Meshorer, E., Yellajoshula, D., George, E., Scambler, P.J., Brown, D.T., and Misteli, T. (2006). Hyperdynamic plasticity of chromatin proteins in pluripotent embryonic stem cells. Dev Cell *10*, 105-116.

Mikkelsen, T.S., Ku, M., Jaffe, D.B., Issac, B., Lieberman, E., Giannoukos, G., Alvarez, P., Brockman, W., Kim, T.K., Koche, R.P.*, et al.* (2007). Genome-wide maps of chromatin state in pluripotent and lineage-committed cells. Nature *448*, 553-560.

Miller, O.L., Jr., and Beatty, B.R. (1969). Visualization of nucleolar genes. Science *164*, 955-957.

Mitsui, K., Tokuzawa, Y., Itoh, H., Segawa, K., Murakami, M., Takahashi, K., Maruyama, M., Maeda, M., and Yamanaka, S. (2003). The homeoprotein Nanog is required for maintenance of pluripotency in mouse epiblast and ES cells. Cell *113*, 631-642.

Morin, R.D., Johnson, N.A., Severson, T.M., Mungall, A.J., An, J., Goya, R., Paul, J.E., Boyle, M., Woolcock, B.W., Kuchenbauer, F.*, et al.* (2010). Somatic mutations altering EZH2 (Tyr641) in follicular and diffuse large B-cell lymphomas of germinal-center origin. Nat Genet *42*, 181-185.

Mosgöller, W. (2004). Nucleolar ultrastructure in vertebrates. (New York, Kluwer Academic/Plenum Publishers).

Moss, T., Langlois, F., Gagnon-Kugler, T., and Stefanovsky, V. (2007). A housekeeper with power of attorney: the rRNA genes in ribosome biogenesis. Cell Mol Life Sci *64*, 29-49.

Muller, J., and Verrijzer, P. (2009). Biochemical mechanisms of gene regulation by polycomb group protein complexes. Curr Opin Genet Dev *19*, 150-158.

Nemeth, A., Conesa, A., Santoyo-Lopez, J., Medina, I., Montaner, D., Peterfia, B., Solovei, I., Cremer, T., Dopazo, J., and Langst, G. (2010). Initial genomics of the human nucleolus. PLoS Genet *6*, e1000889.

Nemeth, A., Guibert, S., Tiwari, V.K., Ohlsson, R., and Langst, G. (2008). Epigenetic regulation of TTF-I-mediated promoter-terminator interactions of rRNA genes. Embo J *27*, 1255-1265.

Nemeth, A., Strohner, R., Grummt, I., and Langst, G. (2004). The chromatin remodeling complex NoRC and TTF-I cooperate in the regulation of the mammalian rRNA genes in vivo. Nucleic Acids Res *32*, 4091-4099.

Nichols, J., and Smith, A. (2012). Pluripotency in the embryo and in culture. Cold Spring Harb Perspect Biol *4*, a008128.

Niwa, H., Miyazaki, J., and Smith, A.G. (2000). Quantitative expression of Oct-3/4 defines differentiation, dedifferentiation or self-renewal of ES cells. Nat Genet *24*, 372-376.

Okano, M., Bell, D.W., Haber, D.A., and Li, E. (1999). DNA methyltransferases Dnmt3a and Dnmt3b are essential for de novo methylation and mammalian development. Cell *99*, 247-257.

Olson, M. (2011). Preface. In The Nucleolus, O. MOJ, ed. (Springer), pp. V-XVII.

Paalman, M.H., Henderson, S.L., and Sollner-Webb, B. (1995). Stimulation of the mouse rRNA gene promoter by a distal spacer promoter. Mol Cell Biol *15*, 4648-4656.

Panov, K.I., Friedrich, J.K., Russell, J., and Zomerdijk, J.C. (2006). UBF activates RNA polymerase I transcription by stimulating promoter escape. Embo J *25*, 3310-3322.

Paredes, S., and Maggert, K.A. (2009). Ribosomal DNA contributes to global chromatin regulation. Proc Natl Acad Sci U S A *106*, 17829-17834.

Park, S.H., Kook, M.C., Kim, E.Y., Park, S., and Lim, J.H. (2004). Ultrastructure of human embryonic stem cells and spontaneous and retinoic acid-induced differentiating cells. Ultrastruct Pathol *28*, 229-238.

Pastor, W.A., Aravind, L., and Rao, A. (2013). TETonic shift: biological roles of TET proteins in DNA demethylation and transcription. Nature reviews Molecular cell biology *14*, 341-356.

Pelletier, G., Stefanovsky, V.Y., Faubladier, M., Hirschler-Laszkiewicz, I., Savard, J., Rothblum, L.I., Cote, J., and Moss, T. (2000). Competitive recruitment of CBP and Rb-HDAC regulates UBF acetylation and ribosomal transcription. Mol Cell *6*, 1059-1066.

Peng, J.C., and Karpen, G.H. (2007). H3K9 methylation and RNA interference regulate nucleolar organization and repeated DNA stability. Nat Cell Biol *9*, 25-35.

Peric-Hupkes, D., Meuleman, W., Pagie, L., Bruggeman, S.W., Solovei, I., Brugman, W., Graf, S., Flicek, P., Kerkhoven, R.M., van Lohuizen, M.*, et al.* (2010). Molecular maps of the reorganization of genome-nuclear lamina interactions during differentiation. Mol Cell *38*, 603-613.

Peters, A.H., O'Carroll, D., Scherthan, H., Mechtler, K., Sauer, S., Schofer, C., Weipoltshammer, K., Pagani, M., Lachner, M., Kohlmaier, A.*, et al.* (2001). Loss of the Suv39h histone methyltransferases impairs mammalian heterochromatin and genome stability. Cell *107*, 323-337.

Phillips, J.E., and Corces, V.G. (2009). CTCF: master weaver of the genome. Cell *137*, 1194-1211.

Pinheiro, I., Margueron, R., Shukeir, N., Eisold, M., Fritzsch, C., Richter, F.M.,

Mittler, G., Genoud, C., Goyama, S., Kurokawa, M.*, et al.* (2012). Prdm3 and Prdm16 are H3K9me1 methyltransferases required for mammalian heterochromatin integrity. Cell *150*, 948-960.

Pluta, A.F., Mackay, A.M., Ainsztein, A.M., Goldberg, I.G., and Earnshaw, W.C. (1995). The centromere: hub of chromosomal activities. Science *270*, 1591-1594.

Poot, R.A., Dellaire, G., Hulsmann, B.B., Grimaldi, M.A., Corona, D.F., Becker, P.B., Bickmore, W.A., and Varga-Weisz, P.D. (2000). HuCHRAC, a human ISWI chromatin remodelling complex contains hACF1 and two novel histone-fold proteins. Embo J *19*, 3377-3387.

Postepska-Igielska, A., Krunic, D., Schmitt, N., Greulich-Bode, K.M., Boukamp, P., and Grummt, I. (2013). The chromatin remodelling complex NoRC safeguards genome stability by heterochromatin formation at telomeres and centromeres. EMBO Rep *14*, 704-710.

Powell, M.A., Mutch, D.G., Rader, J.S., Herzog, T.J., Huang, T.H., and Goodfellow, P.J. (2002). Ribosomal DNA methylation in patients with endometrial carcinoma: an independent prognostic marker. Cancer *94*, 2941-2952.

Putnam, C.D., and Pikaard, C.S. (1992). Cooperative binding of the Xenopus RNA polymerase I transcription factor xUBF to repetitive ribosomal gene enhancers. Mol Cell Biol *12*, 4970-4980.

Qu, G.Z., Grundy, P.E., Narayan, A., and Ehrlich, M. (1999). Frequent hypomethylation in Wilms tumors of pericentromeric DNA in chromosomes 1 and 16. Cancer Genet Cytogenet *109*, 34-39.

Reik, W. (2007). Stability and flexibility of epigenetic gene regulation in mammalian development. Nature *447*, 425-432.

Rinn, J.L., and Chang, H.Y. (2012). Genome regulation by long noncoding RNAs. Annu Rev Biochem *81*, 145-166.

Robinson, M.D., McCarthy, D.J., and Smyth, G.K. (2010). edgeR: a Bioconductor package for differential expression analysis of digital gene expression data.

Bioinformatics *26*, 139-140.

Rosner, M.H., Vigano, M.A., Ozato, K., Timmons, P.M., Poirier, F., Rigby, P.W., and Staudt, L.M. (1990). A POU-domain transcription factor in early stem cells and germ cells of the mammalian embryo. Nature *345*, 686-692.

Sander, E.E., and Grummt, I. (1997). Oligomerization of the transcription termination factor TTF-I: implications for the structural organization of ribosomal transcription units. Nucleic Acids Res *25*, 1142-1147.

Santoro, R. (2005). The silence of the ribosomal RNA genes. Cell Mol Life Sci *62*, 2067-2079.

Santoro, R. (2011). The nucleolus. The epigenetics of the nucleolus: structure and function of active and silent ribosomal RNA genes In The Nucleolus, M.O.J. Olson, ed. (Springer), pp. 57-82.

Santoro, R. (2012). The nucleolus. The epigenetics of the nucleolus : structure and function of active and silent ribosomal RNA genes. In The nucleolus (Olson MOJ) Springer, 57-82.

Santoro, R. (2014). Analysis of chromatin composition of repetitive sequences: the ChIP-Chop assay. Methods Mol Biol *1094*, 319-328.

Santoro, R., and Grummt, I. (2001). Molecular mechanisms mediating methylation-dependent silencing of ribosomal gene transcription. Mol Cell *8*, 719-725.

Santoro, R., and Grummt, I. (2005). Epigenetic mechanism of rRNA gene silencing: temporal order of NoRC-mediated histone modification, chromatin remodeling, and DNA methylation. Mol Cell Biol *25*, 2539-2546.

Santoro, R., Li, J., and Grummt, I. (2002). The nucleolar remodeling complex NoRC mediates heterochromatin formation and silencing of ribosomal gene transcription. Nat Genet *32*, 393-396.

Santoro, R., Schmitz, K.M., Sandoval, J., and Grummt, I. (2010a). Intergenic transcripts originating from a subclass of ribosomal DNA repeats silence

ribosomal RNA genes in trans. EMBO Rep *11*, 52-58.

Santoro, R., Schmitz, K.M., Sandoval, J., and Grummt, I. (2010b). Intergenic transcripts originating from a subclass of ribosomal DNA repeats silence ribosomal RNA genes in trans. EMBO Rep *11*, 52-58.

Sarma K, R.D. (2005). Histone variants meet their match. Nat Rev Mol Cell Biol *6*, 139-149.

Sato, N., Meijer, L., Skaltsounis, L., Greengard, P., and Brivanlou, A.H. (2004). Maintenance of pluripotency in human and mouse embryonic stem cells through activation of Wnt signaling by a pharmacological GSK-3-specific inhibitor. Nat Med *10*, 55-63.

Schlesinger, S., Selig, S., Bergman, Y., and Cedar, H. (2009). Allelic inactivation of rDNA loci. Genes Dev *23*, 2437-2447.

Schmitz, K.M., Mayer, C., Postepska, A., and Grummt, I. (2010). Interaction of noncoding RNA with the rDNA promoter mediates recruitment of DNMT3b and silencing of rRNA genes. Genes Dev *24*, 2264-2269.

Scholer, H.R., Dressler, G.R., Balling, R., Rohdewohld, H., and Gruss, P. (1990). Oct-4: a germline-specific transcription factor mapping to the mouse t-complex. Embo J *9*, 2185-2195.

Schotta, G., Lachner, M., Sarma, K., Ebert, A., Sengupta, R., Reuter, G., Reinberg, D., and Jenuwein, T. (2004). A silencing pathway to induce H3-K9 and H4-K20 trimethylation at constitutive heterochromatin. Genes Dev *18*, 1251-1262.

Shi, Y., Lan, F., Matson, C., Mulligan, P., Whetstine, J.R., Cole, P.A., and Casero, R.A. (2004). Histone demethylation mediated by the nuclear amine oxidase homolog LSD1. Cell *119*, 941-953.

Shiraishi, M., Sekiguchi, A., Chuu, Y.H., and Sekiya, T. (1999). Tight interaction between densely methylated DNA fragments and the methyl-CpG binding domain of the rat MeCP2 protein attached to a solid support. Biol Chem *380*, 1127-1131.

Silva, J., Nichols, J., Theunissen, T.W., Guo, G., van Oosten, A.L., Barrandon, O.,

Wray, J., Yamanaka, S., Chambers, I., and Smith, A. (2009). Nanog is the gateway to the pluripotent ground state. Cell *138*, 722-737.

Smith, A.G., Heath, J.K., Donaldson, D.D., Wong, G.G., Moreau, J., Stahl, M., and Rogers, D. (1988). Inhibition of pluripotential embryonic stem cell differentiation by purified polypeptides. Nature *336*, 688-690.

Sogo, J.M., Ness, P.J., Widmer, R.M., Parish, R.W., and Koller, T. (1984). Psoralen-crosslinking of DNA as a probe for the structure of active nucleolar chromatin. J Mol Biol *178*, 897-919.

Solovei, I., Wang, A.S., Thanisch, K., Schmidt, C.S., Krebs, S., Zwerger, M., Cohen, T.V., Devys, D., Foisner, R., Peichl, L.*, et al.* (2013). LBR and lamin A/C sequentially tether peripheral heterochromatin and inversely regulate differentiation. Cell *152*, 584-598.

Stancheva, I., Lucchini, R., Koller, T., and Sogo, J.M. (1997). Chromatin structure and methylation of rat rRNA genes studied by formaldehyde fixation and psoralen cross-linking. Nucleic Acids Res *25*, 1727-1735.

Stefanovsky, V., Langlois, F., Gagnon-Kugler, T., Rothblum, L.I., and Moss, T. (2006). Growth factor signaling regulates elongation of RNA polymerase I transcription in mammals via UBF phosphorylation and r-chromatin remodeling. Mol Cell *21*, 629-639.

Strahl, B.D., and Allis, C.D. (2000). The language of covalent histone modifications. Nature *403*, 41-45.

Strohner, R., Nemeth, A., Jansa, P., Hofmann-Rohrer, U., Santoro, R., Langst, G., and Grummt, I. (2001). NoRC--a novel member of mammalian ISWI-containing chromatin remodeling machines. EMBO J *20*, 4892-4900.

Sylvester, J.E., Gonzales, I.L., and Mougey, E.B. (2004). Structure and organisation of vertebrate ribosomal DNA. In The Nucleolus,, O. MO, ed. (New York, Kluwer Acad./Plenum), pp. 58-72.

Takahashi, K., and Yamanaka, S. (2006). Induction of pluripotent stem cells from

mouse embryonic and adult fibroblast cultures by defined factors. Cell *126*, 663-676.

Tesar, P.J., Chenoweth, J.G., Brook, F.A., Davies, T.J., Evans, E.P., Mack, D.L., Gardner, R.L., and McKay, R.D. (2007). New cell lines from mouse epiblast share defining features with human embryonic stem cells. Nature *448*, 196-199.

Towbin, B.D., Gonzalez-Aguilera, C., Sack, R., Gaidatzis, D., Kalck, V., Meister, P., Askjaer, P., and Gasser, S.M. (2012). Step-wise methylation of histone H3K9 positions heterochromatin at the nuclear periphery. Cell *150*, 934-947.

Tower, J., Henderson, S.L., Dougherty, K.M., Wejksnora, P.J., and Sollner-Webb, B. (1989). An RNA polymerase I promoter located in the CHO and mouse ribosomal DNA spacers: functional analysis and factor and sequence requirements. Mol Cell Biol *9*, 1513-1525.

Tsai, M.C., Manor, O., Wan, Y., Mosammaparast, N., Wang, J.K., Lan, F., Shi, Y., Segal, E., and Chang, H.Y. (2010). Long noncoding RNA as modular scaffold of histone modification complexes. Science *329*, 689-693.

van de Nobelen, S., Rosa-Garrido, M., Leers, J., Heath, H., Soochit, W., Joosen, L., Jonkers, I., Demmers, J., van der Reijden, M., Torrano, V.*, et al.* (2010). CTCF regulates the local epigenetic state of ribosomal DNA repeats. Epigenetics Chromatin *3*, 19.

van Koningsbruggen, S., Gierlinski, M., Schofield, P., Martin, D., Barton, G.J., Ariyurek, Y., den Dunnen, J.T., and Lamond, A.I. (2010). High-resolution whole-genome sequencing reveals that specific chromatin domains from most human chromosomes associate with nucleoli. Mol Biol Cell *21*, 3735-3748.

Wang, J., Rao, S., Chu, J., Shen, X., Levasseur, D.N., Theunissen, T.W., and Orkin, S.H. (2006). A protein interaction network for pluripotency of embryonic stem cells. Nature *444*, 364-368.

Wen, B., Wu, H., Shinkai, Y., Irizarry, R.A., and Feinberg, A.P. (2009). Large histone H3 lysine 9 dimethylated chromatin blocks distinguish differentiated from embryonic stem cells. Nat Genet *41*, 246-250.

Whetstine, J.R., Nottke, A., Lan, F., Huarte, M., Smolikov, S., Chen, Z., Spooner, E., Li, E., Zhang, G., Colaiacovo, M.*, et al.* (2006). Reversal of histone lysine trimethylation by the JMJD2 family of histone demethylases. Cell *125*, 467-481.

Wiblin, A.E., Cui, W., Clark, A.J., and Bickmore, W.A. (2005). Distinctive nuclear organisation of centromeres and regions involved in pluripotency in human embryonic stem cells. J Cell Sci *118*, 3861-3868.

Williams, R.L., Hilton, D.J., Pease, S., Willson, T.A., Stewart, C.L., Gearing, D.P., Wagner, E.F., Metcalf, D., Nicola, N.A., and Gough, N.M. (1988). Myeloid leukaemia inhibitory factor maintains the developmental potential of embryonic stem cells. Nature *336*, 684-687.

Wilmut, I., Schnieke, A.E., McWhir, J., Kind, A.J., and Campbell, K.H. (1997). Viable offspring derived from fetal and adult mammalian cells. Nature *385*, 810-813.

Wolffe, A.P. (1997). Histone H1. Int J Biochem Cell Biol *29*, 1463-1466.

Wong, L.H., Ren, H., Williams, E., McGhie, J., Ahn, S., Sim, M., Tam, A., Earle, E., Anderson, M.A., Mann, J.*, et al.* (2009). Histone H3.3 incorporation provides a unique and functionally essential telomeric chromatin in embryonic stem cells. Genome Res *19*, 404-414.

Wray, J., Kalkan, T., and Smith, A.G. (2010). The ground state of pluripotency. Biochem Soc Trans *38*, 1027-1032.

Wu, S.C., and Zhang, Y. (2010a). Active DNA demethylation: many roads lead to Rome. Nat Rev Mol Cell Biol *11*, 607-620.

Wu, S.C., and Zhang, Y. (2010b). Active DNA demethylation: many roads lead to Rome. Nature reviews Molecular cell biology *11*, 607-620.

Yeo, J.C., and Ng, H.H. (2013). The transcriptional regulation of pluripotency. Cell Res *23*, 20-32.

Ying, Q.L., Nichols, J., Chambers, I., and Smith, A. (2003). BMP induction of Id proteins suppresses differentiation and sustains embryonic stem cell self-renewal

in collaboration with STAT3. Cell *115*, 281-292.

Ying, Q.L., Wray, J., Nichols, J., Batlle-Morera, L., Doble, B., Woodgett, J., Cohen, P., and Smith, A. (2008). The ground state of embryonic stem cell self-renewal. Nature *453*, 519-523.

Young, R.A. (2011). Control of the embryonic stem cell state. Cell *144*, 940-954.

Zhang, L.F., Huynh, K.D., and Lee, J.T. (2007). Perinucleolar targeting of the inactive X during S phase: evidence for a role in the maintenance of silencing. Cell *129*, 693-706.

Zhang, W.Y., de Almeida, P.E., and Wu, J.C. (2008). Teratoma formation: A tool for monitoring pluripotency in stem cell research.

Zhou, Y., Santoro, R., and Grummt, I. (2002). The chromatin remodeling complex NoRC targets HDAC1 to the ribosomal gene promoter and represses RNA polymerase I transcription. EMBO J *21*, 4632-4640.

Zhou, Y., Schmitz, K.M., Mayer, C., Yuan, X., Akhtar, A., and Grummt, I. (2009). Reversible acetylation of the chromatin remodelling complex NoRC is required for non-coding RNA-dependent silencing. Nat Cell Biol *11*, 1010-1016.

Zink, D., Fischer, A.H., and Nickerson, J.A. (2004). Nuclear structure in cancer cells. Nat Rev Cancer *4*, 677-687.

Zomerdijk, J.C., Beckmann, H., Comai, L., and Tjian, R. (1994). Assembly of transcriptionally active RNA polymerase I initiation factor SL1 from recombinant subunits. Science *266*, 2015-2018.

Zwaka, T.P., and Thomson, J.A. (2005). A germ cell origin of embryonic stem cells? Development *132*, 227-233.

Curriculum Vitae

PERSONAL INFORMATION

Surname	**Savić (born Đorđević)**
Name	**Nataša**
Date of Birth	**June 7, 1984**
Hometown	**Belgrade, Serbia**
Nationality	**Serbian**

EDUCATION

2010 – present	Doctoral Thesis in Molecular Biology (Dr. sc. nat./Ph.D.) University of Zurich
2003 – 2009	Bachelor and Master studies in Molecular Biology and Physiology (MSc University of Belgrade) Faculty of Biology, University of Belgrade, Serbia Diploma Thesis: ”High Throughput Screening for Soluble DAPK1-Calmodulin Complexes”
1999 – 2003	High School - Life Sciences (Matura) IX Belgrade Gymnasium – “Mihailo Petrovic – Alas” Belgrade, Serbia

Grants during doctorate studies: Forschungskredit 2012, the University of Zurich

Acknowledgements

Completing this PhD would not have been possible without the support of many people.

My outmost gratitude goes to my supervisor, Dr. Raffaella Santoro for giving me the opportunity to pursue my PhD in her laboratory. My work would not have reached the same quality without her continuous motivation, highly dedicated scientific guidance and constant support.

I would like to thank to Prof. Dr. Michael O. Hottiger for being my doctoral father, for his time and helpful suggestions in the numerous discussions related to my project. I am very grateful to Dr. Paolo Cinelli, for giving me the opportunity to enter the stem cell field as well as for his generous help and advices throughout my PhD. I am also very grateful to the remaining members of my dissertation committee, Prof. Dr. Massimo Lopes and Prof. Dr. Witold Filipowicz, for their academic support and constructive criticism through this important period. Furthermore, I would like to thank to Dr. Patrick Heun for providing an external expertise of this thesis.

I am also very grateful to Dominik Bär, Sergio Leone, Fabienne A. Weber, Eva Vollenweider, Elena Ferrari and Olga Shakova, who unselfishly helped complement my work with their expertise. My gratitude extends to the Molecular Life Science Program of the Life Science Zurich Graduate School. I would also like to acknowledge the support I had at the Center for Microscopy and Image

Analysis and Functional Genomics Center of the University of Zurich.

Many thanks goes to all the members of IVBMB and CABMM institutes for creating great working atmosphere on a daily basis and making my PhD an enjoyable experience. Big thanks to my current and former lab-mates, Claudio, Fabian, Dominik, Sandra, Eva, Sergio, Nina, Anita, Maria and Damian, among which I have found not only great colleagues, but life-long friends. I am especially grateful to Florian, Anneli, Stephan, Gregor, Ali, Nicki, Sameera, Fabienne and Urs. Big thanks to Ivana for the warmest welcome in Zurich.

My faithful supporters have been my closest friends, Marija, Irena, Marija, Ana and Natasa. Thank you for always being there no matter how far away I was.

I would like to express my deepest gratitude to my parents and my sister, for their unlimited support and blind belief in my capabilities that made it possible to continue to study for my PhD.

Finally, very special thanks to Nemanja for making me smile and being there for me through thick and thin.